

University of Strathclyde Faculty of Engineering

**Analysis of the Maximum Wind Energy
Penetration in the Island of Crete**

**A thesis submitted for the degree of Master in Science In Energy
Systems and the Environment**

Kiriakos Antonakis

Glasgow September 2005



Declaration of Author's Right

The copyright of this Thesis belongs to the author under the terms of the United Kingdom Copyright Acts as qualified by the University of Strathclyde Regulation 3.49. Due acknowledgement must always be made of the use of any material contained in, or derived from, this dissertation.

DEDICATION

Πρώτ' απ' όλα θα ήθελα να αφιερώσω την πτυχιακή αυτή στους γονείς μου θέλοντας να τους ευχαριστήσω για την ηθική και υλική στήριξη των προσπαθειών μου, με όλες τους τις δυνάμεις όλα αυτά τα χρόνια. Στο θείο μου Νίκο, τη Μιμή, την Τιτή, και τη Μπεμπέ για την υποστήριξη που μου πρόσφεραν με τον δικό τους μοναδικό τρόπο.

Ιδιαίτερη αφιέρωση στη Μαρία για τη βοήθεια, τη συμπαράσταση και την υπομονή της όλο αυτό το χρονικό διάστημα.

ACKNOWLEDGEMENTS

I would like to express my sincere appreciation to all those who helped me throughout my thesis. First of all I would like to thank my supervisor Dr. Andrew Cruden for his meaningful suggestions and his guidance throughout this thesis. More than important for the completeness of my thesis was Dr. Aristides Kiprakis help. Many thanks to Mrs. Antiopi Gigantidou and Mr. George Plokamakis from the Public Power Company (PPC) in Greece, for providing me with valuable technical data.

The Student Awards Agency for Scotland (SAAS) for the financial support during my studies in Glasgow.

I would like also to thank everyone in Strathclyde University who helped during this course and especially Prof. Joe Clarke and Mrs. Janet Harbidge.

A big thank to my Scottish 'life-mates' Mcis, Vassilis, George, Lefteris, Kostas K., Christos and Popi.

Special thanks to Kostas and Vicky. Without their help, life in Scotland would be much more difficult.

ABSTRACT

This thesis tries to determine and analyse from a technical aspect the penetration of wind energy in the island of Crete in Greece. Crete is an island with an autonomous electric grid and high wind energy potential. The average wind speed is more than 7m/sec while in some areas; especially in the eastern part, the annual average speed exceeds 10m/sec. The electricity cost produced by the conventional power plants in Crete is quite high reaching 5 to 7 times the power production on the Mainland. Considering also the environmental benefits the use of wind energy becomes an essential factor for the sustainable development of the area. In 2003 almost 10% of the electricity produced in Crete was from wind turbines located in the eastern part of the island. However it is recognised that electricity produced by wind turbines can create some technical problems in the electric grid (such as stability problems), typically due to the unpredicted, variable and non constant form of wind energy.

In this thesis the Cretan electric grid is simulated using Matlab software, in order to analyse the power flows in this system. The power flow solution by both Newton-Raphson and Gauss-Seidel models was developed in order to estimate the additional wind capacity that can be added to each one of the 23 buses in the Cretan electric grid. Furthermore other technical parameters such as the thermal limits of the high voltage transmission lines and power losses were calculated.

By the followed analysis it was estimated that additional 11.7MW of wind energy can be added to the existing Cretan electricity grid. This increase results in a maximum wind energy penetration, which reaches the 12.8% of the total produced energy. This value is quite satisfying in comparison to the present one that is 11.2%. Additionally, the production of 11.7MW by wind turbines provides a further saving of CO₂ emissions on the island (21,852 tonnes), due to the replacement of diesel generation.

CONTENTS

1	Introduction.....	9
2	Wind Energy in Greece	10
2.1	The Electricity System in Greece	12
2.2	Electricity System in Greek Islands.....	14
2.3	The Development of Renewable Energy Sources in Greece	15
2.4	Wind Energy Development in Greece.....	16
2.5	The Case Study of Crete.....	17
2.6	Wind Energy Development in Crete.....	19
3	Wind Turbines - technical issues	21
3.1	Wind Turbine's Components and Electricity Generation.....	21
3.2	Considerations for Wind Turbines Development.....	22
3.2.1	Small unit sizes.....	22
3.2.2	Wind Variability	22
3.2.3	Electrical properties	23
3.3	Electrical Machines.....	23
3.3.1	Synchronous machine	24
3.3.2	Asynchronous or Induction machine	27
3.4	Generator Systems used in Wind Industry.....	31
3.4.1	Constant speed WT with squirrel cage induction generator (CT).....	31
3.4.2	Variable speed WT with doubly-fed (wound-rotor) induction generator (VTDI)	31
3.4.3	Variable speed WTs with direct-drive synchronous generator (VTDD).....	32
3.5	Transmission to the Grid	32
3.6	The Electrical grid.....	33



3.6.1	Frequency control	33
3.6.2	Fast frequency control on the level of an individual station: the droop line;	34
3.6.3	Integral control to reset the frequency to 50 Hz after an offset has occurred;	35
3.6.4	Production switching	35
3.6.5	Finally in case of emergency: load shedding, switching of grid sections off the grid.	35
3.7	Voltage control.....	35
3.8	Impact of Connecting Wind Turbines to the Distribution Network.....	36
3.8.1	Voltage flicker	37
3.8.2	Harmonics.....	39
3.8.3	Voltage Variation	39
3.8.4	Reverse Power Flows.....	40
3.8.5	Fault Levels.....	40
3.8.6	Thermal Limits	40
3.8.7	Transient Stability	41
3.8.8	Protection.....	41
4	Power Flow Analysis	42
4.1	Bus Admittance Matrix.....	43
4.2	Solution of Non-Linear Algebraic Equations	46
4.2.1	Gauss–Siedel Method	46
4.2.2	Newton-Raphson Method	48
4.3	Power Flow Solution.....	50
4.4	Power Flow Equation.....	51
4.5	Gauss-Seidel Power Flow Solution	52
4.6	Line Flows and Losses	54



4.7	Tap Changing Transformers	55
4.8	Power Flow Programs	56
4.9	Data Preparation	57
4.10	Newton-Raphson Power Flow Solution	58
4.11	Fast Decoupled Power Flow Solution	62
5	Methodology and Results.....	66
5.1	The Electric Grid in the Island of Crete	66
5.2	Demand and Electricity Production in Crete	68
5.3	Power Flow Analysis	70
5.3.1	Data Preperation.....	70
5.3.2	Newton-Raphson Method	73
5.3.3	Gauss-Seidel Method	75
5.3.4	Line Flow Analysis and Losses.....	77
5.4	Thermal Limitations	79
6	Conclusions.....	80
7	References	84

1 INTRODUCTION

This thesis tries to determine and analyse from a technical perspective the maximum penetration of wind energy capable in the existing electricity grid in the remote island of Crete in Greece. In chapter 2 the main issues for the development of Renewable Energy Sources and especially Wind Energy in Greece and Crete are reported. The electrical system in Greece is being described as well as the Cretan one, highlighting the major differences between these two systems and pointing out the special characteristics of the Cretan autonomous electric grid.

Chapter 3 describes the technical aspects concerning wind turbines and the considerations that should be taken for the development of wind farms, especially in autonomous electric grids. The special characteristics of the wind turbines as electric machines and the resulting power transmission to the electric grid are described. Ultimately the impacts that wind turbines cause when connected to the electric grid are highlighted.

In Chapter 4 the background and theory of the power flow analysis that was used to determine the penetration level of wind energy in Crete is introduced. The analysis program used within the Matlab software environment is described, pointing out the two main solver methods that were used, in order to evaluate the penetration level of wind energy in Crete.

The whole methodology, the data preparation and the results from the power flow analyses are presented in chapter 5. The main impact that the connection of power plants and especially wind farms have to the electric grid of Crete are also presented.

Finally in chapter 6, the conclusions from the whole analysis are made and a determination of the maximum wind penetration within the existing Cretan electricity grid is stated. Solutions to problems that the development of such systems causes to the Cretan electric grid, are also given.

2 WIND ENERGY IN GREECE

The meaning of the term “Power of the Wind” was first used by the Ancient Greeks. As all great phenomena it was tried to be explained and determined by the wise men of those ages. Although it was very difficult for them to give a convincing explanation, so people deified the phenomenon. According to Mythology all winds were governed by a god named Aeolos, son of Poseidon god of the sea. He was the one who enclosed all the unfavourable winds in a sack and gave it to Odysseus to safeguard them during his journey back to Ithaca. Unfortunately the crew’s curiosity and greed led them to open the sack and release all the winds, throwing the ship off its course and causing Odysseus more difficulties.

Because of Ancient Greeks’ interest an ancient Observatory called "Wind Tower" was built in Athens during the 1st century BC. On its 8 sides, it brings emboss figures of the eight winds that Aristotelis had noticed has centuries earlier.



The “Wind Tower” In Athens



The Tower of the Winds (Horologion of Andronikos of Kyrrhos). The building is octagonal in shape, and was designed as an elaborate timepiece. On each of the 8 sides of the building are reliefs depicting the 8 winds. There are also fixtures for sundials on the exterior, below the personifications of the winds, so that you could tell the time from several different points of view from the outside. But inside the building was an elaborate, water-powered device that turned to show the passing of the hours, the days, and even the phases of the moon. The Tower of the Winds was probably built in the mind 2nd century B.C.





 <p>East Wind (Apiliotis) a young man who carries fruits and grains in his cloak.</p>	 <p>Western Wind (Zephyros)</p>
 <p>North Wind (Borias). Since Boreas brings the cold, he wears a thick garment and blows the howling north wind through a large shell.</p>	 <p>South Wind (Notos) Since this wind brings rain, he pours out a jar of water.</p>

Figure 2.1: Wind Energy in Ancient Greece



 <p>Old wind mills in Chios Island (Greece)</p>	 <p>A damaged windmill and a modern wind generator. The continuity of Man's history and his efforts to exploit the wind energy.</p>
--	---

Figure 2.2 Examples of uses of wind energy in Greece the last centuries

Man has been exploiting the wind energy since very early in his history. The first use of the wind energy was as a motive force for the ships. For many centuries BC the Greeks, Persians, Chinese and Egyptians have largely used the windmills mostly for the cereals grinding. In addition windmills were also used for water pumping. In Greece and in specific in Eastern Crete almost 6,000 water pumping wind mills were used to pump water for agricultural purposes. During the 17th century the discovery of the steam engines started to replace the wind mills. In 1900, the Danish produced electricity by the wind. In 1940 in Vermont (USA) a testing wind motor with two blades was constructed. But wind

energy had not been taken under serious consideration till the oil crisis in 1973-74 when Man realized the energy and environmental problem of our planet and tried to develop the wind technologies.

2.1 The Electricity System in Greece

The Ministry of Development is the state authority that monitors all activities relating to the energy sector. Greece has limited primary energy sources, which, apart from coal (lignite) do not contribute significantly to the national energy balance. The oil and gas fields discovered in the early seventies were relatively small and are being rapidly depleted, whilst the available renewable energy potential is yet to be developed. Furthermore, Greece is highly dependant on imported petroleum, which accounts for almost 69% of its primary energy supply. Indigenous brown coal (lignite) contributes 32% to energy supply with the balance coming from renewable energies, mainly hydro and biomass.

Greece is an exceptionally difficult region for electric power development, with its rugged topography and numerous islands. The mainland transmission system consists of 66, 150 and 400 kV networks. The total length of transmission lines at 66 kV and above, including isolated island transmission systems is more than 10,500 km. The HTSO (Hellenic Transmission System Operator) has an on-going programme for connecting some of the closer islands directly to the mainland grid. In 1991 the power lines in former Yugoslavia were destroyed and Greece became unable to import electricity from the EU. In 2001 a 500 MW submarine cable connected the Greek Electric Grid to the Italian one, connecting Greece with the EU electric grid. Other options are being examined. Several gas-fired retrofit projects are underway or planned at existing power plants as the government tries to offset the use of lignite for power generation. Plans for the development of electric power include the construction and/or completion of 3 natural gas and 4 lignite-fired power stations, a bituminous coal-fired unit, as well as a number of wind, biomass, hydroelectric and solar energy units. Changes in support measures for renewables are likely to increase the role of non-PPC (Public Power Corporation) generators in renewable energy supply.

Since 1990 the power consumption per capita in Greece has been increasing about 4% per year. In 2002, the installed electricity generation capacity in Greece was 12.236 GW, increased about 6.8 % since 2001. In 2003, the installed capacity increased 3.6% reaching the value of 12.679 GW (Table 2.1). Out of the total installed capacity, 88% is on the mainland whereas 12 % is produced on the so called "Non Interconnected Islands" which are islands with autonomous systems not connected to the mainland grid. [2]

Until 1999 the electric power industry in Greece was dominated by the state owned electric utility, the Public Power Corporation (PPC). The PPC was monopolising electricity transmission and distribution. Although the legal framework (L 2244/94) had been modified to encourage private power production, the PPC was generating 98% of all electricity in 1998. With huge investments in lignite mining, the company was remaining vertically integrated to a great degree.

Table 2.1: Installed Electric Power Generation capacity (MW)

	2000	2001	2002	2003	Annual change (%)		
					01/00	02/01	03/02
MAINLAND AND INTERCONNECTED ISLANDS							
Thermal Power Plants							
Coal	4908	4933	4958	5288	0,51	0,51	6,66
HFO	777	771	858	858	-0,72	11,20	0,00
Natural Gas	1100	1103	1693	1693	0,25	53,54	0,00
Total Thermal	6785	6807	7509	7839	0,33	10,31	4,39
Hydroelectric Plants							
Small (1-10 MW)	24	31	35	38	29,17	12,90	8,57
Large (>10 MW)	3039	3039	3039	3039	0,00	0,00	0,00
Total Hydroelectric	3063	3070	3074	3077	0,23	0,13	0,10
Other RES	137	199	217	308	45,65	8,58	42,40
TOTAL	9985	10077	10799	11224	0,92	7,17	3,93
NON-INTERCONNECTED ISLANDS							
Thermal Power Plants							
Coal	-	-	-	-	-	-	-
HFO & LFO	1290,0	1315,0	1365,0	1365,0	1,94	3,80	
Natural Gas	-	-	-	-	-	-	-
Total Thermal	1290,0	1315,0	1365,0	1365,0	1,94	3,80	0,00
Hydroelectric Plants							
Small (1-10 MW)	0,3	0,3	0,3	0,3	0,00	0,00	0,00
Large (>10 MW)	-	-	-	-	-	-	-
Total Hydroelectric	0,3	0,3	0,3	0,3	0,00	0,00	0,00
Other RES	76,3	78,8	83,0	107,1	3,28	5,33	29,04
TOTAL	1366,6	1394,1	1448,3	1472,4	2,01	3,89	1,66
TOTAL	11351,5	11470,6	12247,7	12696,6	1,05	6,77	3,67

Source [2]

Greece is making intense efforts in many sectors such as engineering, funding, institutional and regulatory, in order to meet the indicative target set by Directive 2001/77/EC. Because of the present fluid state of liberalization of the utility market that was dominated by the single utility company in the nation for more than a half century, the approach to the Directive 2001/77/EC is difficult.

The first step was done in 1999 with the voting of the Law 2773/99, "Liberalization of the Electricity Market – Regulation of Energy Policy Issues and other Provisions, constitutes the basic legal background". According to this law, the Regulatory Authority for Energy (RAE) and the Hellenic Transmission System Operator (HTSO), were created.

RAE is an independent, public authority that manages, suggests, and promotes the existence of equal opportunities and fair competition. It gives operation licenses to producers, providers, and any other related to the market. In addition, RAE formulates suggestions to the Minister of Development with regard to the issue of power generation authorizations. Thereafter, RAE monitors the implementation progress of the Renewable Energy Sources (RES) projects through quarterly reports and recommends which investors should be removed from the sector due to unjustifiable delay. RAE also recommends legislative measures for further deregulation of the electricity market within which critical RES issues can be addressed (as is the case of hybrid plants). On a more long-term basis, RAE considers the introduction of green certificates and the establishment of a network of large-scale, dispersed energy production. [1]

HTSO is the company that handles the Hellenic Transmission System of Electric Energy and has a double role. Its task is to set in balance between production and consumption and to ensure that quality electric energy is provided reliably and safely. This role had been being played by the Public Power Corporation (PPC). Additionally according to Law 3175/2003 HTSO has to settle the market – in other words, to act like an energy “stock market” that arranges on a daily basis who owes to whom. HTSO does not provide electricity, and whatever basic exchanging relations exist are bilateral between producers/providers and their customers. [1]

2.2 Electricity System in Greek Islands

Greek islands have every characteristic of the so called “remote areas”. Today there are more than 25 islands of different size in Greece that are not connected to the mainland’s electric grid and possess small autonomous grids. Those grids are usually powered by diesel generators which are neither the cleanest nor the most efficient generators. Diesel fuel should also be transferred on site, and this poses other problems. During the winter months ship link is sometimes difficult to be established due to bad weather. In addition the cost of transporting diesel to the islands is quite high and this means that the cost of producing electricity is also high. People in the islands actually buy the electricity cheaper than it is produced, since there is a common price for the whole country. The cost of producing electricity in the islands is 5 to 7 times higher than that of producing it in the mainland. In the recent years some Renewable Energy Sources have been integrated to the small island grids but without – most of the times- exploiting a great deal of the Renewable Energy potential available. [22], [23]

The Renewable Energy potential of those islands is quite high, one of the highest in the country. Wind speed potential is quite high in most islands varying from 7 to 12m/sec while the mean wind speed is up to 8m/sec [24]. It is also well known that even in the ancient years people were exploiting this potential by using numerous windmills. A bright example is that of the 10,000 windmills in Lasithi tableland in the eastern part of the island of Crete.



Figure 2.3: The tableland in Lasithi with 10,000 windmills

2.3 The Development of Renewable Energy Sources in Greece

The Centre for Renewable Energy Sources (CRES) is the state institution that is responsible for the promotion of Renewable Energy Sources (RES), the Rational Use of Energy (RUE) and Energy Saving (ES) in Greece.

To date, the PPC is the basic owner of Renewable Energy Systems in Greece. It owns exclusively all the large hydro power stations, 97% of the small hydro capacity and 72% of photovoltaic capacity. Since the voting of Law 2244/94 “Production of Electricity from Renewable Energy Sources” in 1994 and Law 2702/99 “Liberalization of the Electricity Market”, individuals were encouraged to develop Renewable Energy Systems and especially wind farms. The wind energy exploitation has been a part of a larger policy since 1998, concerning the development of Renewable Energy Sources that Greek Government supports. The major strategic goals of the national policy for the development of the renewable energy sources are the following [1]:

1. Increase the efficiency of the energy system.
2. Protect the environment by decreasing the emission of atmospheric pollutants.
3. Improvement of the safety of the energy system by diversifying energy supplies.
4. Reduce CO₂ emissions by 2000 to the levels of 1990.
5. Decentralize energy production.
6. Actively involve Greek industry in creating new jobs.
7. Develop new technology.

Table 2.2: Installed and forecasted installed until 2010 Renewable Energy Systems in Greece

	Installed Power in April 2003 (MW)	Forecasted Installed Power in 2010 (MW)	Electricity Generation in 2003 (TWh)	Forecasted Electricity Generation in 2010 (TWh)	Percentage Electricity Generation in 2003 (%)	Percentage Electricity Generation in 2010 (%)
Wind Energy	420	2,170		6.08		8.45
Small Hydro	66	475		1.66		2.31
Large Hydro	3,060	3,680		5.47		7.59
Biomass	8	125		0.99		1.37
Geothermy	0	8		0.06		0.09
Photovoltaics	0	5		0.01		0.01
Total	3461	6463		14.27		19.82

2nd National Report for Renewable Energy Sources Penetration in Greece – Ministry of Development

2.4 Wind Energy Development in Greece

Wind energy is now firmly established as a mature technology for electricity generation and over 13,900 MW of capacity is now installed worldwide. Greece is one of the European countries possessing high wind energy potential and it is among the aims of the government to encourage developers to exploit this potential, aiming at the largest possible replacement of the existing diesel and coal generators, which are currently used for producing electricity.

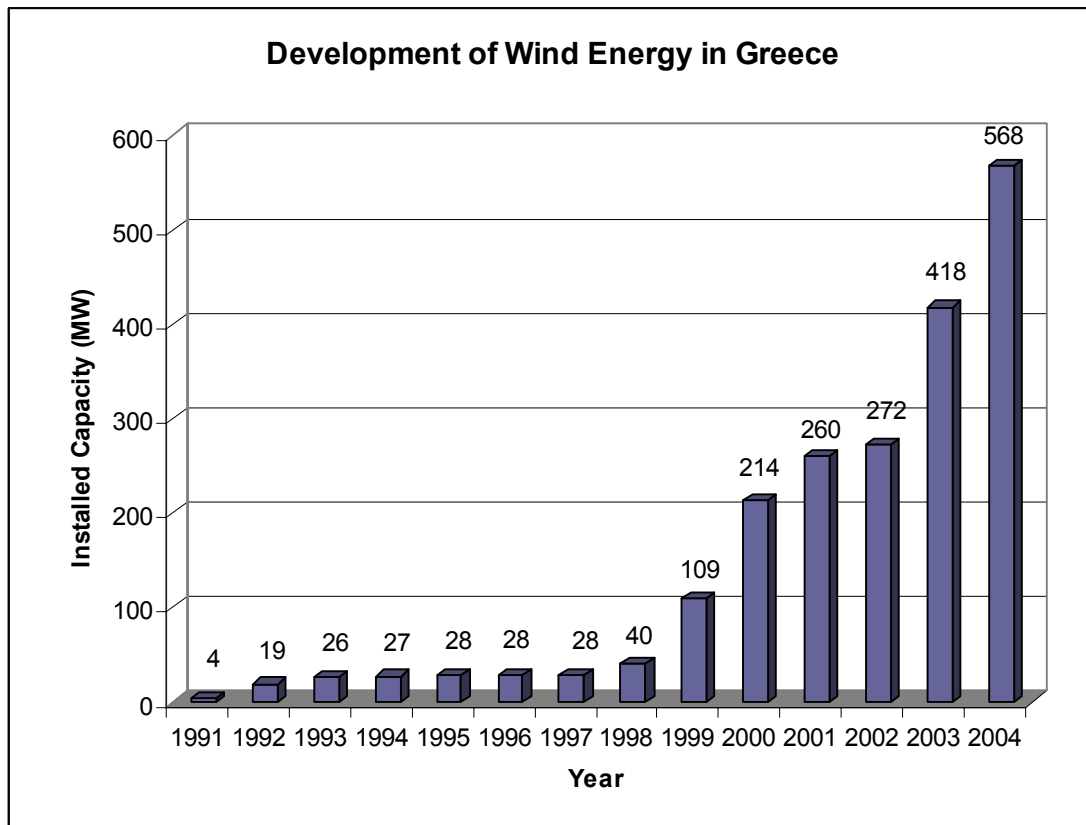
Prior to 1 February 2003, RAE had approved a number of applications for power production from wind energy – 304 WTs with a total installed capacity of 3,533.9 MW.

Table 2.3: Approved Wind projects in Greece prior February 2003

	Approved projects prior February 2003	
	Capacity	Number of WTs
Interconnected System of Mainland	2,967.25	195
Crete	166.7	31
Islands of the Aegean Sea	229.36	70
Islands of the Ionian Sea	70.6	8

Source: Regulatory Authority for Energy

In 2003, the installed capacity of WTs reached 424.4 MW (from 772 WTs). The current national target for wind energy is now 2,000 MW for the year 2010, following EU directives. The new Law 2773/99, introducing electricity market liberalization, maintains energy support from renewable sources in the framework of the competitive market, yet the effect of liberalization on the development of wind energy is not obvious. [6]



An optimistic estimation of wind-energy penetration up to the year 2010 is 2,170 MW. This estimation takes into account the 30% restriction on penetration of wind energy into the electric network. More specifically, 700 MW will be developed in Central Greece and especially in Evia and the connected with the main grid islands of Andros, Tinos islands. In addition 350 MW will be developed in Thraki in the north-east Greece; 280 MW in Lakonia and East Arkadia in Peloponnesus; 240 MW in Crete, Rhodes and other non-interconnected islands; and finally 600 MW in the rest of the country.

According to Law 2773/99, HTSO uses wind energy as first priority during generation unit dispatching. The price paid to the producer is a percentage of the tariff paid by the medium and low-voltage consumers. An important point of that law is that the Minister of Development is allowed to ask the RES producers for a discount on price.

2.5 The Case Study of Crete

Crete is the fourth largest island in the Mediterranean Sea and the biggest in the Aegean Sea in Greece. Its area is 8,335Km² (6.3% of the area that Greece covers). Crete has a population of 594,368 resident inhabitants (2001) most of whom live in the 5 biggest Cretan cities Heraklion (142,112), Hania (55,838), Rethimno (32,694), Ierapetra (23,729) and Agio Nikolao (19,593). Population in Crete increases during summer time due to tourists who in 2003 reached the number of 3 million. [21]

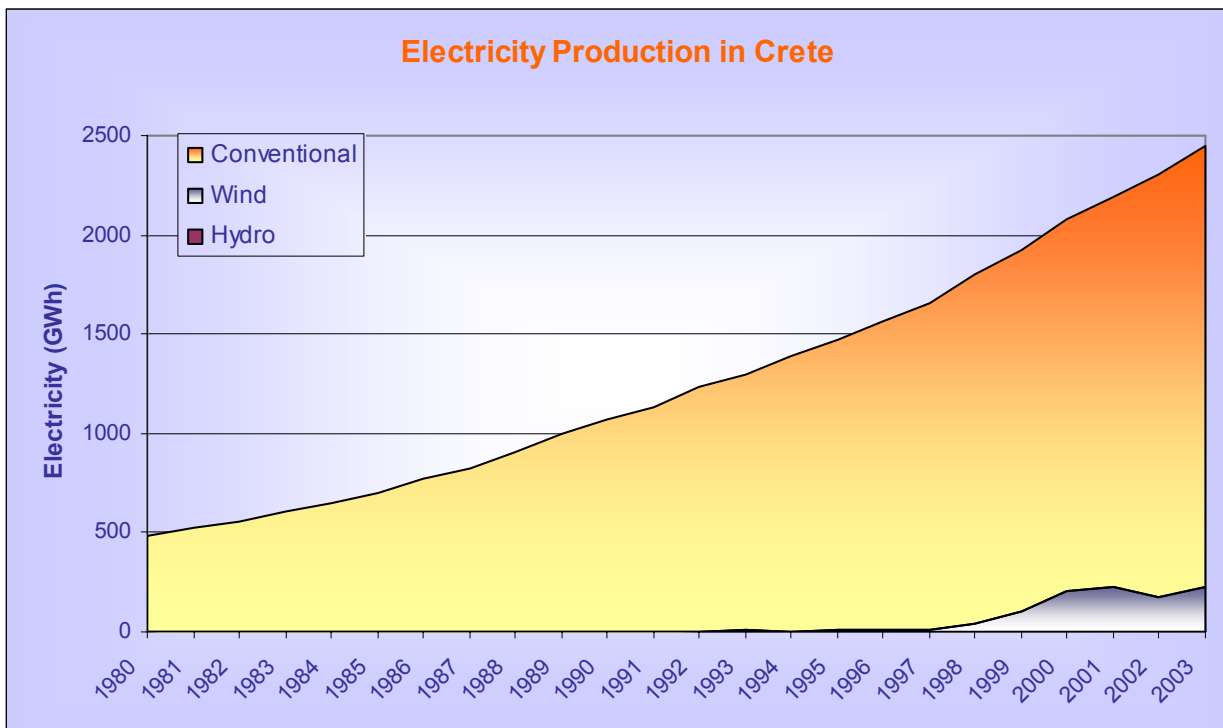
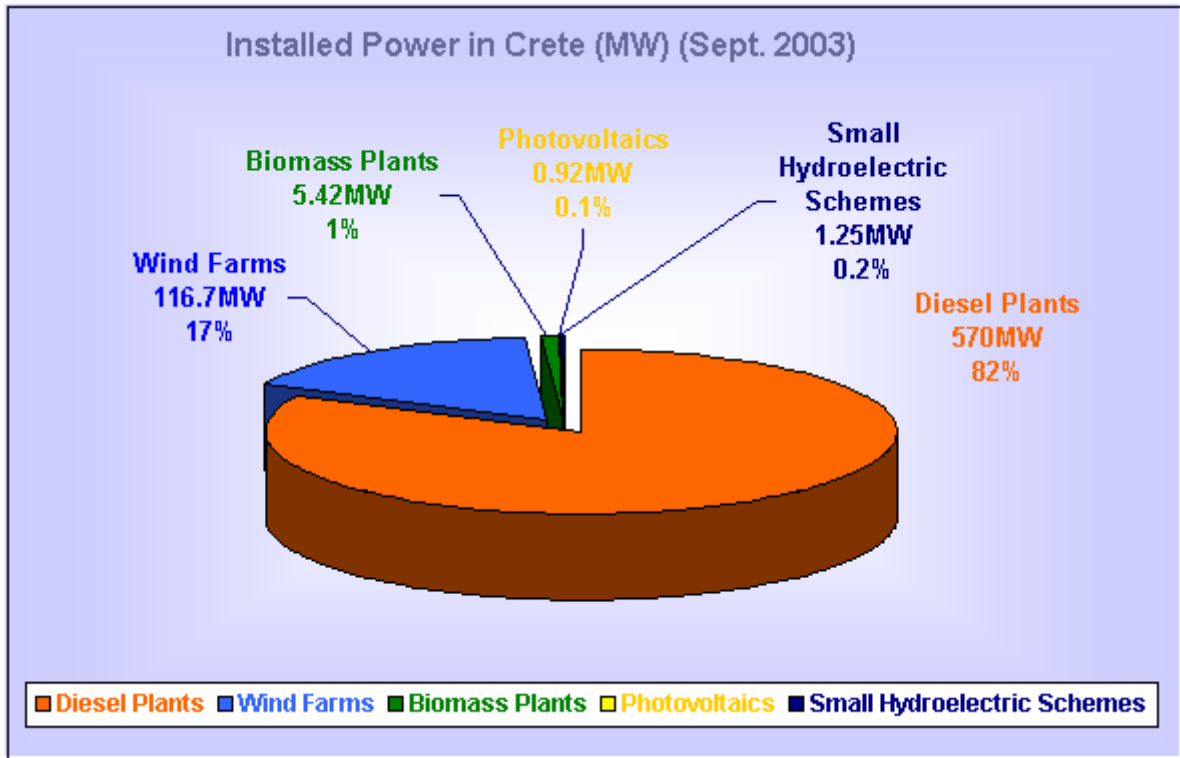
The rate of increase in electricity demand is the highest nationwide reaching up to double as much as the national average. This increase causes power problems that require expensive and non sustainable solutions in coping with the peak power loads from seasonal variations.

As it is mentioned in paragraph 2.1 Greece has implemented several policies for the development of Renewable Energy Sources and especially wind energy. The most important one is the “Implementation Plan for Renewable Energy Sources in Crete”. This policy was planned to last for the period of 1998-2010 and it is mainly focused on the large scale deployment of Renewable Energy Sources for electricity production. This policy is formulated on the basis of the available Renewable Energy potential, the technical constrains for the Renewables penetration and the existing legislative framework.

Actions taken so far in Crete included the exploitation of Renewable Energy potential and its use in systems such as wind farms, biomass plants and solar hot water systems. Further plans included energy savings measures such as the replacement of incandescent bulbs in the residential sector and in street lighting, as well as the use of passive and hybrid systems for cooling and heating of dwellings and hotels. Thirdly actions were applied for smoothing of the daily average hourly load curve, such as time zone pricing systems. Nowadays 10% of the electricity production of the island is being produced by the wind farms placed in the eastern part of the island near Lasithi and central Crete near the biggest city, Heraklio.

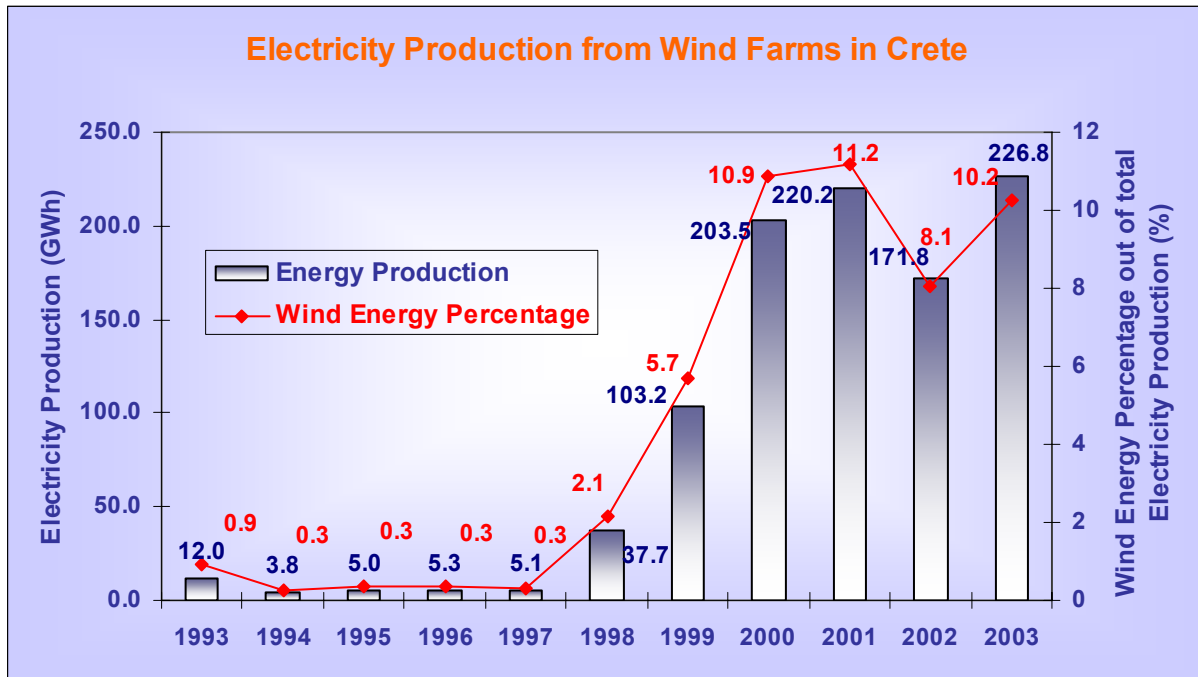
In 2001, the Region of Crete and the Cretan Regional Agency received from the European Commission the first Award for the Best Regional Renewable Energy Partnership, in the framework of 2001 Campaign for the Take-off Awards, for the existing Renewable plants in Crete and their successful integrated programme “Large Scale Deployment of Renewable Energy Sources in Crete”. [24]

Almost 99% of Electricity in Crete is being produced from 2 Diesel Plants in Hania (Ksilokamara) and Heraklio (Linoperamata) and 8 Wind farms that are located at the eastern part of the island especially at Lasithi, Agio Nikolao and central Crete near Heraklio city. [22]



2.6 Wind Energy Development in Crete

In the following diagram the electricity production from Wind Turbines and the percentage of this production the whole Electricity system is presented.



As it can be observed more than 10% of the electricity consumed in the island of Crete was produced from the Wind Farms. This wind penetration has not presented any serious technical problems yet through the system's energy production and supply. Additionally many are the benefits, specially economical and environmental from such a wind energy penetration. However here comes the question of how much more wind energy can be produced and supplied to the Electric Grid of Crete.

3 WIND TURBINES - TECHNICAL ISSUES

Wind Turbines (WT) are the machines that can exploit some of the wind's kinetic energy and convert it into electricity. WTs are usually located in rural or upland areas, where the electrical connection to the nearest electricity substation can be weak, and where local demand for electricity may be much less than the wind generation capacity. WTs are possible to be connected to the supply grid to the low voltage, medium voltage, and high voltage as well as to the extra high voltage system. Nowadays most of the onshore turbines are connected to the medium voltage system of the grid but large offshore wind farms will be connected to the high and extra high voltage level.[9]

3.1 Wind Turbine's Components and Electricity Generation

The common three-blade turbines are placed upwind so that the blades face the wind. They are usually set up on over 30 meters off the ground exploiting the wind velocity which increases as altitude increases, leading to greater turbine performance. The wind causes the blades to rotate through a "lift" force. The rotation turns that wind energy into rotational shaft energy, which causes the generator to generate an electric current.

As the wind turns the blades, the low speed shaft in the nacelle spins, running usually at about 50 rotations per minute. That power is transmitted through the gearbox, which spins the high-speed shaft, increasing the speed to about 1800 rotations per minute. In the end, the gearbox makes the high-speed shaft rotate about fifty times faster than the low-speed shaft. The high-speed shaft turns the connected generator, producing electricity.

As it is shown in figure 3.1 a WT consists of four main parts: the base, the tower, the nacelle, and the blades. The blades capture the wind's energy, spinning a generator in the nacelle. The tower contains the electrical conduits, supports the nacelle, and provides access to the nacelle for maintenance. The base, made of concrete and steel, supports the whole structure. [8]

The three main components for energy conversion in WTs are the rotor, the gear box and the generator. The rotor is the driving device in the conversion system that converts the fluctuating wind energy into mechanical energy. The generator and gearbox are in the nacelle. The gear box adapts rotor to generator speed. The gears increase the rotational speed of the blades to the generator speed of over 1,500 RPM. As the generator spins, electricity is produced. The generator and possibly an electronic inverter convert the mechanical power into electrical energy, supplying the electric grid. Generators can be either variable or fixed speed. Variable speed generators produce electricity at a varying frequency, which must be corrected to 50 cycles per second (Hz) before it is fed onto the grid. Fixed speed generators don't need to be corrected, but aren't as able to take advantage of fluctuations in wind speed. [7], [8]

3.2 Considerations for Wind Turbines Development

Energy production from Wind Turbines (WT) differs in several respects from the “conventional” way of electricity generation. Key differences are the small sizes of individual units, the variable nature of the wind and the type of electrical generator.

3.2.1 Small unit sizes

The small unit sizes mean that both wind farms and individual WTs are usually connected into low voltage distribution networks rather than the high voltage transmission systems and this means that a number of issues related to power flows and protection systems need to be addressed. Electrical safety is an important issue under this heading.[7]

3.2.2 Wind Variability

The wind speed fluctuation is depending both on the weather and on local surface conditions and obstacles. Also in most locations around the globe it is windier during the daytime than at night. The wind is also more turbulent and tends to change direction more frequently during the day than at night. The energy content of the wind is always changing because of the continuous wind speed fluctuation; although to some point the most rapid variations can be compensated by the inertia of the WT rotor. [10]

The variable nature of wind is often perceived as a difficulty, but in fact poses few problems. The variations in output do not cause any difficulty in operating electricity systems, as they are not usually detectable above the normal variations in supply and demand. With significant amounts of wind power – roughly 30 % or more of demand - low cost solutions can be found and some island systems operate with high proportions of wind energy. Variability also needs to be taken into account at the local level, to ensure consumers are not affected by “flicker”. However appropriate care in electrical design can eliminate this problem. [7]

From the point of view of WT electricity producers, it is an advantage that most of the wind energy is produced during the daytime, since electricity consumption is higher then than at night.

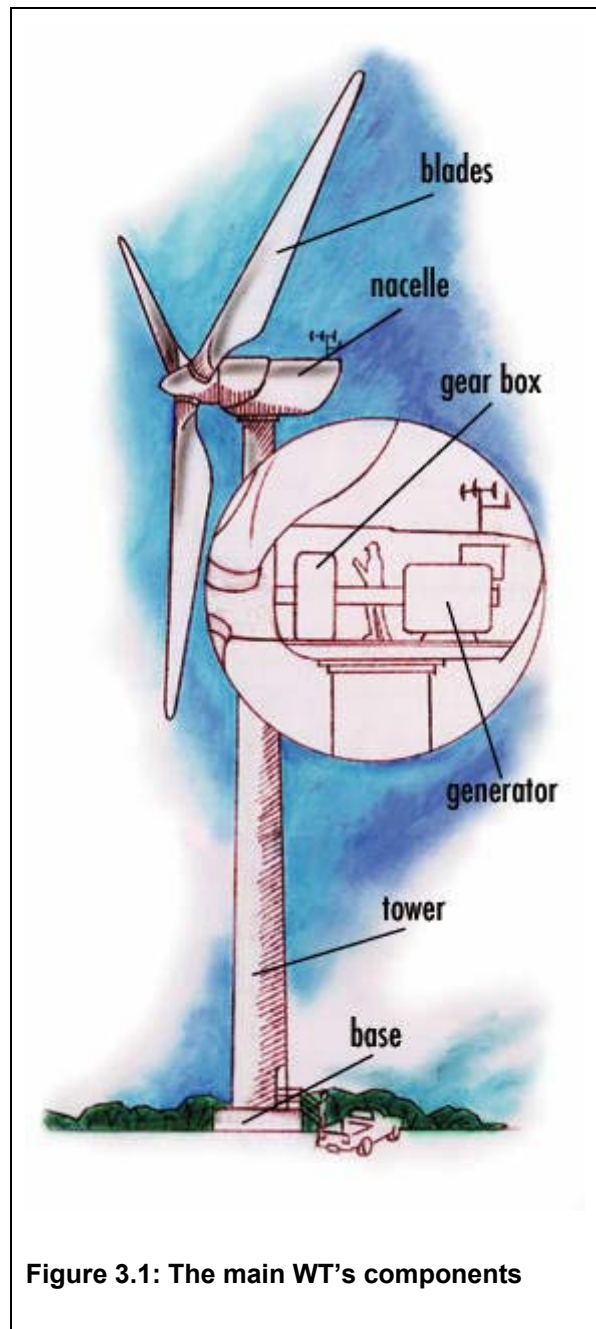


Figure 3.1: The main WT's components

3.2.3 Electrical properties

Early WT followed steam turbine practice with synchronous generators, but many modern WT have induction generators. These draw reactive power from the electricity network, necessitating careful thought to electrical power flows. Other machines, however, are capable of conditioning the electrical output and providing a controllable power factor. This is an asset, especially in rural areas, where it may be undesirable to draw reactive power from the network.

Advances in wind-turbine technology and the results of nearly two decades of research mean that the integration of WT and wind farms into electricity networks generally poses few problems. The characteristics of the network and of the turbines do nevertheless need to be evaluated but there is now a wealth of experience upon which to draw. The fact that Denmark is planning to supply 30 percent of its electricity needs from wind energy is testimony to the fact that its potential is considerable.[7]

3.3 Electrical Machines

Electrical machines can operate as a generator, for instance driven by WT, or as a motor. In the first case electric power is fed into the grid, in the second case the grid supplies power to the machine. Most electrical machines are able to operate in either way. Only rotating machines are considered, which are connected to a three phase AC grid.

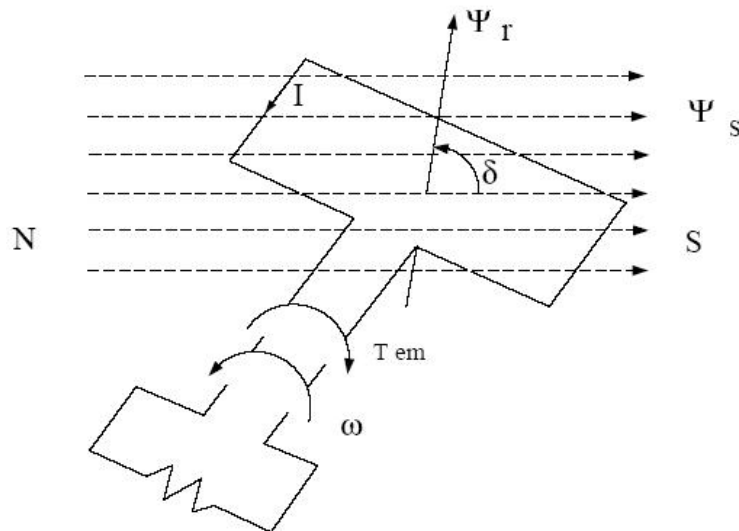


Figure 3.2: A primitive electro-mechanical converter (from Freris)

Electro-mechanical energy conversion is realized through the forces exerted by rotating magnetic fields, in combination with the Electro Motive Force (EMF) induced in conductors in changing magnetic fields.

In [figure 3.2](#) a primitive electro-mechanical machine is shown. A single-turn coil is rotating in a stationary magnetic field of strength Ψ_s . The rotation induces an EMF in the winding and when the winding is closed, this produces a current I . Due to this current a second magnetic field Ψ_r is produced, with its main direction perpendicular to the coil. The interaction between the two magnetic fields results in a clockwise electromagnetic torque aiming to align the two fields. The torque magnitude is proportional to the misalignment angle δ and the magnetic field strengths Ψ_s and Ψ_r :

$$T_{em} = K \cdot \Psi_s \cdot \Psi_r \cdot \sin \delta \quad (3.1)$$

The electromagnetic torque T_{em} opposes the external torque T_m which caused the winding to rotate in the shown direction.

If the coil was stationary and connected to a current source, this would also give a current I and a magnetic field Ψ_r . Again there is a force between the two fields, which tries to align them. The force is constant if the angle between the two fields remains constant. This situation also occurs in 3-phase AC generators and motors. An example is the synchronous machine. [11]

3.3.1 Synchronous machine

Synchronous is a Greek word which means “contemporary”. The reason why it is called synchronous motor, is that the magnet in the centre will rotate at a constant speed which is synchronous with the rotation of the magnetic field. [10]

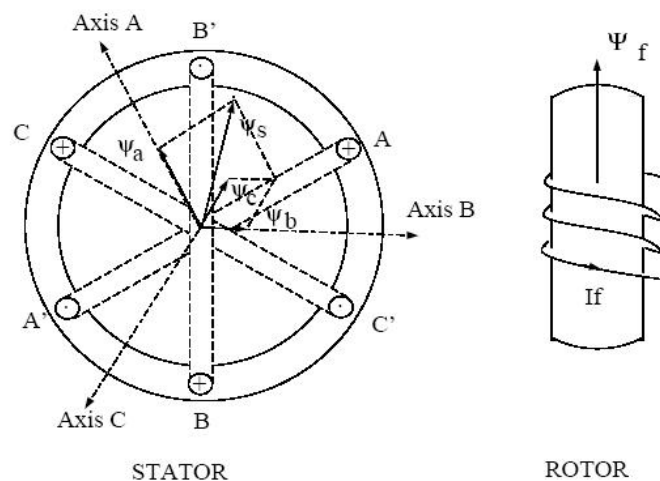


Figure 3.3: Synchronous machine with one pole pair (from Evdokimov)

All 3-phase generators use a rotating magnetic field which is created by three electromagnets around a circle that each one is connected to one of the three phases of the electrical grid. The fluctuation in magnetism corresponds exactly to the fluctuation in voltage of each phase. When one phase is at its peak, the other two have the current running in the opposite direction, at half the voltage. Since the timing of current in the three magnets is one third of a cycle apart, the magnetic field will make one

complete revolution per cycle. The setup with the three electromagnets is called the stator because this part of the motor remains static. The compass needle in the centre is called the rotor, obviously because it rotates.

Figure 3.3 illustrates the main features of the synchronous machine. The stator is a hollow steel cylinder with slots for the wires of a three phase winding system. The windings of phases A, B and C are displaced by 120° . The + and the - indicate the direction of the current: + into the plane of the paper and - out of it. The current in phase “A” produces a flux perpendicular to the winding, according to the cork-screw rule, as indicated by Ψ_a . An alternating current in phase A will give an oscillating flux Ψ_a . Adding the vectors of the individual phase magnetic fields gives the total field Ψ_s caused by stator currents, as indicated by the vector diagram in [figure 3.3](#):

$$\Psi_s = \Psi_a + \Psi_b + \Psi_c \quad (3.2)$$

When the three phases carry alternating currents of angular velocity ω_s , which are 120° out of phase, the oscillating fluxes produced in each phase add up to a rotating magnetic flux Ψ_s of constant magnitude.

The rotor of the synchronous machine consists of magnetic steel and a winding carrying a direct current. Rotation creates a second rotating field of constant magnitude Ψ_f . If the rotor moves with the same angular speed as the stator flux Ψ_s , the angle between the two fields is constant and a constant force between the rotor and the stator results: the electromagnetic torque, as discussed for the primitive machine. Again the angle δ between the stator and rotor flux, called the load angle, determines the magnitude of the produced electromagnetic torque and the produced electrical power. [Figure 3.4](#) shows the position of the stator and rotor fluxes for the two operating modes of the machine:

- the rotor flux Ψ_f leads the stator flux Ψ_s (the load angle is positive) and the machine generates electrical power (generator operation)
- the rotor flux lags the stator flux (the load angle is negative) and the machine consumes electrical power (motor operation).

[Figure 3.5](#) gives an example of the torque as function of the load angle, calculated for a small machine of rated power 15 kVA. The following relation approximately holds:

$$P_{el} = \omega_s \cdot K \cdot \Psi_s \cdot \Psi_f \cdot \sin \delta \quad (3.3)$$

with ω_s the angular speed of the rotating field and K a constant.

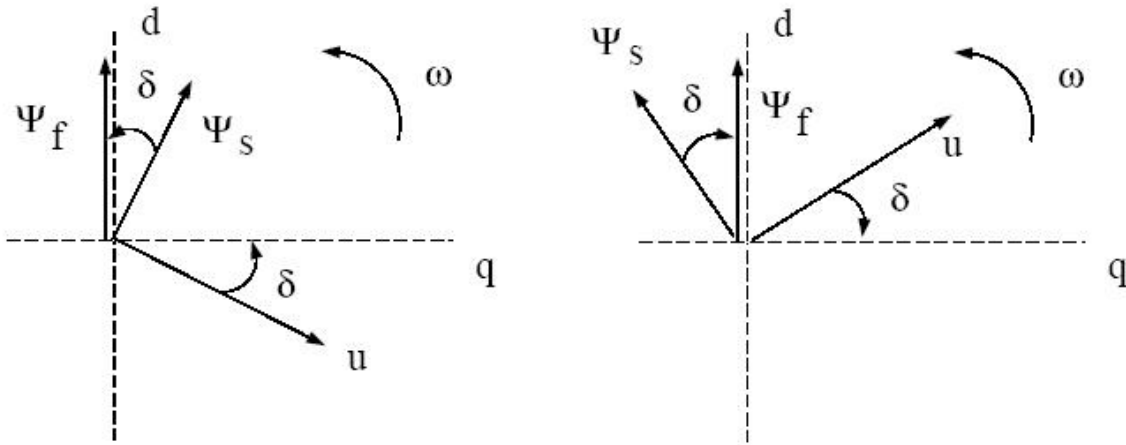


Figure 3.4: Voltage, stator flux and rotor flux of a synchronous machine in d-q ref. frame

The field flux Ψ_f depends on the field current. Variation of the field current at constant grid voltage will influence the power factor of the current delivered to the grid. The power factor $\cos\phi$, with ϕ the phase angle between the current "I" and the voltage "V", is a parameter that gives the fraction of the alternating current which transfers power.

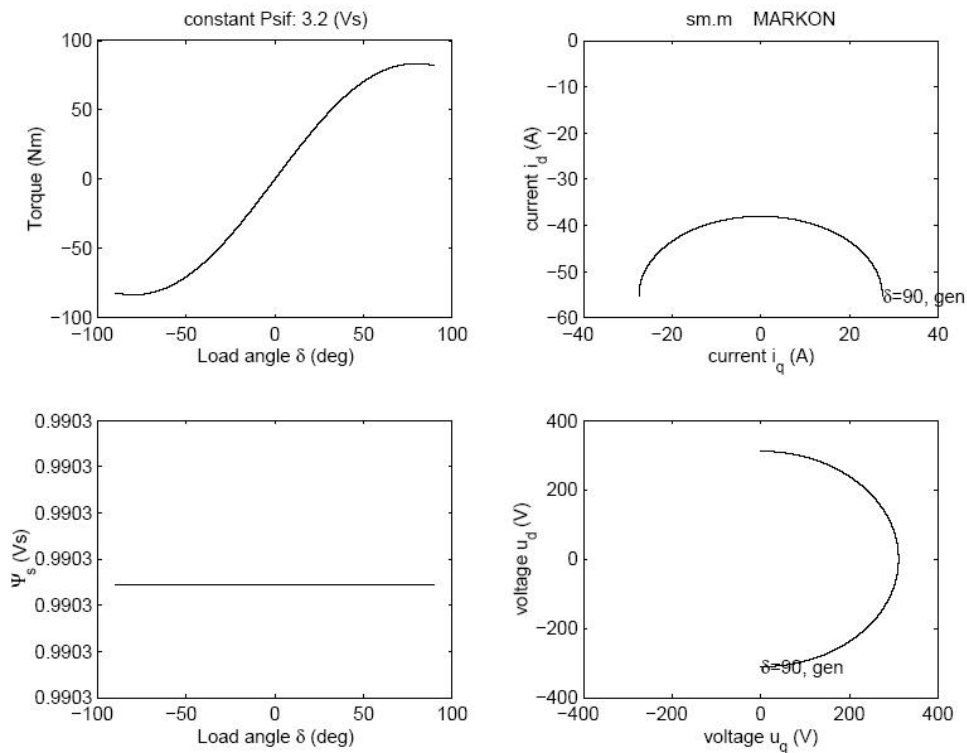


Figure 3.5: Torque as function of the load angle, Ψ_s and Ψ_f are constant

WTs which use synchronous generators normally use electromagnets in the rotor which are fed by direct current from the electrical grid. Since the grid supplies alternating current, they first have to convert alternating current AC to direct current DC before sending it into the coil windings around the

electromagnets in the rotor. The rotor electromagnets are connected to the current by using brushes and slip rings on the axle (shaft) of the generator. [11]

In practice, permanent magnet synchronous generators are not used because permanent magnets tend to become demagnetised by working in the powerful magnetic fields inside a generator. Also the powerful magnets (made of rare earth metals, e.g. Neodymium) are quite expensive. [10]

3.3.2 Asynchronous or Induction machine

Asynchronous machines are the most common electrical machines used worldwide. This is primarily due to their rugged and simple construction, allowing for a low maintenance service life and low cost. One third of the world's electricity is used for running applications where electrical energy should be converted into mechanical energy.

Most WTs in the world use a so-called three phase asynchronous generator generating alternating current. This type of generator is not widely used outside the WT industry, and in small hydropower units. One reason for choosing this type of generator is that it is very reliable, and tends to be comparatively inexpensive. The generator also has some mechanical properties which are useful for WTs, such as generator slip and a certain overload capability. [10]

In figure 3.6 the main features of the induction machine are shown. The structure of the stator is the same as for a synchronous machine, and when connected to a three phase grid, it produces a magnetic flux Ψ_{ss} rotating at synchronous speed, as discussed before.

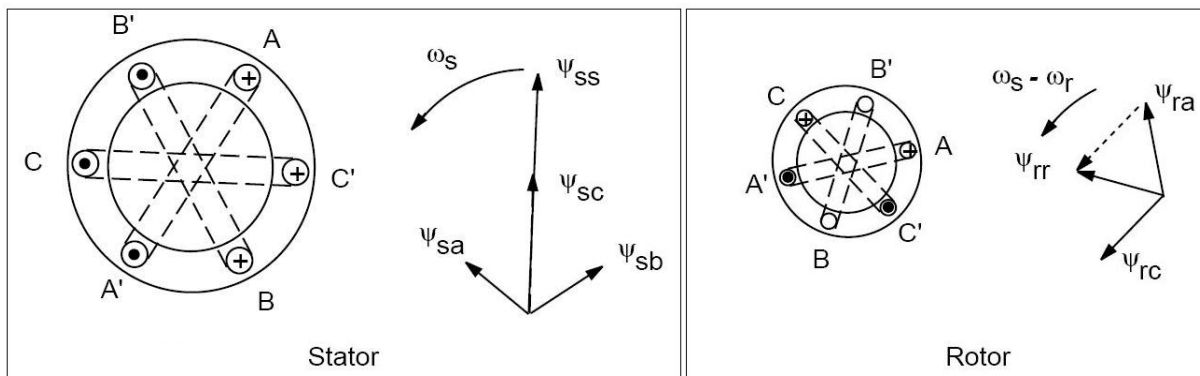


Figure 3.6: Induction machine with one pole pair

The rotor differs from the synchronous machine rotor. It consists of an iron cylinder with slots that carry copper bars, short circuited by rings at the two flat ends of the rotor. This construction is frequently referred to as a squirrel cage. As it was fore mentioned two magnetic fields, one on the stator and one on the rotor, interact. Since there is no external current source connected to the rotor, a current must be produced in a different way, namely by electromagnetic induction. The rotor speed and the speed of the rotating magnetic field must be different. Then there is a movement of the squirrel cage relative to

the stator flux, and the enclosed flux changes. The relative difference between the rotor speed ω_r and the angular speed of the stator flux ω_s is called the slip s :

$$S = \frac{\omega_s - \omega_r}{\omega_s} \quad (3.4)$$

It can be shown that the induced Electro-Magnetic Forces (EMF) and currents in the rotor have the frequency: $\frac{\omega_s - \omega_r}{2\pi}$. When the stator field speed is higher than the rotor speed, the induced flux rotates in the direction of the stator field rotation and the induction machine operates as motor. When the rotor speed is higher than the stator field speed, the induced flux rotates backwards, in the opposite direction of the stator field rotation. The induction machine operates as generator.

Figure 3.6 only shows the fluxes created by stator and rotor currents. The linked fluxes on rotor and stator result from all currents:

$$\begin{aligned} \Psi_s &= L_s i_s + L_m i_r \\ \Psi_r &= L_m i_s + L_r i_r \end{aligned} \quad (3.5)$$

In order to calculate the torque any two space vectors and the angle between them can be chosen. This also implies that there is no unique load angle, but that it depends on the choice of the fluxes.

The stator and rotor fluxes, seen by an observer fixed to the stator, rotate at the same speed, as was the case for a synchronous machine. This is a requirement for constant electromagnetic torque and power. Again the load angle δ between the stator flux and rotor flux (in the synchronously rotating reference frame) is a measure for the electromagnetic torque:

$$T_{em} = -K \cdot \hat{\Psi}_s \cdot \hat{\Psi}_r \cdot \sin \delta \quad (3.6)$$

Figure 3.7 shows the components of the above equation as function of the slip (-30% to 30%).

In figure 3.8 an example of the load angle as a function of the speed of the machine is given. The load angle is equivalent to the load angle of the synchronous machine. Three situations are considered:

- when the speed of the rotor is less than the synchronous speed, the stator flux leads the rotor flux and the machine is operating as a motor (0-3000 rpm). The load angle δ is negative and the electromagnetic torque is positive;
- the load angle is zero at the synchronous speed (3000 rpm): there is no current induced in the rotor, and no electromagnetic torque is produced;
- above the synchronous speed the rotor flux leads the stator flux. The sign of the load angle δ and of the generated torque have changed, the machine is now operating as generator.

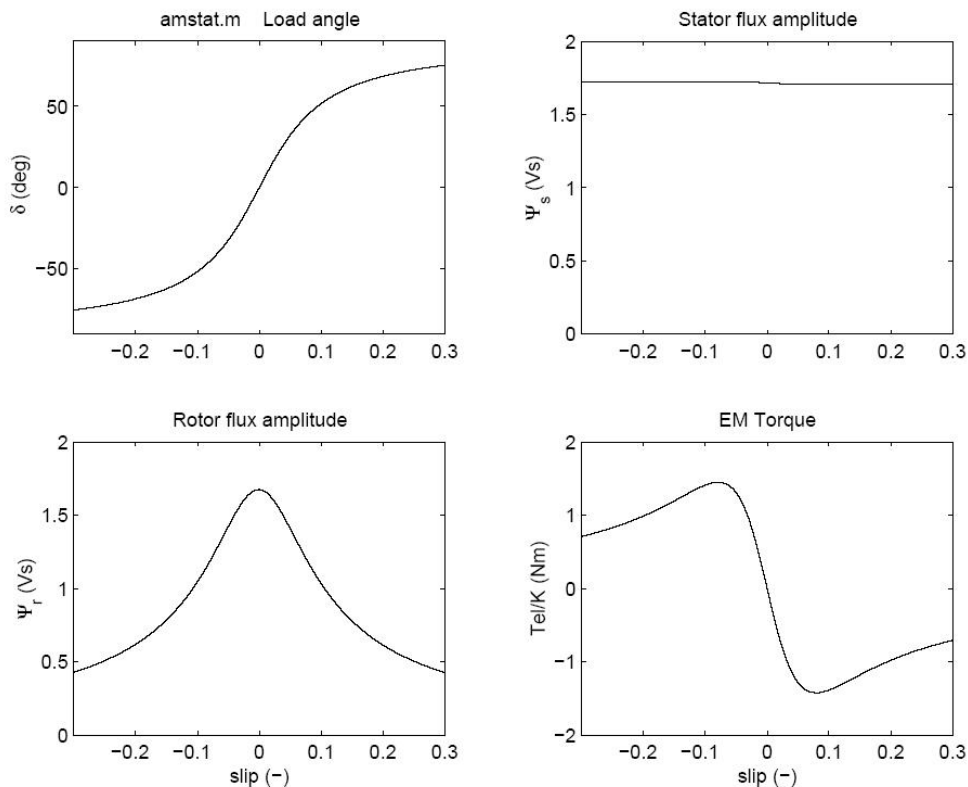


Figure 3.7: Induction machine torque from fluxes and load angle

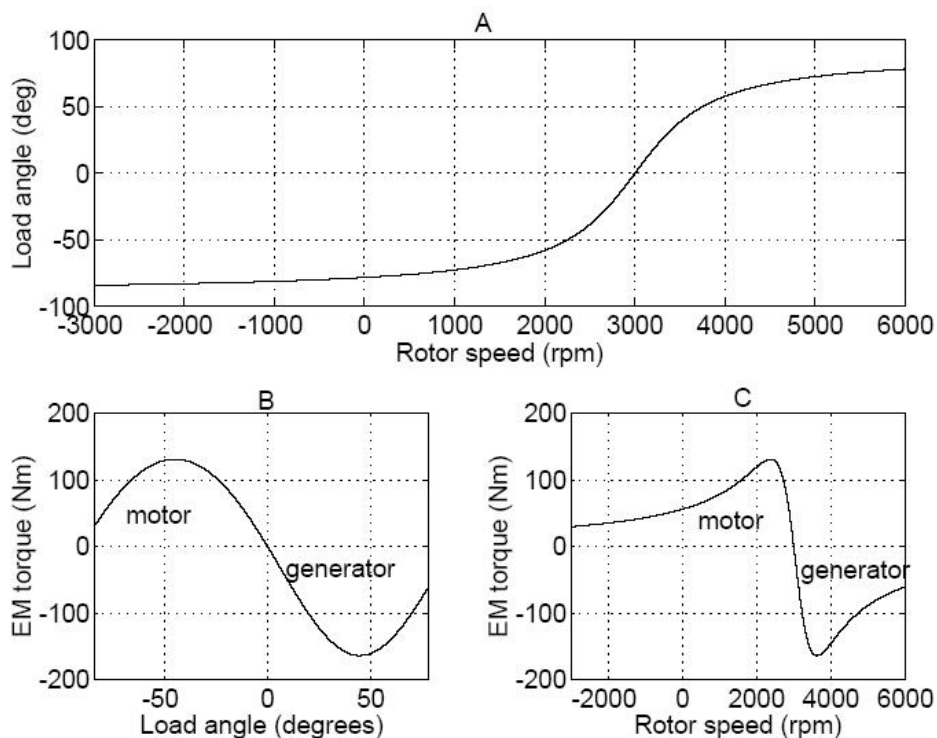


Figure 3.8: Induction machine load angle and torque as function of the rotor speed and load angle

The sign convention for the torque of an induction machine is chosen opposite to that of the synchronous machine due to the different application of the machines. The synchronous machines are mostly used as generators, while the induction machines most frequent application is as motors for driving tools or vehicles. Apart from this minor difference the relation between torque and load angle is similar to that for the synchronous machine. However, as it shown in figure 3.8 B, the maximum torque is reached at a lower value of the load angle. Looking at the torque as a function of the speed in figure 3.8 C, it shows that there is a maximum value at 2370 rpm and a minimum value at 3870 rpm. The maximum and minimum are called stalling torque or pull-out torque. For speeds from 2500 to 3500 the torque-speed curve is practically a linear function of the slip:

$$T_{em} = k \cdot s \quad (3.7)$$

When a synchronous machine or an induction machine is directly connected to a three phase grid, the grid frequency dictates the synchronous speed of the machine:

$$\omega = f_{grid} \frac{2\pi}{p} \quad (3.8)$$

with p the number of pole pairs of the machine. For a synchronous machine this speed is the rotor speed.

For an induction machine there is a small difference between the synchronous speed and the rotor speed, depending on the load, which is proportional to the slip:

$$\omega - r = (1 - s) \cdot \omega \quad (3.9)$$

Between no-load and full load the slip changes from zero to only a few percent, so the speed of an induction machine is also practically constant. From a practical point of view it is a constant speed system.

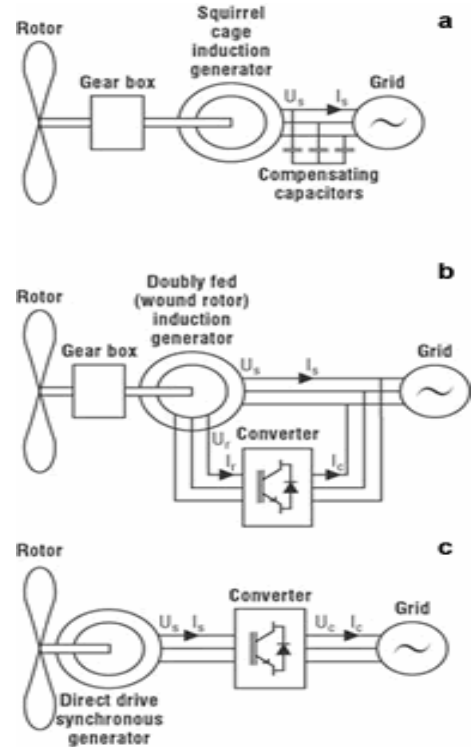
The disadvantages of (directly grid connected) induction machines are twofold: the stator voltage and current are out of phase, i.e. the power factor is less than one and can not be controlled, and the speed can not be controlled either. A major disadvantage of the synchronous machine, relevant to operation in WTs, is that the speed is completely fixed, so all torque variations are instantaneously converted into electric power variations.

Synchronous generators could run as a generator without connection to the public grid. An asynchronous generator is different, because it requires magnetisation of the stator from the grid before it starts operates. An asynchronous generator can be run in a stand alone system only when it is provided with capacitors which supply the necessary magnetisation current. It also requires the existence of some remnant in the rotor iron, i.e. some leftover magnetism when the turbine is started.

Otherwise a battery and power electronics or a small diesel generator is needed to start the system. [10]

3.4 Generator Systems used in Wind Industry

There can be distinguished two main types of WTs, the namely variable speed and constant speed turbines. The constant speed turbines are usually the induction generators that are directly connected to the grid. The main type of these turbines that is used widely is the one with squirrel cage induction generator. In contrast the variable speed turbines need a variety of conversions systems in order to be connected to the main electrical grid. The two most commonly used generator systems of variable WTs are the one with doubly fed induction generator and the one with direct drive wind generation.



3.4.1 Constant speed WT with squirrel cage induction generator (CT)

Between the rotor and the generator, there is a gearbox so that a standard (mostly 1500 rpm) squirrel cage induction generator can be used. A squirrel cage generator always draws reactive power from the grid, which is undesirable, especially in weak networks. The reactive power consumption of squirrel cage generators is therefore nearly always compensated by capacitors. The generator is directly connected to the 50 Hz or 60 Hz utility grid (50 Hz for the Greek Electrical Grid). The generator slip varies with the generated power. Actually the speed variations are very small (just 1-2%), but is accepted that speed remains constant in that variations and it is commonly referred to as a “constant speed” turbine. [13] Mostly, the power is limited using the classic stall principle where when the wind speed increases above the rated wind speed, the power coefficient inherently reduces, so that the power produced by the turbine stays near the rated power. Sometimes active stall is used where negative pitch angles are used to limit the power. In order to increase energy yield and reduce audible noise one pole changing generators with two stator windings with different numbers of pole pairs is used so that the turbine can operate at two constant speeds. Also with the semi variable speed WT, larger speed variations can be achieved by using two generators with electronically variable rotor resistance resulting mechanical loads reduction. [12]

3.4.2 Variable speed WT with doubly-fed (wound-rotor) induction generator (VTDI)

In a variable speed turbine with doubly fed induction generator DFIG, the converter feeds the rotor winding, while the stator winding is connected directly to the grid. The power converter provides the

DFIG the ability of reactive power control. It decouples active and reactive power control by independent control of the rotor excitation current. Therefore, in the case of a weak grid, where the grid voltage may fluctuate, it is advantageous to use a DFIG which can produce or absorb an amount of reactive power to or from the grid, with the purpose of voltage control. By means of the bi-directional converter in the rotor circuit, the DFIG is able to work as a generator in both sub-synchronous (positive slip $s > 0$) and over-synchronous (negative slip $s < 0$) operating area. [13][15]

In contrast to a conventional, singly-fed induction generator, the electrical power of a doubly-fed induction machine is independent from the speed. Therefore in a variable speed wind generator the mechanical speed is adjusted to the wind speed and hence the turbine operates at the aerodynamically optimal point for a certain wind speed range. [14] A speed range from roughly 60% to 110 % of the rated speed is sufficient for a good energy yield, that is achieved by using the variable speed capability to keep the tip speed ratio λ at the value resulting in optimal energy capture. If the gearbox ratio is chosen such that the synchronous speed of the generator just falls in the middle of the speed range (in this case at 85% of rated speed), then the lowest converter power rating is obtained. A converter rating of roughly 35 % of the rated turbine power is sufficient, particularly when star-delta switching at the rotor winding is applied. At wind speeds above the rated wind speed, the power is reduced by pitching the blades.[12]

3.4.3 Variable speed WTs with direct-drive synchronous generator (VTDD)

In variable speed WTs with direct-drive synchronous generator, the generator and the grid are completely decoupled by means of a power electronic converter, also allowing variable speed operation. [13] In these WTs the generator rotates at very low speed, typically 10 to 25 rpm for turbines in the MW range, thus gearbox is unnecessary. Standard generators can therefore not be used and generators have to be developed specifically for this application. These generators are very large because they have to produce a huge torque. A converter converts the varying generator frequency to the constant grid frequency. At wind speeds above the rated wind speed, the power is again reduced by pitching the blades. [12]

3.5 Transmission to the Grid

Most WTs run at almost constant speed with direct grid connection. The speed of the generator and the rotor is given by the grid. Therefore the rotor cannot always work with the optimal aerodynamic efficiency unless the rotor blade can be mechanically controlled. Another way for connecting WT to the grid is a generator with a pole switching system. This allows for operation under reduced speed and a better adaptation of the current on the rotor during low wind speeds.

The main WTs (WT) components for their connection to the grid are the transformer and the substation with the circuit breaker and the electricity meter inside it. Because of the high losses in low voltage lines, each of the turbines has its own transformer from the voltage level of the WT (400 or 690 V) to

the medium voltage line. The transformer is located beside the WT to avoid long low-voltage cables. However it is possible to connect small WT directly to the low voltage line of the grid without a transformer or, to connect to one transformer some of the small WT in a wind farm.

For large wind farms a separate substation for transformation from the medium voltage system to the high voltage system is necessary. At the point of common coupling (PCC) between the single WT or the wind farm and the grid a circuit breaker for the disconnection of the whole wind farm or of the WT must exist. In general this circuit breaker is located at the medium voltage system inside a substation, where also the electricity meter for the settlement purposes is installed. This usually has its own voltage and current transformers. The medium voltage connection to the grid can be performed as a radial feeder or as a ring feeder, depending on the individual conditions of the existing supply system.

3.6 The Electrical grid

The electricity grid consists of three parts, the interconnection network, the transmission network and the distribution network. For the reliability and the normal operation of the network two important aspects of grid control, the control of frequency and voltage (amplitude), have to be taken into consideration.

The interconnection network links the large production units and is primarily intended to come into action in case of station failures. It operates at the highest voltage levels: 380 and 220kV and the connections are made by overhead lines.

The transmission network is located between production units and the distribution network and operates at voltages of 150kV and 50kV. It connects to the distribution network at 10 kV level. The apparent power of transformer unit typically is 30-100MVA at 150/10kV and 20-60MVA at 50/10kV units. At the transmission network level voltages, power and reactive power distribution are controlled. The connections can be made by overhead lines or cables. Transport of AC power over cables at high voltages is less practical though due to the reactive power demand of the cables, caused by the capacitive nature of the isolation.

The distribution network connects the consumers, also referred to as loads, to the transmission network. Common distribution network voltage levels are 10.5 kV and 380 (400) V. [11]

3.6.1 Frequency control

The grid frequency is the result of the combined action of all the power controllers on the grid, mainly influenced by the large power stations. The frequency is the same in all the electrical grids worldwide. The frequency is determined by the equilibrium between the power demand and the power produced minus the losses. A mismatch in power will change the frequency:

$$\omega \cdot J \frac{d}{dt} \omega = P_{produced} - P_{demand} - P_{losses} \quad (3.10)$$

J is the total moment of inertia of all rotating equipment on the grid.

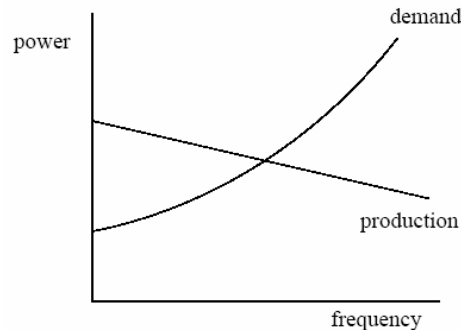


Figure 3.9: Steady state frequency condition

As it is shown in Figure 3.9, both the load power and the production power depend on the frequency. A decrease in frequency will reduce the power demand P_{dem} , due to the power-speed dependency of mechanical tools, pumps, fans and compressors. Resistive loads do not depend on the frequency however inductive and capacitive loads do without consuming active power. The power production P_{prod} also depends on the frequency, this dependency is intentionally implemented in the control for stability reasons. Controller settings determine how much power a station will deliver compared to the other power stations. For steady state conditions the produced and consumed reactive powers have to be equal and both depend on the frequency and voltage and are controlled through the voltage.

Four levels of frequency control, also referred to as frequency-power control, are distinguished:

3.6.2 Fast frequency control on the level of an individual station: the droop line;

The primary frequency control intends to reduce the effect of load changes on the frequency at the expense of a small frequency offset. The offset is the result of the characteristics of the individual controllers: a decrease in frequency (called droop) gives an increase in produced power (figure 3.9).

The primary control acts fast: within 2 to 3 seconds after a disturbance (mismatch of the power balance). The time delay is determined by the controller settings and the delays of the fuel injection system of the producer. Droop is incorporated to make the sharing of power over a number of units more easy. The slopes of the droop lines need not be equal to have an acceptable distribution of power over different units, see for example figure 14.

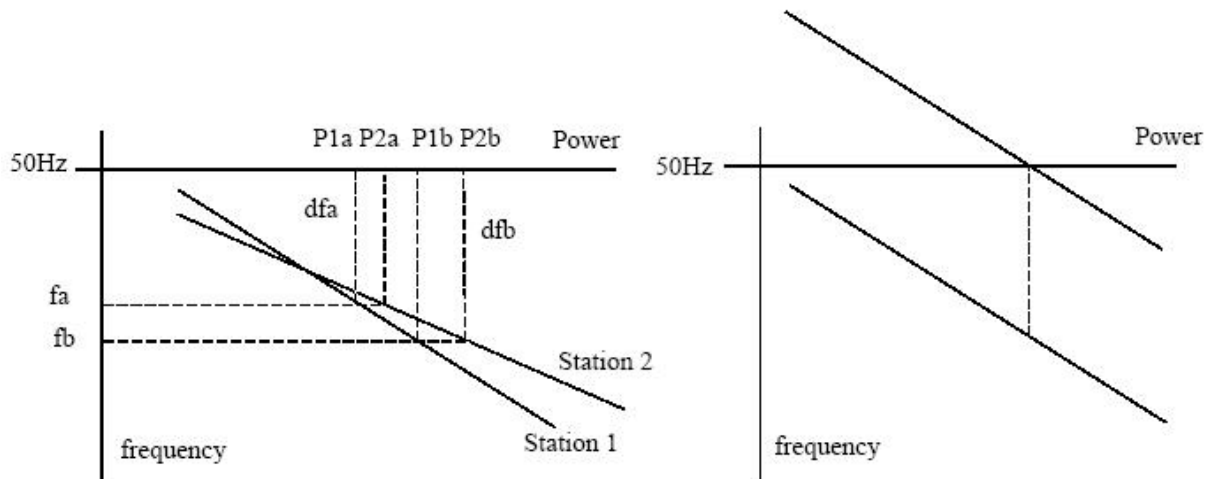


Figure 3.10: Load sharing and step of load for 2 units, secondary correction station 1

3.6.3 Integral control to reset the frequency to 50 Hz after an offset has occurred;

On a longer time scale, minutes to tens of minutes, the droop lines of power stations are shifted vertically, at constant power of the production unit, to regain the frequency of 50 Hz (figure 3.10).

The shifting of the droop-lines can also intentionally change the power distribution over the units, either to locate power production closer to the demand and thereby reducing the losses, or to maintain enough reserved capacity on a specific production station.

3.6.4 Production switching

The third level of control ensures that there is an adequate amount of "spinning reserve" on a grid. Aspects such as start up times for hot and cold starts and the expectations about the power demand and independent production play an important role here. Additionally this level of control aims at an economical optimization of the production system.

3.6.5 Finally in case of emergency: load shedding, switching of grid sections off the grid.

Under emergency conditions, viz. overload or loss of production capacity due to technical failures which result in a frequency drop, sections of the grid are switched off to protect production equipment.

3.7 Voltage control

Dynamic voltage control takes place at the interconnection level and the transmission level. The voltage is a local variable, meaning that its value is location dependent. Power normally flows from the interconnection level to the transmission and distribution level.

The tasks of voltage control at the interconnection network level are:

1. to maintain a constant voltage at the power stations;
2. to maintain a stable distribution of reactive power over all power stations;
3. to prevent high voltages in case of loss of load;
4. to increase the grid stability at short circuit situations by increasing the excitation and thereby the synchronism of the grid (meanwhile fuses at the shortcircuit will be destroyed).

The primary voltage control of the grid is executed by the set of voltage controllers of all the synchronous generators of the power stations. An automatic voltage regulator AVR measures the voltage and adjusts the field current on the rotor of the synchronous machine through an exciter. An increase in field current will increase the stator voltage at constant stator current and phase angle (the angle between the fundamental sinusoidal component of the voltage and current). At constant stator voltage, an increase in field current will increase the reactive power to the grid, i.e. the share of reactive power of this particular generator.

The current and phase angle will increase. Similar to the primary frequency control, the voltage control is given droop to obtain a well defined a steady state condition and reactive power distribution over different stations.

Types of voltage controllers are the electronic regulator and the compound regulator. The electronic regulator compares the measured voltage to a given setpoint and a PID controller adjusts the field current of the synchronous machine. In a compound regulator, also referred to as the magnetic amplifier regulator, the field is determined by two contributions, one proportional to the rectified voltage and the other proportional to the amplitude of the out-of-phase current. Sometimes a combination of both types is used.

The voltage at a given location on the distribution grid depends on the grid parameters (reactance, capacitance and to a lesser degree resistance) and current. The distribution network is not controlled, it is based on a passive design philosophy and assumes power flow from the MV side to the LV side. Reverse power flow could cause control problems. Power production at the low voltage side will also have consequences for the safety of the system. Unlike conventional power plants, most WTs feed into the distribution network at 10.5 kV level.

3.8 Impact of Connecting Wind Turbines to the Distribution Network

Production and consumption of electric power puts a demand on the transport capacity of the electricity grid and causes local deviations in voltage level and wave form. Voltage deviations are undesirable but inherent to the application of electricity. In this respect, electricity production by means of WTs is no exception. On the contrary, the effect of wind power on the grid is likely to be more severe, due to the

highly variable character of wind power. With increasing turbine size and number, this is of increasing importance and is currently receiving more attention from developers as well as manufacturers.

The effect of an electricity producer on the grid is summarized by the term Power Quality, which includes a number of aspects on different time scales:

- flicker;
- voltage and current harmonics;
- reactive power and power factor;
- switching transients;
- WT power variability.

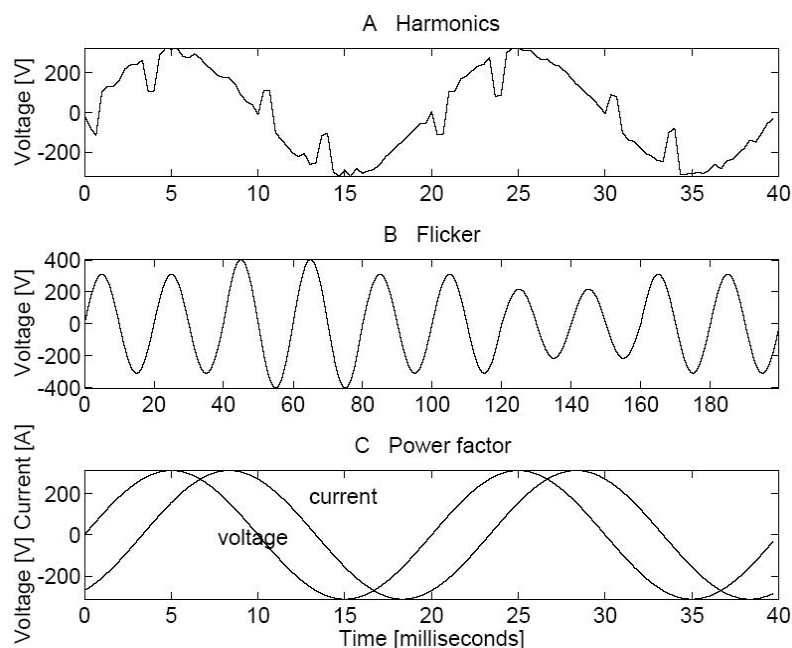


Figure 3.11: Harmonics, flicker and reactive power the basic effects to Grid Power Quality

3.8.1 Voltage flicker

Voltage variations caused by fluctuating loads and/or production is the most common cause of complaints over the voltage quality. [7] These fluctuations can be very annoying for local electricity users, as they cause light bulbs to 'flicker' instead of producing a steady light. [16] Figure 3.10 gives the level of voltage changes as function of the frequency of the changes that is just visible. This curve, called the flicker curve, is empirically determined by subjecting persons to light from a 60W lamp fed by a voltage with rectangular variations of different intensity and frequency. [11]

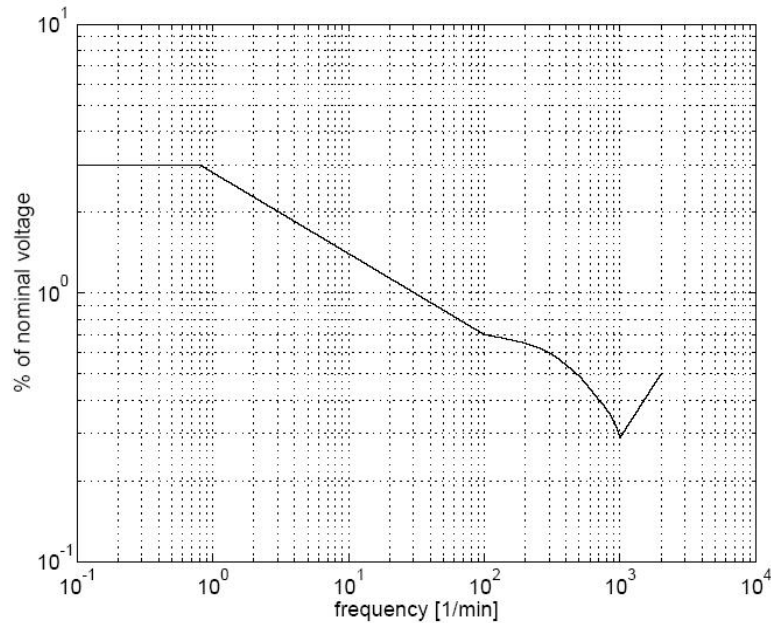


Figure 3.12: The level of voltage variation visible by the human eye

The issue of voltage flicker is often raised in connection with wind energy schemes. [16] Flicker is caused to changes in power output of WTs and switching operations. Power fluctuations in the range relevant for flicker (0.5-35Hz) are mainly caused by: [11]:

- • wind turbulence;
- • wind shear;
- • tower shadow;
- • yaw misalignment.

For frequencies above 1Hz the blade passing frequency and its multiples dominate the power spectrum and therefore are critical in the assessment of flicker. In constant speed systems, the variations in aerodynamic power are almost instantaneously transmitted to variations in electric power.

In variable speed systems the relation between the instantaneous wind and electric power is less direct. To deliver more electric power, the system first has to increase in speed, which damps the power variations considerably. Electric power variations from the tower shadow effect are negligible in variable speed systems, which eliminate an important source of flicker. This does not necessarily mean that variable speed systems cause less flicker than constant speed ones. Flicker can also be caused by fast oscillations in the active and or reactive power resulting from the control system. Especially oscillations near the critical frequency of 8.8Hz have to be avoided. [11]

As a result, many people in the electricity industry still associate wind energy schemes with voltage flicker. In fact, the vast majority of wind energy schemes have not caused problems with flicker. A common example for voltage flicker is when one or two fixed-speed WTs are connected to a weak rural

network with low fault levels. In such systems the power output of WTs varies rapidly due to wind turbulence and speed and this can result in voltage fluctuations. When there are more WTs is less likely to cause flicker, as the variations in the power outputs of the different turbines tend to normalise it. In contrast a system with normal fault levels is affected from flicker as a result of the connection of one or two WTs. The potential to cause voltage flicker is peculiar to fixed-speed WTs, and is due to the electrical characteristics of induction generators. Variable-speed WTs are less likely to cause flicker. Gensets and other types of generators operating at constant power output do not cause flicker. [16]

3.8.2 Harmonics

Harmonics are a phenomenon associated with the distortion of the fundamental sinewave of the grid voltages, which is purely sinusoidal in the ideal situation. Ideally, the voltage at any point in a distribution system should have a perfectly sinusoidal, 50Hz waveform. [16] However, this is rarely achieved in practice as harmonic disturbances are produced by many types of electrical equipment. Depending on their harmonic order they may cause different types of damage to different types of electrical equipment.[7]

Rectified power supplies, compact fluorescent lights variable speed motor drives and other switched loads introduce harmonic components, which distort the voltage waveform. Harmonics can also be introduced by inverter-coupled embedded generation schemes using technologies such as fuel cells, photovoltaics and machine-based generators that are connected to the network through a power electronic converter, e.g. some variable speed WTs. The limits on the level of harmonic currents that generators and loads are permitted to inject into distribution networks are usually specified in special recommendations. [16]

All harmonics causes increased currents and possible destructive overheating in capacitors as the impedance of a capacitor goes down in proportion to the increase in frequency. As harmonics with order 3 and odd higher multiples of 3 are in phase in a three phase balanced network, they cannot cancel out between the phases and cause circulating currents in the delta windings of transformers, again with possible overheating as the result. The higher harmonics may further give rise to increased noise in analogue telephone circuits. Highly distorting loads are older unfiltered frequency converters based on thyristor technology and similar types of equipment. It is characteristic for this type that it switches one time in each half period and it may generate large amounts of the lower harmonic orders. [7]

3.8.3 Voltage Variation

Power flows along the feeder towards the load will create a voltage drop between the substation and the local load. When the presence of a distributed generator causes the power flow to reverse there will be a local voltage rise at the location of the generator and load. At transmission level, reactive impedance (X) is much greater than resistive impedance (R), and the voltage excursion is brought about by reactive power flow. However, in the distribution network where R can be comparable with or

exceed X , the voltage rise is influenced by both active and reactive power flows. Hence, the relatively high line resistance at the edges of distribution networks can restrict active power export from a DG due to the excessive voltage variations.

3.8.4 Reverse Power Flows

Since the 1950s, the design and operation of most electricity distribution networks in the UK has been based on a key assumption - which power always flows from high voltage systems to lower voltage systems. However, this 'rule' is being undermined by the recent development of renewable electricity generation, combined heat and power, and waste-to energy schemes. In some cases, the connection schemes for these embedded generators result in reverse power flows in distribution transformers. In these cases, the generator exports more than enough power to supply all the loads on the system to which it is connected. The surplus power is transferred back through the distribution transformer, and is fed into a higher voltage system. The possibility of reverse power flows in transformers can sometimes present a problem with the operation of automatically controlled tap changers which are fitted to the transformers to provide voltage regulation on the low voltage side of the transformer. The critical issue is the type of voltage control scheme which is used to operate these tap changers. Most of the commonly-used voltage control schemes operate perfectly well with reverse power flows, but there are problems with certain schemes.[18]

3.8.5 Fault Levels

In the event of a short circuit fault on the network all generators will contribute to the fault currents flowing. As such, the switchgear in the DNO network and that of the DG must be rated to withstand the effects of the combined network and DG fault currents. As the point of connection becomes more remote from the transmission network the intervening impedance increases, and the network fault contribution falls. Where connection of the DG would increase fault levels beyond the rating of existing DNO switchgear, it must be replaced. [17]

Fault levels also affected by the type of the machines that are used from the developers. There are two basic categories of Asynchronous (Induction) Machines (AM), the Squirrel Cage Induction Machines (SCIM), which is categorized in SCIM of Constant Speed and SCIM of Variable Speed and the Wound Rotor Asynchronous Machines (Doubly Fed Induction Machines). In the two last types of machines there is a converter between the machine and load, which can automatically stop the production of electric power depending the fault level in contrast with the SCIM with Constant Speed where there is no converter in order to control the fault level.[18]

3.8.6 Thermal Limits

Each element of the existing distribution infrastructure- lines, cables, transformers and so on- has a limited current-carrying capacity. If it is loaded above this limit for an extended period of time. it will overheat. For this reason, the current-carrying capacity of the device is referred to as its thermal rating.

Loading a device beyond its thermal rating may lead to permanent damage, or even to a dangerous event such as a fire or explosion. Connecting a generator to a distribution system has the effect of changing the current flows in the system. With a suitable choice of site and connection scheme, connecting a generator can have an entirely beneficial effect. With no increases in current levels and some significant reductions. Although this is clearly a desirable outcome, it is not always possible or cost-effective. In many cases, the most 'convenient' connection design results in higher current levels in parts of the system. These new current levels may exceed the thermal ratings of existing cables or lines. If so, the developer may opt to pay for these existing assets to be reinforced or up-rated. However, if the cost of this reinforcement is very high, it may be worth considering an alternative connection arrangement.. possibly at a higher voltage level. [16][18]

3.8.7 Transient Stability

The ability of DG to remain connected to the network during transient conditions caused by load changes or network reconfiguration depends on the topography of the network, the nature of the perturbation and the characteristics of the DG. During the transient conditions network stability is reduced. Some DGs can assist in restoring stable conditions and hence it is mutually beneficial for the DNO and developer that such plant should remain connected. Those that cannot may be disconnected. In terms of overall system stability, current levels of DG penetration are not a concern but this may alter if, as the capacity of renewable energy DG increases it displaces high-energy thermal plant that currently ensures stability. [17][18]

3.8.8 Protection

Prior to the installation of a DG, operation of the distribution network is made safe and reliable by the provision and coordination of protection devices at energy sources, switching points or loads. This ensures the integrity and security of supply to consumers based on the traditional operation of the network. The protection schemes were designed and co-ordinated largely for uni-directional flow and their use with bi-directional power flows may lead to unstable or spurious operation. While settings may be adjusted so that protection remains effective during DG operation, it must also be effective when the DG is shut down. The achievement of such a balance may leave the network less closely protected than before, and this must be carefully evaluated. [18]

4 POWER FLOW ANALYSIS

In order to study the possible problems that wind farms could cause to the electric grid in Crete the resulting power flows were analysed. This chapter deals with the steady-state analysis of an interconnected power system during normal operation. The system is assumed to be operating under balanced conditions and is represented by a single-phase network. The network contains nodes and branches with impedances specified in per unit on a common MVA base. [27]

Network equations can be formulated systematically in a variety of forms. However, the most commonly used method is the node-voltage method, which is the most suitable form for many power system analyses. The formulation of the network equations in the nodal admittance form results in complex linear simultaneous algebraic equations in terms of node currents. When node currents are specified, the set of linear equations can be solved for the node voltages. However, in a power system, powers are known rather than currents. Thus, the resulting equations in terms of power, known as the power flow equation, become nonlinear and must be solved by iterative techniques. Power flow studies, commonly referred to as load flow, are the backbone of power system analysis and design. They are necessary for planning, operation, economic scheduling and exchange of power between utilities. In addition, power flow analysis is required for many other analyses such as transient stability and contingency studies.

In order to analyse the power flow the bus admittance matrix of the node-voltage equation is formulated, while a MATLAB function named `ybus` is developed for the systematic formation of the bus admittance matrix. Power flow problems usually are solved by the use of Gauss-Seidel and Newton-Raphson methods that are two commonly used iterative techniques and are used for the solution of nonlinear algebraic equations. For the solution of power flow problems by Gauss-Seidel, Newton-Raphson and the fast decoupled power flow methods, three programs (`lfgauss`, `lfnewton`, and `decouple` respectively) were developed by Hadi Saadat in the Milwaukee School of Engineer.

MATLAB is a high-performance language for technical computing. It integrates computation, visualization, and programming in an easy-to-use environment where problems and solutions are expressed in familiar mathematical notation. The name MATLAB stands for matrix laboratory. MATLAB is an interactive system whose basic data element is an array that does not require dimensioning. This allows the user to solve technical computing problems, especially those with matrix and vector formulations. MATLAB features a family of add-on application-specific solutions called toolboxes. Very important to most users of MATLAB, toolboxes allow the user to learn and apply specialized technology. Toolboxes are comprehensive collections of MATLAB functions (M-files) that extend the MATLAB environment to solve particular classes of problems. Areas in which toolboxes are available include signal processing, control systems, neural networks, fuzzy logic, wavelets, simulation, and many others.

4.1 Bus Admittance Matrix

In Figure 4.1 a simple power system is shown where impedances are expressed in per unit on a common MVA base and resistances are neglected as in most real transmission systems a line's resistance is negligible compared to its reactance, which allows such simplification. Since the nodal solution is based upon Kirchhoff's current law, impedances are converted to admittance, i.e.,

$$y_{ij} = \frac{1}{z_{ij}} = \frac{1}{r_{ij} + jx_{ij}} \quad (4.1)$$

Where y =admittance, z =impedance, r =resistance and x =reactance between buses 'i' and 'j', as declared by subscripts 'i' and 'j' respectively. Therefore y_{12} is the admittance from bus 1 to bus 2, etc. From these values, it is set $Y_{ij}=Y_{ji}=-y_{ij}$, for $i \neq j$. Additionally, we set $Y_{ii}=y_{i0}+y_{i1}+\dots+y_{ij}$, for $i \neq j$.

In Figure 4.2 the circuit has been redrawn in terms of admittances and transformation to current sources. Node 0 (which is normally earth) is taken as reference. Applying Kirchhoff's current law to the independent nodes 1 through 4 results in

$$\begin{aligned} I_1 &= y_{10}V_1 + y_{12}(V_1 - V_2) + y_{13}(V_1 - V_3) \\ I_2 &= y_{20}V_2 + y_{12}(V_2 - V_1) + y_{23}(V_2 - V_3) \\ 0 &= y_{23}(V_3 - V_2) + y_{13}(V_3 - V_1) + y_{34}(V_3 - V_4) \\ 0 &= y_{34}(V_4 - V_3) \end{aligned} \quad (4.2)$$

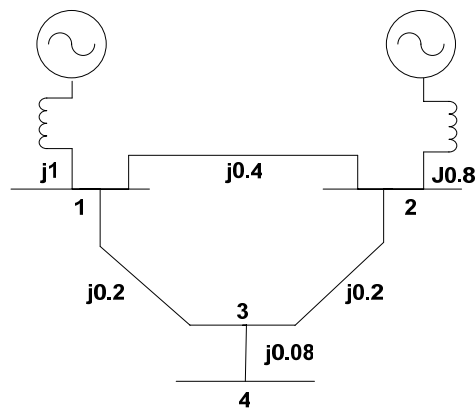


Figure 4.1: The impedance diagram of a simple system

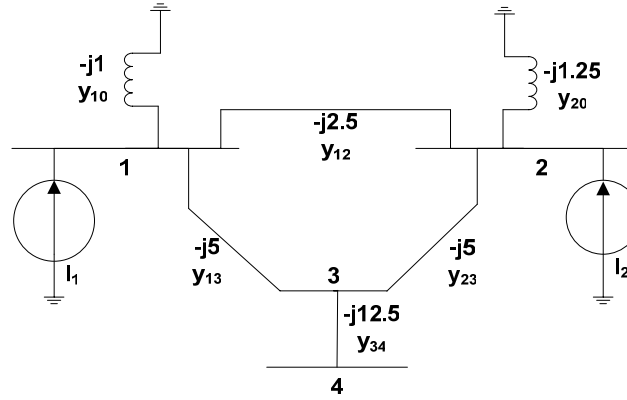


Figure 4.2: The admittance diagram for system in Figure 4.1

Rearranging these equation yields

$$\begin{aligned}
 I_1 &= (y_{10} + y_{12} + y_{13})V_1 - y_{12}V_2 - y_{13}V_3 \\
 I_2 &= -y_{12}V_1 + (y_{20} + y_{12} + y_{23})V_2 - y_{23}V_3 \\
 0 &= -y_{13}V_1 - y_{23}V_2 + (y_{13} + y_{23} + y_{34})V_3 - y_{34}V_4 \\
 0 &= -y_{34}V_3 + y_{34}V_4
 \end{aligned} \tag{4.3}$$

The total admittance at each node is defined as the sum of the admittances connected to that node i.e. for Y_{ii} , where $i = 1-n$, where n is the total number of nodes, and the off-diagonal elements Y_{ij} are given by:

$$\begin{aligned}
 Y_{11} &= y_{10} + y_{12} + y_{13} \\
 Y_{22} &= y_{20} + y_{21} + y_{23} \\
 Y_{33} &= y_{31} + y_{32} + y_{34} \\
 Y_{44} &= y_{34} \\
 Y_{21} &= Y_{12} = -y_{12} \\
 Y_{31} &= Y_{13} = -y_{13} \\
 Y_{23} &= Y_{32} = -y_{23} \\
 Y_{34} &= Y_{43} = -y_{34}
 \end{aligned} \tag{4.4}$$

The node equation reduces to

$$\begin{aligned}
 I_1 &= Y_{11}V_1 + Y_{12}V_2 + Y_{13}V_3 + Y_{14}V_4 \\
 I_2 &= Y_{21}V_1 + Y_{22}V_2 + Y_{23}V_3 + Y_{24}V_4 \\
 I_3 &= Y_{31}V_1 + Y_{32}V_2 + Y_{33}V_3 + Y_{34}V_4 \\
 I_4 &= Y_{41}V_1 + Y_{42}V_2 + Y_{43}V_3 + Y_{44}V_4
 \end{aligned} \tag{4.5}$$

Because of the connection between Bus 1 and 4, $Y_{14} = Y_{41} = 0$ and similarly $Y_{24} = Y_{42} = 0$. Extending the above relation to an n bus system, the node voltage equation in matrix form is

$$\begin{bmatrix} I_1 \\ I_2 \\ \vdots \\ I_i \\ \vdots \\ I_n \end{bmatrix} = \begin{bmatrix} Y_{11} & Y_{12} & \dots & Y_{1i} & \dots & Y_{1n} \\ Y_{21} & Y_{22} & \dots & Y_{2i} & \dots & Y_{2n} \\ \vdots & \vdots & & \vdots & & \vdots \\ Y_{i1} & Y_{i2} & \dots & Y_{ii} & \dots & Y_{in} \\ \vdots & \vdots & & \vdots & & \vdots \\ Y_{n1} & Y_{n2} & \dots & Y_{ni} & \dots & Y_{nn} \end{bmatrix} \begin{bmatrix} V_1 \\ V_2 \\ \vdots \\ V_i \\ \vdots \\ V_n \end{bmatrix} \quad (4.6)$$

$$\text{Or } I_{bus} = Y_{bus} V_{bus} \quad (4.7)$$

Where I_{bus} is the vector of the injected bus currents, such as external current sources. The current is positive when flowing towards the bus and negative when flowing away from the bus. V_{bus} is the vector of bus voltages measured from the reference node. Y_{bus} is the bus admittance matrix. The diagonal element of each node is the self-admittance or driving point admittance and is the sum of admittances connected to each node.

$$Y_{ii} = \sum_{j=0}^n y_{ij} \quad (4.8)$$

The off diagonal element is the mutual admittance or transfer admittance and it is equal to the negative of the admittance between the nodes.

$$Y_{ij} = Y_{ji} = -y_{ij} \quad (4.9)$$

When the bus currents are known, the equation 4.7 can be solved for the n bus voltages.

$$V_{bus} = Y_{bus}^{-1} I_{bus} \quad (4.10)$$

The inverse of the bus admittance matrix is known as the bus impedance matrix Z_{bus} . The admittance matrix obtained with one of the buses as reference is non-singular. Otherwise the nodal matrix is singular.*

Inspection of the bus admittance matrix reveals that the matrix is symmetric along the leading diagonal, and have only the upper triangular nodal admittances needed to be found. In a typical power system network, each bus is connected to only a few nearby buses. Consequently, many off-diagonal elements are zero. Such a matrix is called sparse, and efficient numerical techniques can be applied to compute its inverse. By means of an appropriately ordered triangular decomposition, the inverse of a sparse matrix can be expressed as a product of sparse matrix factors, thereby giving an advantage in computational speed, storage and reduction of round-off errors. However, Z_{bus} , which is required for

* Singular is a square matrix whose determination is zero and has no inverse.

short-circuit analysis, can be obtained directly by the method of building algorithm without the need for matrix inversion.

A function called $Y = ybus(zdata)$ was written [27] for the formation of the bus admittance matrix. $zdata$ is the line data input and contains four columns. The first two columns are the line bus numbers and the remaining columns contain the line resistance and reactance in per unit. The function returns the bus admittance matrix. The algorithm for the bus admittance program is very simple and basic to power system programming. Y is then initialized to zero. In the first loop, the line data is searched, and the off-diagonal elements are entered. Finally, in a nested loop, line data is searched to find the elements connected to a bus, and the diagonal elements are thus formed.

The $Y = ybus(zdata)$ function is used to obtain the bus admittance matrix and then the bus impedance matrix is estimated by inversion. The solution of equation $I_{bus} = Y_{bus} V_{bus}$ by inversion is very inefficient. The inverse of Y_{bus} is not necessary to be obtained. Instead, direct solution is obtained by optimally ordered triangular factorisation. In MATLAB, the solution of linear simultaneous equations $A \cdot X = B$ is obtained by using the matrix division operator \backslash (i.e., $X = A \backslash B$), which is based on the triangular factorisation and Gaussian elimination. This technique is superior in both execution time and numerical accuracy. It is two to three times as fast and produces residuals on the order of machine accuracy.

4.2 Solution of Non-Linear Algebraic Equations

Gauss-Seidel, Newton-Raphson, and Quasi-Newton methods are the most common techniques used for the iterative solution of nonlinear algebraic equations. The Gauss-Seidel and Newton-Raphson methods are discussed for one-dimensional equation, and are then extended to n-dimensional equations.[27]

4.2.1 Gauss–Seidel Method

The Gauss-Seidel method is also known as the method of successive displacements. To illustrate the technique, consider the solution of the nonlinear equation given by

$$f(x) = 0 \quad (4.11)$$

The above function is rearranged and written as

$$x = g(x) \quad (4.12)$$

If $x^{(k)}$ is an initial estimate of the variable x , the following iterative sequence is formed

$$x^{(k+1)} = g(x^{(k)}) \quad (4.13)$$

A solution is obtained when the difference between the absolute value of the successive iteration is less than a specified accuracy, i.e.

$$\left| x^{(k+1)} - x^{(k)} \right| \leq \varepsilon \tag{4.14}$$

Where ε is the desired accuracy.

In some cases the Gauss-Seidel method needs many iterations to achieve the desired accuracy and there is no guarantee that it will converge. Thus an acceleration factor, α , can be used to improve the rate of convergence. If $\alpha > 1$ is the acceleration factor, the Gauss-Seidel algorithm becomes:

$$x^{(k+1)} = x^{(k)} + \alpha \left[g(x^{(k)}) - x^{(k)} \right] \tag{4.15}$$

A very large acceleration factor should not be used since the larger step size may result in an overshoot.*

If a system of n equations in n variables is considered then

$$\begin{aligned} f_1(x_1, x_2, \dots, x_n) &= c_1 \\ f_2(x_1, x_2, \dots, x_n) &= c_2 \\ &\dots\dots\dots \\ f_n(x_1, x_2, \dots, x_n) &= c_n \end{aligned} \tag{4.16}$$

Solving for one variable from each equation, the above functions are rearranged and written as:

$$\begin{aligned} x_1 &= c_1 + g_1(x_1, x_2, \dots, x_n) \\ x_2 &= c_2 + g_2(x_1, x_2, \dots, x_n) \\ &\dots\dots\dots \\ x_n &= c_n + g_n(x_1, x_2, \dots, x_n) \end{aligned} \tag{4.17}$$

The iteration procedure is initiated by assuming an approximate solution for each of the independent variables $x_1^{(0)}, x_2^{(0)}, \dots, x_n^{(0)}$. Equation 4.17 results in a new approximate solution $x_1^{(1)}, x_2^{(1)}, \dots, x_n^{(1)}$. In the Gauss-Seidel method, the updated values of the variables calculated ($x_{cal}^{(k+1)}$) in the preceding equations are immediately used in the solution of the subsequent equations. At the end of each

* Experience shows that no of iteration in Gauss-Seidel method can be reduced considerably if the correction in voltage at each bus is multiplied by some constant that increases the amount of correction to bring the voltage closer to the value it is approaching. The multiplier that improves the convergence is known as acceleration factor. Usually the acceleration factor “ α ” is: $1 < \alpha < 2$. [28]

iteration, the calculated values of all variables are tested against the previous values. If all changes in the variables are within the specified accuracy, a solution has converged; otherwise another iteration must be performed. The rate of convergence can often be increased by using a suitable acceleration factor α , and taking into account eq.4.13 the iterative sequence becomes

$$\mathbf{x}^{(k+1)} = \mathbf{x}^{(k)} + \alpha(\mathbf{x}_{cal}^{(k+1)} - \mathbf{x}^{(k)}) \quad (4.18)$$

$\mathbf{x}_{cal}^{(k+1)}$ arises from the inversion of $g(x^{(k)})$ where x_{cal} is the calculated value of variable x . Indicator k indicates the number of the current iteration while indicator $k+1$ is the input of the next iteration.

4.2.2 Newton-Raphson Method

The most widely used method for solving simultaneous nonlinear algebraic equations is the Newton-Raphson method. Newton's method is a successive approximation procedure based on an initial estimate of the unknown and the use of Taylor's series expansion. [27] Consider the solution of the one-dimensional equation given by

$$f(x) = c \quad (4.19)$$

If $x^{(0)}$ is an initial estimate of the solution, and $\Delta x^{(0)}$ is a small deviation from the correct solution, we must have

$$f(x^{(0)} + \Delta x^{(0)}) = c$$

Expanding the left-hand side of the above equation in Taylor's series about $x^{(0)}$ yields

$$f(x^{(0)}) + \left(\frac{df}{dx}\right)^{(0)} \Delta x^{(0)} + \frac{1}{2!} \left(\frac{d^2f}{dx^2}\right)^{(0)} (\Delta x^{(0)})^2 + \dots = c$$

Assuming the error $\Delta x^{(0)}$ is very small, the higher-order terms can be neglected, which results in

$$\Delta c^{(0)} \cong \left(\frac{df}{dx}\right)^{(0)} \Delta x^{(0)}$$

where

$$\Delta c^{(0)} = c - f(x^{(0)})$$

Adding $\Delta x^{(0)}$ to the initial estimate will result in the second approximation

$$\mathbf{x}^{(1)} = \mathbf{x}^{(0)} + \frac{\Delta \mathbf{c}^{(0)}}{\left(\frac{df}{dx}\right)^{(0)}}$$

The Newton-Raphson algorithm arise where:

$$\Delta \mathbf{c}^{(k)} = \mathbf{c} - \mathbf{f}\left(\mathbf{x}^{(k)}\right) \quad (4.20)$$

$$\Delta \mathbf{x}^{(k)} = \frac{\Delta \mathbf{c}^{(k)}}{\left(\frac{df}{dx}\right)^{(k)}} \quad (4.21)$$

$$\mathbf{x}^{(k+1)} = \mathbf{x}^{(k)} + \Delta \mathbf{x}^{(k)} \quad (4.22)$$

Equation 4.21 can be rearranged as

$$\Delta \mathbf{c}^{(k)} = \mathbf{j}^{(k)} \Delta \mathbf{x}^{(k)} \quad (4.23)$$

where

$$\mathbf{j}^{(k)} = \left(\frac{df}{dx}\right)^{(k)}$$

The relation in 4.23 demonstrates that the nonlinear equation $f(\mathbf{x}) - \mathbf{c} = 0$ is approximated by the tangent line on the curve at $\mathbf{x}^{(k)}$. Therefore, a linear equation is obtained in terms of the small changes in the variable. The intersection of the tangent line with the x-axis results in $\mathbf{x}^{(k+1)}$.

Expanding the left side of the n-dimensional equation 4.16 in the Taylor's series about the initial estimates and neglecting all higher order terms, leads to the expression

$$\begin{aligned} (\mathbf{f}_1)^{(0)} + \left(\frac{\partial \mathbf{f}_1}{\partial \mathbf{x}_1}\right)^{(0)} \Delta \mathbf{x}_1^{(0)} + \left(\frac{\partial \mathbf{f}_1}{\partial \mathbf{x}_2}\right)^{(0)} \Delta \mathbf{x}_2^{(0)} + \dots + \left(\frac{\partial \mathbf{f}_1}{\partial \mathbf{x}_n}\right)^{(0)} \Delta \mathbf{x}_n^{(0)} &= \mathbf{c}_1 \\ (\mathbf{f}_2)^{(0)} + \left(\frac{\partial \mathbf{f}_2}{\partial \mathbf{x}_1}\right)^{(0)} \Delta \mathbf{x}_1^{(0)} + \left(\frac{\partial \mathbf{f}_2}{\partial \mathbf{x}_2}\right)^{(0)} \Delta \mathbf{x}_2^{(0)} + \dots + \left(\frac{\partial \mathbf{f}_2}{\partial \mathbf{x}_n}\right)^{(0)} \Delta \mathbf{x}_n^{(0)} &= \mathbf{c}_2 \\ \vdots & \\ (\mathbf{f}_n)^{(0)} + \left(\frac{\partial \mathbf{f}_n}{\partial \mathbf{x}_1}\right)^{(0)} \Delta \mathbf{x}_1^{(0)} + \left(\frac{\partial \mathbf{f}_n}{\partial \mathbf{x}_2}\right)^{(0)} \Delta \mathbf{x}_2^{(0)} + \dots + \left(\frac{\partial \mathbf{f}_n}{\partial \mathbf{x}_n}\right)^{(0)} \Delta \mathbf{x}_n^{(0)} &= \mathbf{c}_n \end{aligned}$$

Or in matrix form

$$\begin{bmatrix} c_1 - (f_1)^{(0)} \\ c_2 - (f_2)^{(0)} \\ \vdots \\ c_n - (f_n)^{(0)} \end{bmatrix} = \begin{bmatrix} \left(\frac{\partial f_1}{\partial x_1}\right)^{(0)} & \left(\frac{\partial f_1}{\partial x_2}\right)^{(0)} & \dots & \left(\frac{\partial f_1}{\partial x_n}\right)^{(0)} \\ \left(\frac{\partial f_2}{\partial x_1}\right)^{(0)} & \left(\frac{\partial f_2}{\partial x_2}\right)^{(0)} & \dots & \left(\frac{\partial f_2}{\partial x_n}\right)^{(0)} \\ \vdots & \vdots & \ddots & \vdots \\ \left(\frac{\partial f_n}{\partial x_1}\right)^{(0)} & \left(\frac{\partial f_n}{\partial x_2}\right)^{(0)} & \dots & \left(\frac{\partial f_n}{\partial x_n}\right)^{(0)} \end{bmatrix} \begin{bmatrix} \Delta x_1^{(0)} \\ \Delta x_2^{(0)} \\ \vdots \\ \Delta x_n^{(0)} \end{bmatrix}$$

In a short form can be written as

$$\Delta C^{(k)} = J^{(k)} \Delta X^{(k)} \Leftrightarrow \Delta X^{(k)} = [J^{(k)}]^{-1} \Delta C^{(k)} \quad (4.24)$$

Thus the Newton-Raphson algorithm for the n-dimensional case becomes

$$X^{(k+1)} = X^{(k)} + \Delta X^{(k)} \quad (4.25)$$

$$\Delta X^{(k)} = \begin{bmatrix} \Delta x_1^{(k)} \\ \Delta x_2^{(k)} \\ \vdots \\ \Delta x_n^{(k)} \end{bmatrix} \text{ and } \Delta C^{(k)} = \begin{bmatrix} c_1 - (f_1)^{(k)} \\ c_2 - (f_2)^{(k)} \\ \vdots \\ c_n - (f_n)^{(k)} \end{bmatrix} \quad (4.26)$$

$$J^{(k)} = \begin{bmatrix} \left(\frac{\partial f_1}{\partial x_1}\right)^{(k)} & \left(\frac{\partial f_1}{\partial x_2}\right)^{(k)} & \dots & \left(\frac{\partial f_1}{\partial x_n}\right)^{(k)} \\ \left(\frac{\partial f_2}{\partial x_1}\right)^{(k)} & \left(\frac{\partial f_2}{\partial x_2}\right)^{(k)} & \dots & \left(\frac{\partial f_2}{\partial x_n}\right)^{(k)} \\ \vdots & \vdots & \ddots & \vdots \\ \left(\frac{\partial f_n}{\partial x_1}\right)^{(k)} & \left(\frac{\partial f_n}{\partial x_2}\right)^{(k)} & \dots & \left(\frac{\partial f_n}{\partial x_n}\right)^{(k)} \end{bmatrix} \quad (4.27)$$

$J^{(k)}$ is called the Jacobean matrix. Elements of this matrix are the partial derivatives evaluated at $X^{(k)}$. It is assumed that $J^{(k)}$ has an inverse during each iteration. Newton's method, as applied to a set of nonlinear equations, reduces the problem to solving a set of linear equations in order to determine the values that improve the accuracy of the estimates.

The solution of (4.24) by inversion is very inefficient. It is not necessary to obtain the inverse of $J^{(k)}$. Instead, a direct solution is obtained by optimally ordered triangular factorisation. In MATLAB, the solution of linear simultaneous equations $\Delta C = J \Delta X$ is obtained by using the matrix division operator \backslash (i.e., $\Delta X = J \backslash \Delta C$) which is based on the triangular factorisation and Gaussian elimination.

4.3 Power Flow Solution

Power flow studies, commonly known as load flow, form an important part of power system analysis. They are necessary for planning, economic scheduling, and control of an existing system as well as

planning its future expansion. The problem consists of determining the magnitudes and phase angle of voltages at each bus and active and reactive power flow in each line.

In solving a power flow problem, the system is assumed to be operating under balanced conditions and a single-phase model is used. Four quantities are associated with each bus. These are voltage magnitude $|V|$, phase angle δ , real power P , and reactive power Q . The system buses are generally classified into three types.

Slack bus: One bus, known as slack or swing bus, is taken as reference where the magnitude and phase angle of the voltage are specified. This bus makes up the difference between the scheduled loads and generated power that are caused by the losses in the network.

Load buses: At these buses the active and reactive powers are specified. The magnitude and the phase angle of the bus voltages are unknown. These buses are called P-Q buses.

Regulated buses: These buses are the generator buses. They are also known as voltage-controlled buses. At these buses, the real power and voltage magnitude are specified. The phase angles of the voltages and the reactive power are to be determined. The limits on the value of the reactive power are also specified. These buses are called P-V buses.

4.4 Power Flow Equation

Consider a typical bus of a power system network as shown in Figure 4.3. Transmission lines are represented by their equivalent π models where impedances have been converted to per unit admittances on a common MVA base.

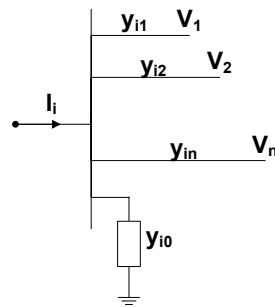


Figure 4.3: A typical bus of the power system

Application of Kirchhoff's Current Law to this bus results in:

$$\begin{aligned}
 I_i &= y_{i0}V_i + y_{i1}(V_i - V_1) + y_{i2}(V_i - V_2) + \dots + y_{in}(V_i - V_n) \\
 &= (y_{i0} + y_{i1} + y_{i2} + \dots + y_{in})V_i - y_{i1}V_1 - y_{i2}V_2 - \dots - y_{in}V_n
 \end{aligned}
 \tag{4.28}$$

$$I_i = V_i \sum_{j=0}^n y_{ij} - \sum_{j=1}^n y_{ij} V_j \quad (4.29)$$

The real and reactive power at bus “i” is:

$$P_i + jQ_i = V_i I_i^* \quad (4.30)$$

$$I_i = \frac{P_i + jQ_i}{V_i^*} \quad (4.31)$$

Substituting for I_i in 4.29 yields:

$$\frac{P_i + jQ_i}{V_i^*} = V_i \sum_{j=0}^n y_{ij} - \sum_{j=1}^n y_{ij} V_j \quad j \neq i \quad (4.32)$$

Considering the above relation, the mathematical formulation, of the power flow problem, results in a system of algebraic nonlinear equations which must be solved by iterative techniques.

4.5 Gauss-Seidel Power Flow Solution

In the power flow study it is necessary to solve the set of nonlinear equations represented by equation 4.12 for two unknown variables at each node. In the Gauss-Seidel method in eq. 4.32 is solved for V_i , and the iterative sequence become:

$$V_i^{(k+1)} = \frac{\frac{P_i^{sch} - jQ_i^{sch}}{V_i^{*(k)}} + \sum y_{ij} V_j^{(k)}}{\sum y_{ij}} \quad j \neq i \quad (4.33)$$

where y_{ij} shown in lowercase letters is the actual admittance in per unit P_i^{sch} and Q_i^{sch} are the net real and reactive powers expressed in per unit. In applying the Kirchhoff's current law, current entering bus i was assumed positive. Thus, P_i^{sch} and Q_i^{sch} have positive values for buses where real and reactive powers are injected into the bus, such as generator buses. In contrary P_i^{sch} and Q_i^{sch} have negative values for load buses where real and reactive powers are flowing away from the bus. If (4.32) is solved for P_i and Q_i , we have

$$P_i^{(k+1)} = \Re \left\{ V_i^{*(k)} \left[V_i^{(k)} \sum_{j=0}^n y_{ij} - \sum_{j=1}^n y_{ij} V_j^{(k)} \right] \right\} \quad j \neq i \quad (4.34)$$

$$Q_i^{(k+1)} = -\Im \left\{ V_i^{*(k)} \left[V_i^{(k)} \sum_{j=0}^n y_{ij} - \sum_{j=1}^n y_{ij} V_j^{(k)} \right] \right\} \quad j \neq i \quad (4.35)$$

The power flow equation is usually expressed in terms of the elements of the bus admittance matrix. Since the off-diagonal elements of the bus admittance matrix Y_{bus} , shown by uppercase letters, are $Y_{ij} = -y_{ij}$, and the diagonal elements are $Y_{ii} = \sum y_{ij}$ thus (4.33) becomes

$$V_i^{(k+1)} = \frac{\frac{P_i^{sch} - jQ_i^{sch}}{V_i^{*(k)}} - \sum_{j \neq i} Y_{ij} V_j^{(k)}}{Y_{ii}} \quad (4.36)$$

And

$$P_i^{(k+1)} = \Re \left\{ V_i^{*(k)} \left[V_i^{(k)} Y_{ii} + \sum_{\substack{j=1 \\ j \neq i}}^n Y_{ij} V_j^{(k)} \right] \right\} \quad j \neq i \quad (4.37)$$

$$Q_i^{(k+1)} = -\Im \left\{ V_i^{*(k)} \left[V_i^{(k)} Y_{ii} - \sum_{\substack{j=1 \\ j \neq i}}^n Y_{ij} V_j^{(k)} \right] \right\} \quad j \neq i \quad (4.38)$$

Y_{ii} includes the admittance to ground of line charging sensitivity and any other fixed admittance to ground.

Since both components of voltage are specified for the slack bus, there are $2(n-1)$ equations which must be solved by an iterative method. Under normal operating conditions, the voltage magnitude of buses is close to 1.0 per unit or close to the voltage magnitude of the slack bus. Voltage magnitude at load buses is somewhat lower than the slack bus value, depending on the reactive power demand, whereas the scheduled voltage at the generator buses is somewhat higher. Also, the phase angle of the load buses are below the reference angle in accordance to the real power demand, whereas the phase angle of the generator buses may be above the reference value depending on the amount of real power flowing into the bus. Thus, for the Gauss-Seidel method, an initial voltage estimate of $1.0 + j0.0$ for unknown voltages is satisfactory, and the converged solution correlates with the actual operating states.

For P-Q buses, the real and reactive powers P_i^{sch} and Q_i^{sch} are known. Starting with an initial estimate, (4.36) is solved for the real and imaginary components of voltage. For the voltage-controlled buses (P-V buses) where P_i^{sch} and $|V_i|$ are specified, first (4.38) is solved for $Q_i^{(k+1)}$ and then is used in (4.36) to solve for $V_i^{(k+1)}$. However, since $|V_i|$ is specified, only the imaginary part of $V_i^{(k+1)}$ is retained, and its real part is selected in order to satisfy the relation

$$\left(e_i^{(k+1)} \right)^2 + \left(f_i^{(k+1)} \right)^2 = |V_i|^2 \quad (4.39)$$

$$e_i^{(k+1)} = \sqrt{|V_i|^2 - \left(f_i^{(k+1)} \right)^2} \quad (4.40)$$

where $e_i^{(k+1)}$ and $f_i^{(k+1)}$ are the real and imaginary components of the voltage $V_i^{(k+1)}$ in the iterative sequence.

The rate of convergence is increased by applying an acceleration factor to the approximate solution obtained from each iteration.

$$V_i^{(k+1)} = V_i^{(k)} + \alpha (V_{ical}^{(k)} - V_i^{(k)}) \quad (4.41)$$

where α is the acceleration factor which depends on the system. For typical systems the range from 1.3 to 1.7 is found to be satisfactory. The updated voltages immediately replace the previous values in the solution of the subsequent equations. The process is continued until changes in the real and imaginary components of bus voltages between successive iterations are within a specified accuracy.

$$|e_i^{(k+1)} - e_i^{(k)}| \leq \varepsilon \quad \text{and} \quad |f_i^{(k+1)} - f_i^{(k)}| \leq \varepsilon \quad (4.42)$$

In order to have a acceptable and reasonably small power mismatch, a very tight tolerance must be specified on both components of the voltage. A voltage accuracy in the range of 0.00001 to 0.00005 pu is satisfying. In practice, the method for determining the completion of a solution is based on an accuracy index set up on the power mismatch. The iteration continues until the magnitude of the largest element in the ΔP and ΔQ columns is less than the specified value. A typical power mismatch accuracy is 0.001 pu. Once a solution is converged, the net real and reactive powers at the slack bus are computed from equations 4.37 and 4.38.

4.6 Line Flows and Losses

An important parameter for the analysis of a power system is the computation of line flows and losses. In Figure 4.4 a line connecting two bases “i” and “j” is presented. The line current I_{ij} , measured at bus “i” and defined positive in the direction $i \rightarrow j$ is given by the equation:

$$I_{ij} = I_\ell + I_{i0} = y_{ij} (V_i - V_j) + y_{i0} V_i \quad (4.43)$$

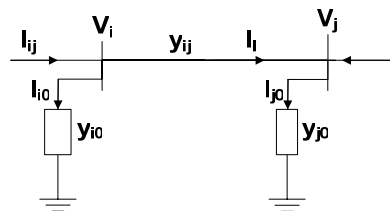


Figure 4.4: Transmission line model for calculating line flows

Similarly, the line current I_{ji} measured at bus j and defined positive in the direction $j \rightarrow i$ is given by equation

$$I_{ij} = I_c + I_{i0} = y_{ij}(V_j - V_i) + y_{i0}V_j \quad (4.44)$$

The complex powers S_{ij} from bus i to j and S_{ji} from bus j to i are

$$S_{ij} = V_i I_{ij}^* \quad (4.45)$$

$$S_{ji} = V_j I_{ji}^* \quad (4.46)$$

The power loss in line $i - j$ is the algebraic sum of the power flows determined for equations 4.45 and 4.46.

$$S_{Lij} = S_{ij} + S_{ji} \quad (4.47)$$

4.7 Tap Changing Transformers

The flow of real power along a transmission line is determined by the angle difference of the terminal voltages, and the flow of reactive power is determined mainly by the magnitude difference of terminal voltages. Real and reactive powers can be controlled by use of tap changing transformers and regulating transformers.

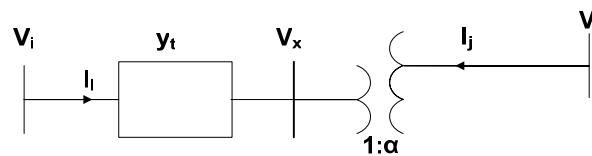


Figure 4.5Transformer with tap setting ratio $1:\alpha$

In a tap changing transformer, when the ratio is at the nominal value, the transformer is represented by a series admittance y_t in per unit. With off-nominal ratio, the per unit admittance is different from both sides of the transformer, and the admittance must be modified to include the effect of the off-nominal ratio. Consider a transformer with admittance y_t in series with an ideal transformer representing the off-nominal tap ratio $1:\alpha$ as shown in Figure 4.5. y_t is the admittance in per unit based on the nominal turn ratio and α is the per unit off-nominal tap position allowing for small adjustment in voltage of usually ± 10 percent. In the case of phase shifting transformers, α is a complex number. Consider a fictitious bus x between the turn ratio and admittance of the transformer. Since the complex power on either side of the ideal transformer is the same, it follows that if the voltage goes through a positive phase angle shift, the current will go through a negative phase angle shift. Thus, for the assumed direction of currents, we have:

$$V_x = \frac{1}{\alpha} V_j \quad (4.48)$$

$$I_i = -a^* I_j \quad (4.49)$$

The current I_i is given by the equation $I_i = y_i (V_i - V_x)$

Substituting for V_x from equation 4.48:

$$I_i = y_i V_i - \frac{y_t}{a} V_j \quad (4.50)$$

Also from 4.49:

$$I_i = -\frac{1}{a^*} I_j$$

Substituting for I_j from equation 4.48:

$$I_i = \frac{y_t}{a^*} V_i - \frac{y_t}{|a|^2} V_j \quad (4.51)$$

Writing 4.50 and 4.52 in a matrix:

$$\begin{bmatrix} I_i \\ I_j \end{bmatrix} = \begin{bmatrix} y_i & -\frac{y_t}{a} \\ -\frac{y_t}{a^*} & \frac{y_t}{|a|^2} \end{bmatrix} \begin{bmatrix} V_i \\ V_j \end{bmatrix} \quad (4.52)$$

When α is real, the π model shown in Figure 4.6 represents the admittance matrix in 4.52. In the π model, the left side corresponds to the non-tap side and the right side corresponds to the tap side of the transformer.

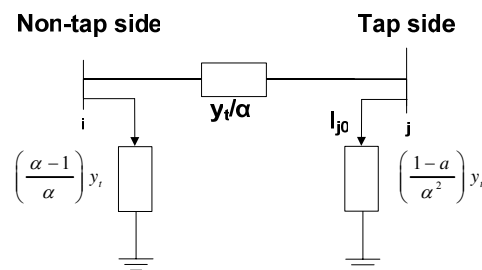


Figure 4.6: Equivalent circuit for a tap changing transformer

4.8 Power Flow Programs

For each fore mentioned power flow solution of practical systems a computer program has been developed. [27] Each method of solution consists of four programs. The program for the Gauss-Seidel

method is Ifgauss, which is preceded by Ifybus, and is followed by busout and lineflow. Programs Ifybus, busout, and lineflow are designed to be used with two more power flow programs. These are Ifnewton for the Newton-Raphson method and decouple for the fast decoupled method. The following is a brief description of the programs used in the Gauss-Seidel method.

Ifybus: This program requires the line and transformer parameters and transformer tap settings specified in the input file named linedata. Ifybus converts impedances to admittances and obtains the bus admittance matrix. The program is designed to handle parallel lines.

Ifgauss: This program obtains the power flow solution by the Gauss-Seidel method and requires the files named busdata and linedata. Ifgauss is designed for the direct use of load and generation in MW and Mvar, bus voltages in per unit, and angle in degrees. Loads and generation are converted to per unit quantities on the base MVA selected. A provision is made to maintain the generator reactive power of the voltage-controlled buses within their specified limits. The violation of reactive power limit may occur if the specified voltage is either too high or too low. After a few iterations (10th iteration in the Gauss method), the Var calculated at the generator buses are examined. If a limit is reached, the voltage magnitude is adjusted in steps of 0.5 percent up to ± 5 percent to bring the Var demand within the specified limits.

busout This program produces the bus output result in a tabulated form. The bus output result includes the voltage magnitude and angle, real and reactive power of generators and loads, and the shunt capacitor/reactor Mvar. Total generation and total load are also included as outlined in the sample case.

lineflow This program prepares the line output data. "lineflow" program is designed to display the active and reactive power flow entering the line terminals and line losses as well as the net power at each bus. Also included are the total real and reactive losses in the system. The output of this portion is also shown in the sample case.

4.9 Data Preparation

In order to perform a power flow analysis by the Gauss-Seidel method in the MATLAB environment, the following variables must be defined: power system base MVA, power mismatch accuracy, acceleration factor, and maximum number of iterations. The name (in lowercase letters) reserved for these variables are basemva, accuracy, accel, and maxiter, respectively. Typical values are as follows:

$$basemva = 100, accuracy = 0.001, accel = 1.6, maxiter = 80.$$

The initial step in the preparation of input file is the numbering of each bus. Buses are numbered sequentially. Although the numbers are sequentially assigned, the buses need not be entered in sequence. In addition, the following data files are required.

BUS DATA FILE – busdata: The format for the bus entry is chosen to facilitate the required data for each bus in a single row. The information required must be included in a matrix called busdata. In the first column the bus number is mentioned. Column 2 contains the bus code. Column 3 is the voltage magnitude in per unit and in Column 4 is the phase angle in degrees. Columns 5 and 6 are load in MW and Mvar respectively. From the 7th Column through 10th are mentioned the MW, Mvar, minimum Mvar and maximum Mvar of generation. The last column is the injected Mvar of shunt capacitors. The bus code entered in column 2 is used for identifying load, voltage-controlled, and slack buses as outlined below:

“1” This code is used for the slack bus. The only necessary information for this bus is the voltage magnitude and its phase angle.

“0” This code is used for load buses. The loads are entered positive in megawatts and megavars. For this bus, initial voltage estimate must be specified. This is usually 1 and 0 for voltage magnitude and phase angle, respectively. If voltage magnitude and phase angle for this type of bus are specified, they will be taken as the initial starting voltage for that bus instead of a flat start of 1 and 0..

“2” This code is used for the voltage-controlled buses. For this bus, voltage magnitude, real power generation in megawatts, and the minimum and maximum limits of the megavar demand must be specified.

LINE DATA FILE – linedata: Lines are identified by the node-pair method. The information required must be included in a matrix called linedata. Columns 1 and 2 are the line bus numbers. Columns 3 through 5 contain the line resistance, reactance, and one-half of the total line charging susceptance in per unit on the specified MVA base. The last column is for the transformer tap setting; for lines, 1 must be entered in this column. The lines may be entered in any sequence or order with the only restriction being that if the entry is a transformer, the left bus number is assumed to be the tap side of the transformer. The IEEE 30 bus system is used to demonstrate the data preparation and the use of the power flow programs by the Gauss-Seidel method.

4.10 Newton-Raphson Power Flow Solution

Newton's method is mathematically superior to the Gauss-Seidel method due to its quadratic convergence, and is less prone to divergence with ill-conditioned problems. For large power systems, the Newton-Raphson method is found to be more efficient and practical. The number of iterations required to obtain a solution is independent of the system size, but more functional evaluations are required at each iteration. Since in the power flow problem real power and voltage magnitude are specified for the voltage-controlled buses, the power flow equation is formulated in polar form. For the typical bus of the power system shown in Figure 4.3, the current entering bus "i" is given by equation 4.29. This equation can be rewritten in terms of the bus admittance matrix as:

$$I_i = \sum_{j=1}^n Y_{ij} V_j \quad (4.53)$$

In the above equation, “j” includes bus “i”. The polar form expression of this equation is:

$$I_i = \sum_{j=1}^n |Y_{ij}| |V_j| \angle \theta_{ij} + \delta_j \quad (4.54)$$

The complex power at bus “i” is

$$P_i - jQ_i = V_i^* I_i \quad (4.55)$$

Substituting from equation 4.54 for I_i in 4.55:

$$P_i - jQ_i = |V_i| \angle -\delta_i \sum_{j=1}^n |Y_{ij}| |V_j| \angle \theta_{ij} + \delta_j \quad (4.56)$$

Separating the real and imaginary parts:

$$P_i = \sum_{j=1}^n |V_i| |V_j| |Y_{ij}| \cos(\theta_{ij} - \delta_i + \delta_j) \quad (4.57)$$

$$Q_i = -\sum_{j=1}^n |V_i| |V_j| |Y_{ij}| \sin(\theta_{ij} - \delta_i + \delta_j) \quad (4.58)$$

Equations 4.57 and 4.58 constitute a set of nonlinear algebraic equations in terms of the independent variables, voltage magnitude in per unit, and phase angle in radians. There are two equations for each load bus, given by 4.57 and 4.58, and one equation for each voltage-controlled bus, given by 4.57. Expanding 4.57 and 4.58 in Taylor's series about the initial estimate and neglecting all higher order terms results in the following set of linear equations.

$$\begin{bmatrix} \Delta P_2^{(k)} \\ \vdots \\ \Delta P_n^{(k)} \\ \Delta Q_2^{(k)} \\ \vdots \\ \Delta Q_n^{(k)} \end{bmatrix} = \begin{bmatrix} \frac{\partial P_2^{(k)}}{\partial \delta_2} & \dots & \frac{\partial P_2^{(k)}}{\partial \delta_n} & \frac{\partial P_2^{(k)}}{\partial |V_2|} & \dots & \frac{\partial P_2^{(k)}}{\partial |V_n|} \\ \vdots & \ddots & \vdots & \vdots & \ddots & \vdots \\ \frac{\partial P_n^{(k)}}{\partial \delta_2} & \dots & \frac{\partial P_n^{(k)}}{\partial \delta_n} & \frac{\partial P_n^{(k)}}{\partial |V_2|} & \dots & \frac{\partial P_n^{(k)}}{\partial |V_n|} \\ \hline \frac{\partial Q_2^{(k)}}{\partial \delta_2} & \dots & \frac{\partial Q_2^{(k)}}{\partial \delta_n} & \frac{\partial Q_2^{(k)}}{\partial |V_2|} & \dots & \frac{\partial Q_2^{(k)}}{\partial |V_n|} \\ \vdots & \ddots & \vdots & \vdots & \ddots & \vdots \\ \frac{\partial Q_n^{(k)}}{\partial \delta_2} & \dots & \frac{\partial Q_n^{(k)}}{\partial \delta_n} & \frac{\partial Q_n^{(k)}}{\partial |V_2|} & \dots & \frac{\partial Q_n^{(k)}}{\partial |V_n|} \end{bmatrix} \begin{bmatrix} \Delta \delta_2^{(k)} \\ \vdots \\ \Delta \delta_n^{(k)} \\ \Delta |V_2^{(k)}| \\ \vdots \\ \Delta |V_n^{(k)}| \end{bmatrix}$$

In the above equation, bus 1 is assumed to be the slack bus. The Jacobian matrix gives the linearized relationship between small changes in voltage angle $\Delta \delta_i^{(k)}$ and voltage magnitude $\Delta |V_i^{(k)}|$ with the small changes in real and reactive power $\Delta P_i^{(k)}$ and $\Delta Q_i^{(k)}$. Elements of the Jacobian matrix are the partial derivatives of 4.57 and 4.58, evaluated at $\Delta \delta_i^{(k)}$ and $\Delta |V_i^{(k)}|$. In short form, it can be written as:

$$\begin{bmatrix} \Delta P \\ \Delta Q \end{bmatrix} = \begin{bmatrix} J_1 & J_2 \\ J_3 & J_4 \end{bmatrix} \begin{bmatrix} \Delta \delta \\ \Delta |V| \end{bmatrix} \quad (4.59)$$

For voltage-controlled buses, the voltage magnitudes are known. Therefore, if m buses of the system are voltage-controlled, m equations involving ΔQ and ΔV and the corresponding columns of the Jacobian matrix eliminated. Accordingly, there are $n-1$ real power constraints and $n-1-m$ reactive power constraints and the Jacobian matrix is of order $(2n-2-m) \times (2n-2-m)$. J_1 is of the order $(n-1) \times (n-1)$, J_2 is of order $(n-1) \times (n-1-m)$, J_3 is of the order $(n-1-m) \times (n-1)$ and J_4 is of the order $(n-1-m) \times (n-1-m)$.

The diagonal and the off diagonal elements of J_1 are:

$$\frac{\partial P_i}{\partial \delta_i} = \sum_{j \neq i} |V_i| |V_j| |Y_{ij}| \sin(\theta_j - \delta_i + \delta_j) \quad (4.60)$$

$$\frac{\partial P_i}{\partial \delta_j} = -|V_i| |V_j| |Y_{ij}| \sin(\theta_j - \delta_i + \delta_j) \quad j \neq i \quad (4.61)$$

The diagonal and the off diagonal elements of J_2 are:

$$\frac{\partial P_i}{\partial |V_i|} = 2|V_i||Y_{ii}|\cos\theta_{ii} + \sum_{j \neq i} |V_j||Y_{ij}|\cos(\theta_{ij} - \delta_i + \delta_j) \quad (4.62)$$

$$\frac{\partial P_i}{\partial |V_j|} = |V_i||Y_{ij}|\cos(\theta_{ij} - \delta_i + \delta_j) \quad j \neq i \quad (4.63)$$

The diagonal and the off diagonal elements of J_3 are:

$$\frac{\partial Q_i}{\partial \delta_i} = \sum_{j \neq i} |V_i||V_j||Y_{ij}|\cos(\theta_{ij} - \delta_i + \delta_j) \quad (4.64)$$

$$\frac{\partial Q_i}{\partial \delta_j} = -|V_i||V_j||Y_{ij}|\cos(\theta_{ij} - \delta_i + \delta_j) \quad j \neq i \quad (4.65)$$

The diagonal and the off diagonal elements of J_4 are:

$$\frac{\partial Q_i}{\partial |V_i|} = -2|V_i||Y_{ii}|\sin\theta_{ii} + \sum_{j \neq i} |V_j||Y_{ij}|\sin(\theta_{ij} - \delta_i + \delta_j) \quad (4.66)$$

$$\frac{\partial Q_i}{\partial |V_j|} = -|V_i||Y_{ij}|\sin(\theta_{ij} - \delta_i + \delta_j) \quad j \neq i \quad (4.67)$$

The terms $\Delta P_i^{(k)}$ and $\Delta Q_i^{(k)}$ are the difference between the scheduled and calculated values, known as power residuals, given by:

$$\Delta P_i^{(k)} = P_i^{sch} - P_i^{(k)} \quad (4.68)$$

$$\Delta Q_i^{(k)} = Q_i^{sch} - Q_i^{(k)} \quad (4.69)$$

The new estimates for bus voltages are:

$$\delta_i^{(k+1)} = \delta_i^{(k)} + \Delta \delta_i^{(k)} \quad (4.70)$$

$$|V_i^{(k+1)}| = |V_i^{(k)}| + \Delta |V_i^{(k)}| \quad (4.71)$$

The procedure for power flow solution by the Newton-Raphson method is as follows:

1. For load buses, where P_i^{sch} and Q_i^{sch} are specified, voltage magnitudes and phase angles are set equal to the slack bus values, or 1.0 and 0.0, i.e., $|V_i^{(0)}| = 1.0$ and $\delta_i^0 = 0.0$. For voltage-regulated buses, where $|V_i|$ and P_i^{sch} are specified, phase angles are set equal to the slack bus angle, or 0, i.e., $\delta_i^0 = 0.0$.

2. For load buses, $P_i^{(k)}$ and $Q_i^{(k)}$ are calculated from 4.57 and 4.58 and $\Delta P_i^{(k)}$ and $\Delta Q_i^{(k)}$ are calculated from 4.68 and 4.69.
3. For voltage-controlled buses, $P_i^{(k)}$ and $\Delta P_i^{(k)}$ are calculated from 4.57 and 4.68, respectively.
4. The elements of the Jacobian matrix ($J_1, J_2, J_3,$ and J_4) are calculated from 4.58 - 4.67.
5. The linear simultaneous equation 4.59 is solved directly by optimally ordered triangular factorisation and Gaussian elimination.
6. The new voltage magnitudes and phase angles are computed from 4.70 and 4.71.
7. The process is continued until the residuals $\Delta P_i^{(k)}$ and $\Delta Q_i^{(k)}$ are less than the specified accuracy, i.e.,

$$\begin{aligned} \left| \Delta P_i^{(k)} \right| &\leq \varepsilon \\ \left| \Delta Q_i^{(k)} \right| &\leq \varepsilon \end{aligned} \quad (4.72)$$

For power flow solution by the Newton-Raphson method for practical power systems a program was developed named `lfnewton`. [27] This program must be preceded by the `lfbus` program. `busout` and `lineflow` programs can be used to Print the load flow solution and the line flow results. The format is the same as the Gauss-Seidel.

lfnewton: This program obtains the power flow solution by the Newton-Raphson method and requires the `busdata` and the `linedata` files described in Section 4.9. It is designed for the direct use of load and generation in MW and Mvar, bus voltages in per unit, and angle in degrees. Loads and generation are converted to per unit quantities on the base MVA selected. A provision is made to maintain the generator reactive power of the voltage-controlled buses within their specified limits. The violation of reactive power limit may occur if the specified voltage is either too high or too low. In the second iteration, the Var calculated at the generator buses are examined. If a limit is reached, the voltage magnitude is adjusted in steps of 0.5 percent up to ± 5 percent to bring the var demand within the specified limits.

4.11 Fast Decoupled Power Flow Solution

Power system transmission lines have a very high X/R ratio. For such a system, real power changes ΔP are less sensitive to changes in the voltage magnitude and are most sensitive to changes in phase angle $\Delta \delta$. Similarly, reactive power is less sensitive to changes in angle and is mainly dependent on changes in voltage magnitude. Therefore, it is reasonable to set elements J_2 and J_3 of the Jacobian matrix to zero. Thus, 4.59 becomes:

$$\begin{bmatrix} \Delta P \\ \Delta Q \end{bmatrix} = \begin{bmatrix} J_1 & 0 \\ 0 & J_4 \end{bmatrix} \begin{bmatrix} \Delta \delta \\ \Delta |V| \end{bmatrix} \quad (4.73)$$

$$\Delta P = J_1 \Delta \delta = \frac{\partial P}{\partial \delta} \Delta \delta \quad (4.74)$$

$$\Delta Q = J_4 \Delta |V| = \frac{\partial Q}{\partial |V|} \Delta |V| \quad (4.75)$$

Equations 4.74 and 4.75 show that the matrix equation is separated into two decoupled equations requiring considerably less time to solve compared to the time required for the solution of 4.59. Furthermore, considerable simplification can be made to eliminate the need for recomputing J_1 and J_4 during each iteration. This procedure results in the decoupled power flow equations developed by Scott and Alsac. [19][20] The diagonal elements of J_1 described by equation 4.60 may be written as:

$$\frac{\partial P_i}{\partial \delta_i} = \sum_{j=1}^n |V_i| |V_j| |Y_{ij}| \sin(\theta_j - \delta_i + \delta_j) - |V_i|^2 |Y_{ii}| \sin \theta_{ii}$$

Replacing the first term of the above equation with $-Q_i$, as given by 4.58, results:

$$\frac{\partial P_i}{\partial \delta_i} = -Q_i - |V_j|^2 |Y_{ij}| \sin \theta_{ij} = -Q_i - |V_j|^2 B_{ij}$$

Where $B_{ii} = |Y_{ii}| \sin \theta_{ii}$ is the imaginary part of the diagonal elements of the bus admittance matrix. B_{ii} is the sum of sensitivity of all elements incident to bus "i". In a typical power system, the self-sensitivity $B_{ii} \ll Q_i$, and Q_j may be neglected. Further simplification is obtained by assuming $|V_i|^2 \approx |V_i|$, which yields:

$$\frac{\partial P_i}{\partial \delta_i} = -|V_i| B_{ii} \quad (4.76)$$

Under normal operating conditions, $\delta_j - \delta_i$ is quite small. Thus, in 4.61 assuming $\theta_{ii} - \delta_j + \delta_i \approx \theta_{ii}$, the off-diagonal elements of J_1 becomes:

$$\frac{\partial P_i}{\partial \delta_j} = -|V_i| |V_j| B_{ij}$$

Further simplification is obtained by assuming $|V_j| \approx 1$

$$\frac{\partial P_i}{\partial \delta_j} = -|V_i| B_{ij} \quad (4.77)$$

Similarly, the diagonal elements of J_4 described by equation 4.46 may be written:

$$\frac{\partial Q_i}{\partial |V_i|} = -|V_i| |Y_{ii}| \sin \theta_{ii} - \sum_{j=1}^n |V_i| |V_j| |Y_{ij}| \sin(\theta_{ij} - \delta_i + \delta_j)$$

Using equation 4.58 in order to replace the second term with $-Q_i$ results in:

$$\frac{\partial Q_i}{\partial |V_i|} = -|V_i| |Y_{ii}| \sin \theta_{ii} + Q_i$$

$B_{ii} = Y_{ii} \sin \theta_{ii}$ and Q_i can be neglected and 4.66 take the following form:

$$\frac{\partial Q_i}{\partial |V_i|} = -|V_i| B_{ii} \quad (4.78)$$

Assuming that $\theta_{ij} - \delta_i + \delta_j \approx \theta_{ij}$ it is yielded that:

$$\frac{\partial Q_i}{\partial |V_j|} = -|V_i| B_{ij} \quad (4.79)$$

With the above assumptions, equations 4.74 and 4.75 becomes:

$$\frac{\Delta P}{|V_i|} = -B' \Delta \delta \quad (4.80)$$

$$\frac{\Delta Q}{|V_i|} = -B'' \Delta |V| \quad (4.81)$$

Here, B' and B'' are the imaginary part of the bus admittance matrix Y_{bus} . Since the elements of this matrix are constant, they need to be triangularized and inverted only once at the beginning of the iteration. B' is of order of $(n-1)$. For voltage-controlled buses where $|V_i|$ and P_i are specified and Q_i is not specified, the corresponding row and column of Y_{bus} are eliminated. Thus, B'' is of order of $(n-1-m)$, where m is the number of voltage-regulated buses. Therefore, in the fast decoupled power flow algorithm, the successive voltage magnitude and phase angle changes are

$$\Delta \delta = \frac{\Delta P}{|V_i|} - [B']^{-1} \quad (4.82)$$

$$\Delta |V| = \frac{\Delta Q}{|V|} - [B'']^{-1} \quad (4.83)$$

The fast decoupled power flow solution requires more iterations than the Newton-Raphson method, but requires considerably less time per iteration, and a power flow solution is obtained very rapidly. This technique is very useful in contingency analysis where numerous outages are to be simulated or a power flow solution is required for on-line control.

A program named decouple is developed for power flow solution by the fast decoupled method for practical power systems. This program must be preceded by the lfybus program. busout and lineflow programs can be used to print the load flow solution and the line flow results. The format is the same as the Gauss-Seidel method. The following is a brief description of the decouple program:

decouple This program finds the power flow solution by the fast decouple method and requires the busdata and the linedata files described in Section 4.9. It is designed for the direct use of load and generation in MW and Mvar, bus voltages in per unit, and angle in degrees. Loads and generation are converted to per unit quantities on the MVA base selected. A provision is made to maintain the generator reactive power of the voltage-controlled buses within their specified limits. The violation of reactive power limit may occur if the specified voltage is either too high or too low. In the 10th iteration, the vars calculated at the generator buses are examined. If a limit is reached, the voltage magnitude is adjusted in steps of 0.5 percent up to ± 5 percent to bring the var demand within the specified limits.

5 METHODOLOGY AND RESULTS

In this chapter the existing Cretan Power System is presented in detailed statistics provided by the Public Power Company. [26] Crete has an autonomous electric grid which is mainly supplied by two conventional power plants and eight wind farms. Crete has high wind energy potential which in some areas exceeds the annual average speed of 10m/sec. The cost of the electricity that is produced by the conventional power plants in Crete is quite high, exceeding the cost of the electricity production on the Mainland by 5 to 7 times.

In the following paragraphs the Cretan electric grid is simulated using Matlab software and analysed using the simulink models that are developed by Sadaat and were described in chapter 4. These models are static and do not take into account certain parameters, such as the fact that wind energy is a variable, non constant and unpredicted energy source, as a dynamic or real time model does.

The power flow solution was developed by both Newton-Raphson and Gauss-Seidel models in order to estimate the additional wind capacity that can be added to each one of the 23 buses of the Cretan electric grid. Afterwards, the results were compared. Furthermore some technical parameters, such as the thermal limits of the high voltage transmission lines and power losses, were calculated.

5.1 The Electric Grid in the Island of Crete

The Electric Grid in Crete consists of 10 power plants and 14 buses connected to the High Voltage.

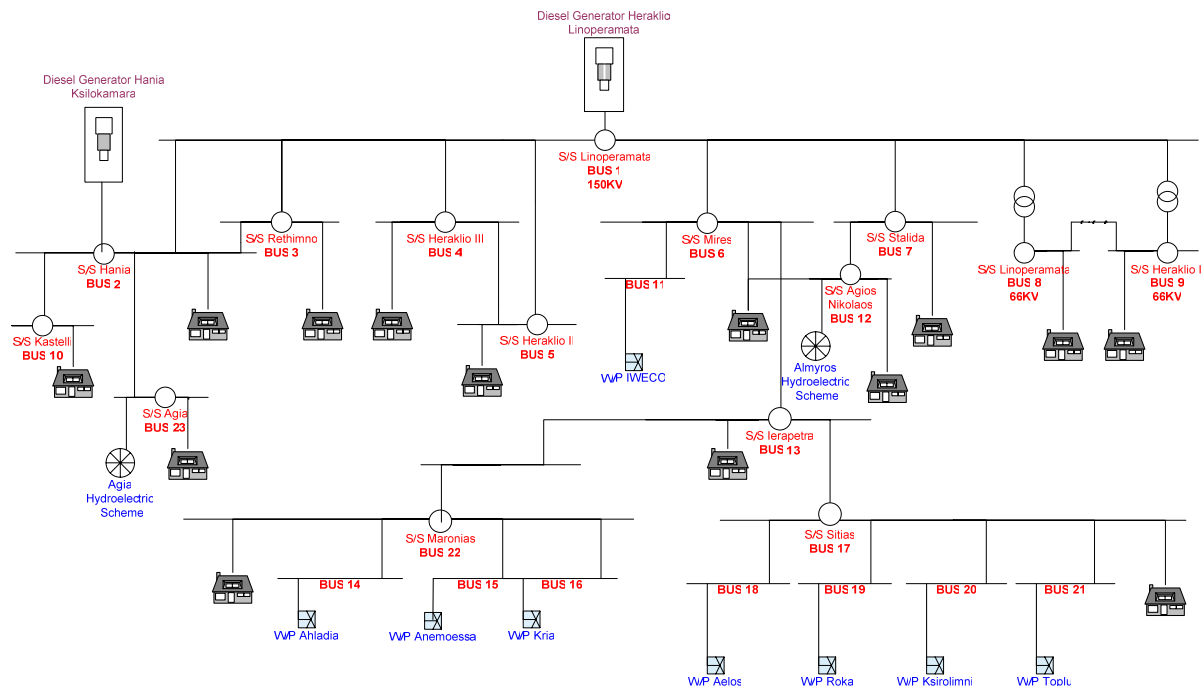


Figure 5.1: The Electrical Grid in the Island of Crete

Basically the electricity is being produced by 2 conventional plants one at Ksilokamara (355MW nominal power) near the city of Hania and one at Linoperamata (284MW nominal power) near Heraklio. The rest power is being produced by 8 wind farms and two small hydroelectric schemes.

Table 5.1: Electricity Generation in the island of Crete

Place or Name of the Plant	Type of Power Plant	Nominal Power (MW)	Operational Hours	Electricity production in 2003 (MWh)	Percentage out of the total
Conventional Power Plants					
Linoperamata	Steam Turbine	111	8760	683879	27.97%
Ksilokamara	Steam Turbine	42.4	8503	196838	8.05%
Total	Steam Turbine	153.2		880717	36.04%
Linoperamata	Diesel Plant	49.2	8730	290375	11.88%
Linoperamata	Gas Turbines	123.82	12957	247064	10.11%
Ksilokamara		312.6	32256	798451	32.66%
Total	Gas Turbines	436.42	32256	1045515	42.77%
Renewable Plants					
Total	Small Hydroelectric schemes	0.6	-	1305	0.05%
Total	Wind Turbines	81.19	-	226812	9.28%
TOTAL		721	-	2444727	100%



The Power Plant in Linoperamata

These generators are connected to the main load buses through a transmission system of 66 and 150 KV networks. The specification of the transmission system is presented in table 5.2.

Table 5.2: Specifications of the Transmission System

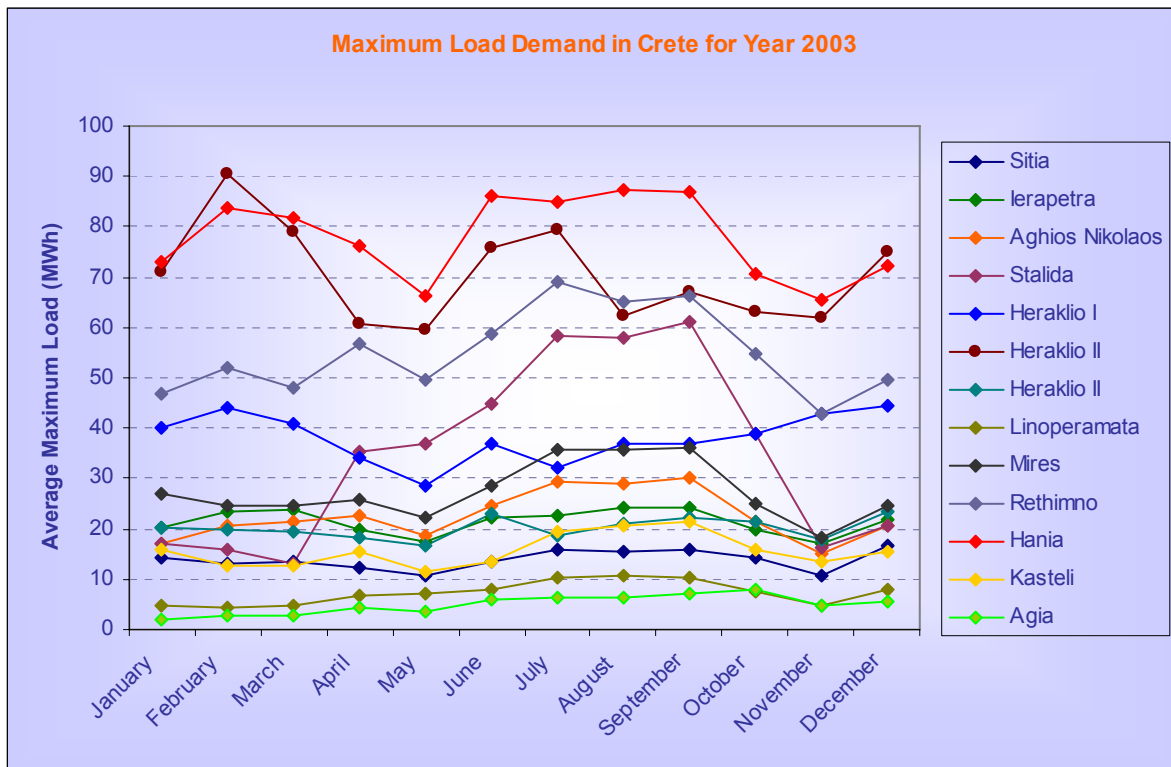
Total length of transmission lines			
Voltage Capacity	Circuit	Type	Length
150KV	Single	Light	160Km
150KV	Double	Light	316
150KV	Single	Heavy	230
150KV	Double	Heavy	109
66KV			29
Installed Transformers Power			
Transformer Type	High Voltage	Step-Down	Subtransmission Coupling
Installed Power (MVA)	989.35	1060	100

5.2 Demand and Electricity Production in Crete

As it can be seen in Figures 5.2 and 5.3 in substations near area of touristic interest such as S.S. Stalida, Heraklio II, Hania, Rethimno, Mires and Aghio Nikolao the electricity demand in some cases might be doubled or tripled. For example in the substation of Stalida the maximum demand in winter time is 15MW, but on the contrary at summer time the maximum demand reaches 61MW, which is four times up the demand in winter. However, in most substations such as Hania, Heraklio II, Moires, Rethimno and Agia maximum demand is almost doubled.



The Substation of Aghia



F

Figure 5.2: Average Maximum load per substation in Crete

Similar conclusions can be made while observing the graph in Figure 5.3 with the average minimum load demand.

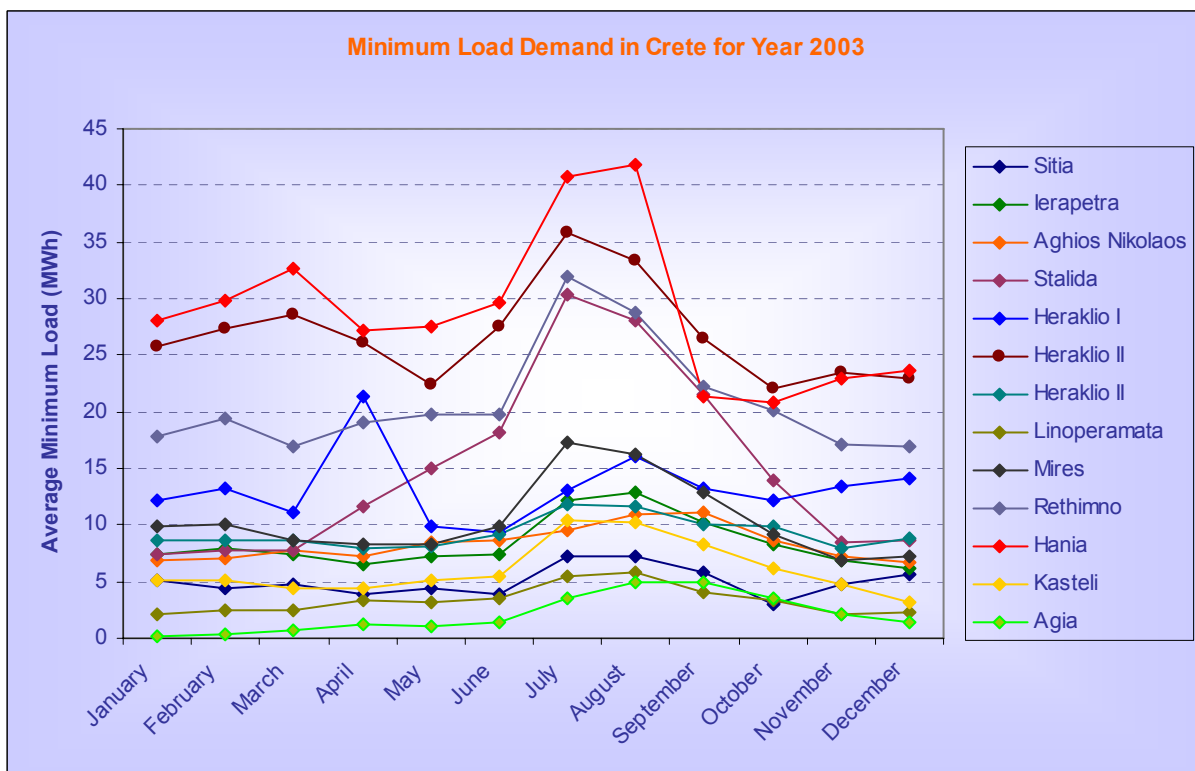


Figure 5.3: Average Minimum load per substation in Crete

In Figure 5.4 it can be observed that most energy is being consumed in the Substations that supply the cities of Hania, Heraklio I and Rethimno. Over 53% of the total energy produced in Crete is being delivered in winter time although in summer time because of the tourist growth, this amount falls to 43%. Also it can be seen that in most substations the demand in August is over doubled in comparison to the demand in winter, autumn and spring time.

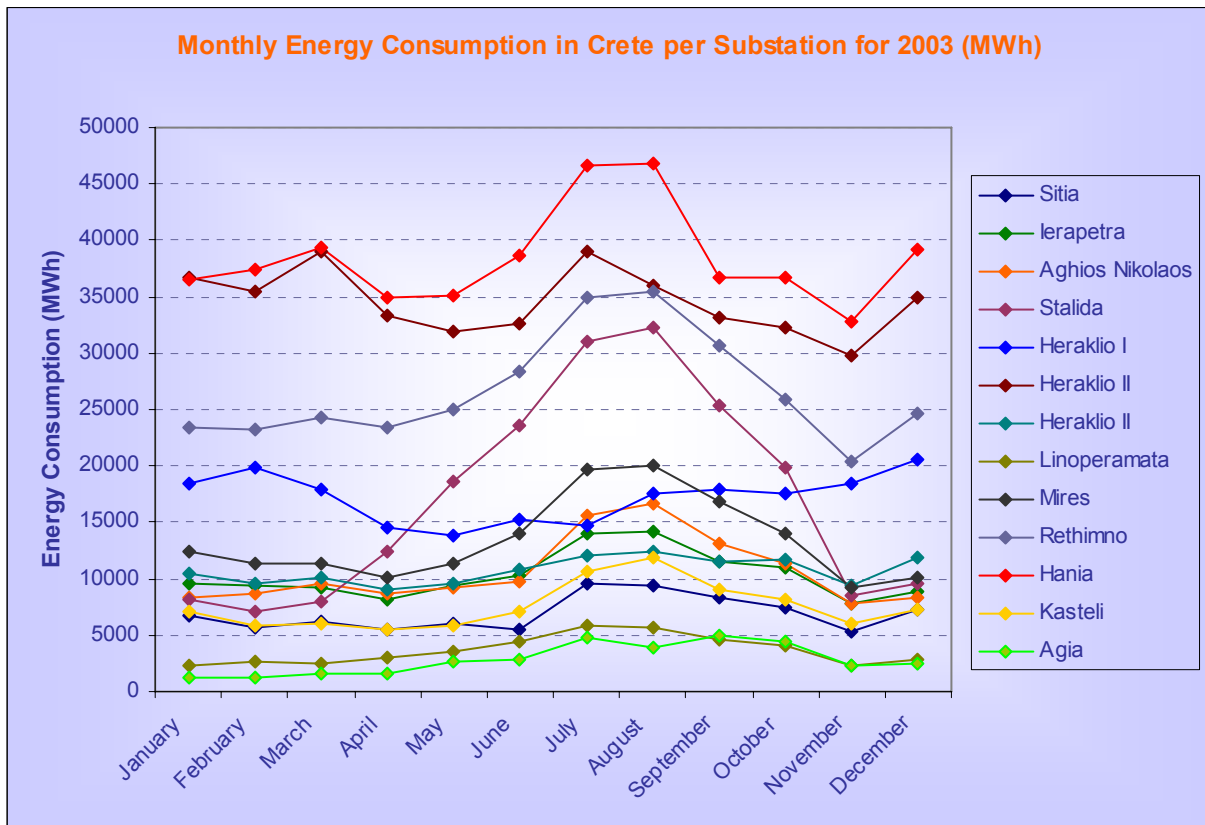


Figure 5.4: The Energy Consumption in the island of Crete per month per substation

5.3 Power Flow Analysis

In order to simulate the power flow in the electricity grid of Crete, the simulation programs in Matlab that was presented in Chapter 4 and developed by Saadat were used. For the definition of the wind penetration in the island of Crete the Newton-Raphson and the Gauss-Seidel methods were used.

5.3.1 Data Preparation

The data used in the simulations was either provided by the Public Power Corporation S.A and the Department of Transmission Sector of Crete and Rhodes or calculated using the data aforementioned.

As it is known the ratio of the active power P to the apparent power S is termed the power factor $\cos\phi$.

$$\frac{\text{Active Power } P}{\text{Apparent Power } S} = \text{power factor or } \cos \phi = \frac{P}{S} = \frac{P}{VI} \quad (5.1)$$

Reactive power Q is given also by the equation:

$$Q = VI \cdot \sin \phi \quad (5.2)$$

From equations 5.1 and 5.2 arises that:

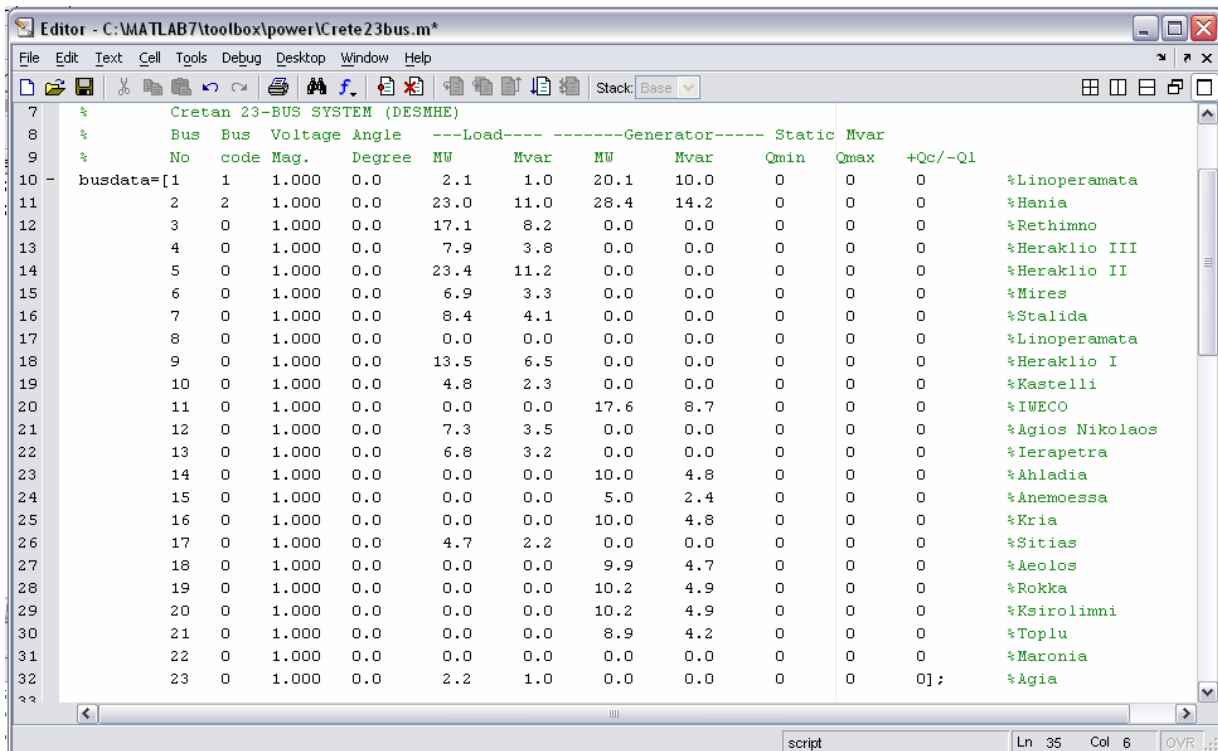
$$\cos \phi = \frac{P \cdot \sin \phi}{Q} \Rightarrow Q = \tan \phi \cdot P \quad (5.3)$$

In order to define the reactive power a value for the power factor should be set. This was chosen to be 0.9 in the Cretan High Voltage Network. This value is empirical and the one that the High Voltage Network is working.

$$\cos \phi = 0.9 \Leftrightarrow \phi = 25.8^\circ \quad (5.4)$$

From equations 5.3 and 5.4 results that:

$$Q = P \cdot 0.483 \quad (5.5)$$

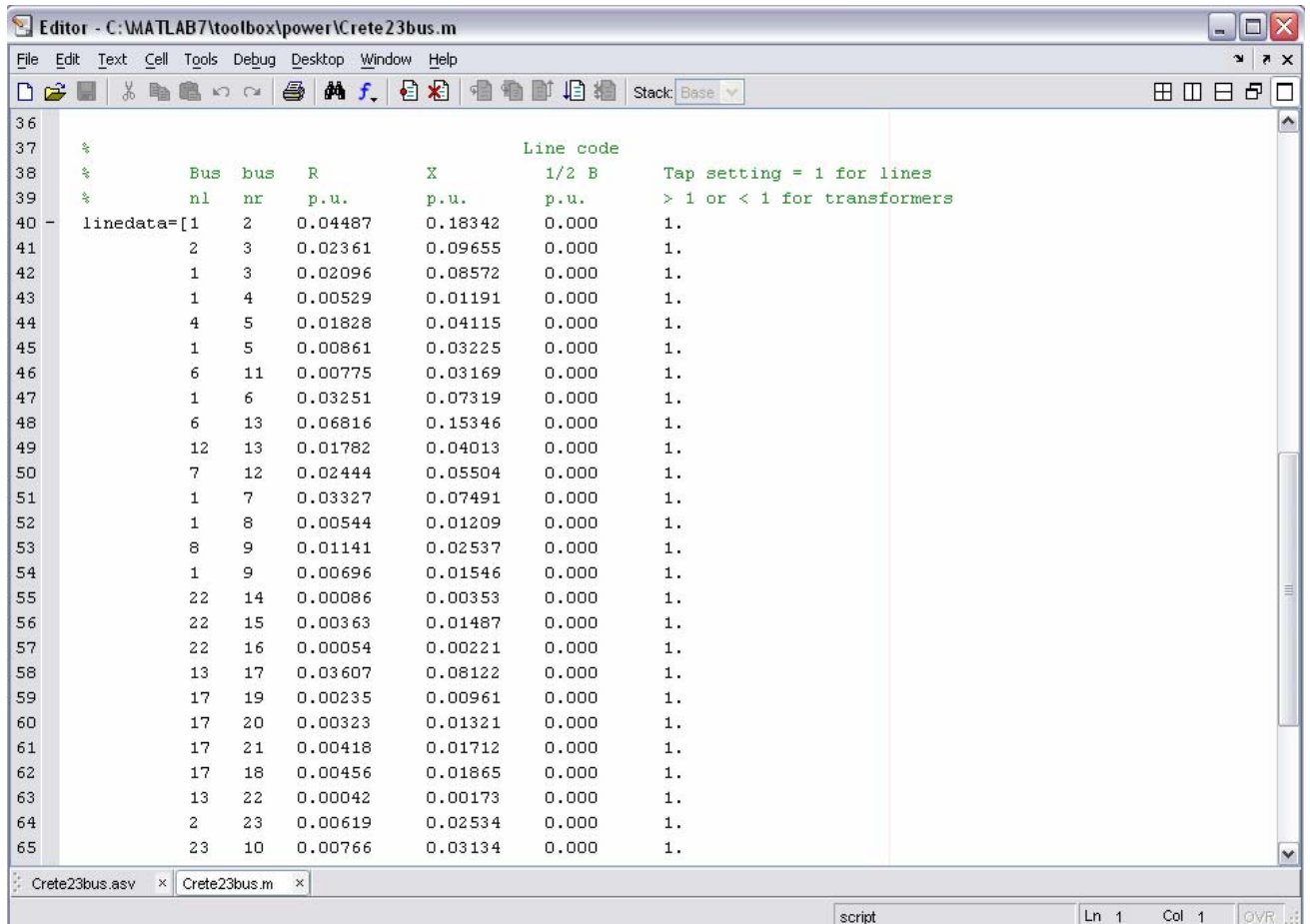


```

7 % Cretan 23-BUS SYSTEM (DESMHE)
8 % Bus Bus Voltage Angle ---Load--- Generator--- Static Mvar
9 % No code Mag. Degree MW Mvar MW Mvar Qmin Qmax +Qc/-Ql
10 busdata=[1 1 1.000 0.0 2.1 1.0 20.1 10.0 0 0 0 %Linoperamata
11 2 2 1.000 0.0 23.0 11.0 28.4 14.2 0 0 0 %Hania
12 3 0 1.000 0.0 17.1 8.2 0.0 0.0 0 0 0 %Rethimno
13 4 0 1.000 0.0 7.9 3.8 0.0 0.0 0 0 0 %Heraklio III
14 5 0 1.000 0.0 23.4 11.2 0.0 0.0 0 0 0 %Heraklio II
15 6 0 1.000 0.0 6.9 3.3 0.0 0.0 0 0 0 %Mires
16 7 0 1.000 0.0 8.4 4.1 0.0 0.0 0 0 0 %Stalida
17 8 0 1.000 0.0 0.0 0.0 0.0 0.0 0 0 0 %Linoperamata
18 9 0 1.000 0.0 13.5 6.5 0.0 0.0 0 0 0 %Heraklio I
19 10 0 1.000 0.0 4.8 2.3 0.0 0.0 0 0 0 %Kastelli
20 11 0 1.000 0.0 0.0 0.0 17.6 8.7 0 0 0 %IWECO
21 12 0 1.000 0.0 7.3 3.5 0.0 0.0 0 0 0 %Agios Nikolaos
22 13 0 1.000 0.0 6.8 3.2 0.0 0.0 0 0 0 %Ierapetra
23 14 0 1.000 0.0 0.0 0.0 10.0 4.8 0 0 0 %Ahladia
24 15 0 1.000 0.0 0.0 0.0 5.0 2.4 0 0 0 %Anemoessa
25 16 0 1.000 0.0 0.0 0.0 10.0 4.8 0 0 0 %Kria
26 17 0 1.000 0.0 4.7 2.2 0.0 0.0 0 0 0 %Sitias
27 18 0 1.000 0.0 0.0 0.0 9.9 4.7 0 0 0 %Aeolos
28 19 0 1.000 0.0 0.0 0.0 10.2 4.9 0 0 0 %Rokka
29 20 0 1.000 0.0 0.0 0.0 10.2 4.9 0 0 0 %Ksirolimni
30 21 0 1.000 0.0 0.0 0.0 8.9 4.2 0 0 0 %Toplu
31 22 0 1.000 0.0 0.0 0.0 0.0 0.0 0 0 0 %Maronia
32 23 0 1.000 0.0 2.2 1.0 0.0 0.0 0 0 0]; %Agia
  
```

Figure 5.5: The busdata file of the power flow analysis process as it is presented in Matlab's Editor

Equation 5.5 was used in order to divert the active power for Load and Generation to reactive power on per unit base. Results are shown on Figure 5.5 in the 6th and 8th column of the busdata file. In the last column the names of the buses are shown in green letters.



```

36
37 %
38 %          Bus bus  R      X      1/2 B      Tap setting = 1 for lines
39 %          nl  nr  p.u.   p.u.   p.u.      > 1 or < 1 for transformers
40 linedata=[1  2  0.04487  0.18342  0.000  1.
41           2  3  0.02361  0.09655  0.000  1.
42           1  3  0.02096  0.08572  0.000  1.
43           1  4  0.00529  0.01191  0.000  1.
44           4  5  0.01828  0.04115  0.000  1.
45           1  5  0.00861  0.03225  0.000  1.
46           6 11  0.00775  0.03169  0.000  1.
47           1  6  0.03251  0.07319  0.000  1.
48           6 13  0.06816  0.15346  0.000  1.
49          12 13  0.01782  0.04013  0.000  1.
50           7 12  0.02444  0.05504  0.000  1.
51           1  7  0.03327  0.07491  0.000  1.
52           1  8  0.00544  0.01209  0.000  1.
53           8  9  0.01141  0.02537  0.000  1.
54           1  9  0.00696  0.01546  0.000  1.
55          22 14  0.00086  0.00353  0.000  1.
56          22 15  0.00363  0.01487  0.000  1.
57          22 16  0.00054  0.00221  0.000  1.
58          13 17  0.03607  0.08122  0.000  1.
59          17 19  0.00235  0.00961  0.000  1.
60          17 20  0.00323  0.01321  0.000  1.
61          17 21  0.00418  0.01712  0.000  1.
62          17 18  0.00456  0.01865  0.000  1.
63          13 22  0.00042  0.00173  0.000  1.
64           2 23  0.00619  0.02534  0.000  1.
65          23 10  0.00766  0.03134  0.000  1.

```

Figure 5.6: In the first two columns of the linedata file there can be seen the line bus n

In the first two columns of the linedata file (Figure 5.6) the two buses that the transmission line connects can be seen. In the 3rd and 4th column the line resistance “R” and reactance “X” can be seen respectively. Both values were calculated from the specifications of the transmission lines that were given by PPC [26]. The total length of the transmission lines, the Resistance and Reactance per kilometre were known. After calculating the resistance and reactance in Ohms both values were divided by the base Resistance R_{base} in order to divert it into per unit.

$$R_{base} = \frac{V_{base}}{I_{base}} \quad \text{and} \quad I_{base} = \frac{P_{base}}{V_{base}} \quad (5.6), (5.7)$$

Taking into consideration equations 5.6 and 5.7 and setting as P_{base} 100MVA:

$$R_{base} = \frac{V_{base}^2}{P_{base}} = \frac{150^2 \text{KV}}{100\text{MVA}} = \frac{22500}{100} = 225\text{ohm} \quad (5.8)$$

In order to investigate the maximum wind penetration in Crete considering, the existing electricity system the following scenario was taken into account. It was accepted that wind speed in the wind farm sites was enough for the wind turbines to produce electricity at their nominal power. In addition the electricity demand was accepted to be the minimum that was recorded through out 2003 and that was for November. This scenario is not far from the reality as the demand data were real and in most wind farms, wind turbines work at their nominal power in November. [26]

5.3.2 Newton-Raphson Method

With **lfnewton** program the power flow solution using the Newton-Raphson method is being obtained. The busdata and linedata files, that are required for the simulation of this program, contain values and data that are being defined in paragraphs 5.2 and 5.3. Several trials have been made in order to define the maximum wind penetration in the existing wind farms in Crete. That has been achieved by increasing the power produced from the wind turbines while decreasing the power produced by the conventional power plants in order to meet the electricity demand.

Power Flow Solution by Newton-Raphson Method							
Maximum Power Mismatch = 0.000181309							
No. of Iterations = 3							
Bus No.	Voltage Mag.	Angle Degree	-----Load-----		---Generation---		Injected Mvar
			MW	Mvar	MW	Mvar	
1	1.000	0.000	2.100	1.000	23.900	13.111	0.000
2	1.000	-0.087	23.000	11.000	36.500	18.637	0.000
3	0.994	-0.436	17.100	8.200	0.000	0.000	0.000
4	0.998	-0.088	7.900	3.800	0.000	0.000	0.000
5	0.996	-0.246	23.400	11.200	0.000	0.000	0.000
6	1.010	0.558	6.900	3.300	0.000	0.000	0.000
7	1.011	0.604	8.400	4.100	0.000	0.000	0.000
8	1.000	-0.021	0.000	0.000	0.000	0.000	0.000
9	0.999	-0.066	13.500	6.500	0.000	0.000	0.000
10	0.998	-0.254	4.800	2.300	0.000	0.000	0.000
11	1.011	0.636	0.000	0.000	5.000	2.400	0.000
12	1.023	1.238	7.300	3.500	0.000	0.000	0.000
13	1.035	1.814	6.800	3.200	0.000	0.000	0.000
14	1.036	1.851	0.000	0.000	10.000	4.800	0.000
15	1.036	1.869	0.000	0.000	5.000	2.400	0.000
16	1.036	1.845	0.000	0.000	10.000	4.800	0.000
17	1.059	2.968	4.700	2.200	0.000	0.000	0.000
18	1.060	3.051	0.000	0.000	9.900	4.700	0.000
19	1.060	3.012	0.000	0.000	10.200	4.900	0.000
20	1.060	3.028	0.000	0.000	10.200	4.900	0.000
21	1.060	3.037	0.000	0.000	8.900	4.200	0.000
22	1.035	1.834	0.000	0.000	0.000	0.000	0.000
23	0.999	-0.177	2.200	1.000	0.000	0.000	0.000
Total			128.100	61.300	129.600	64.848	0.000

Figure 5.7a: The results from the power flow solution by Newton-Raphson as they are printed in Matlab software for a scenario with the existing power system.

Power Flow Solution by Newton-Raphson Method							
Maximum Power Mismatch = 0.000198655							
No. of Iterations = 3							
Bus No.	Voltage Mag.	Angle Degree	-----Load----- MW	Mvar	---Generation--- MW	Mvar	Injected Mvar
1	1.000	0.000	2.100	1.000	20.426	5.927	0.000
2	1.000	-0.533	23.000	11.000	28.500	20.610	0.000
3	0.994	-0.646	17.100	8.200	0.000	0.000	0.000
4	0.998	-0.088	7.900	3.800	0.000	0.000	0.000
5	0.996	-0.246	23.400	11.200	0.000	0.000	0.000
6	1.017	0.862	6.900	3.300	0.000	0.000	0.000
7	1.012	0.674	8.400	4.100	0.000	0.000	0.000
8	1.000	-0.021	0.000	0.000	0.000	0.000	0.000
9	0.999	-0.066	13.500	6.500	0.000	0.000	0.000
10	0.998	-0.699	4.800	2.300	0.000	0.000	0.000
11	1.020	1.119	0.000	0.000	16.700	8.200	0.000
12	1.026	1.357	7.300	3.500	0.000	0.000	0.000
13	1.038	1.966	6.800	3.200	0.000	0.000	0.000
14	1.039	2.003	0.000	0.000	10.000	4.800	0.000
15	1.039	2.021	0.000	0.000	5.000	2.400	0.000
16	1.039	1.997	0.000	0.000	10.000	4.800	0.000
17	1.062	3.113	4.700	2.200	0.000	0.000	0.000
18	1.064	3.196	0.000	0.000	9.900	4.700	0.000
19	1.063	3.157	0.000	0.000	10.200	4.900	0.000
20	1.063	3.173	0.000	0.000	10.200	4.900	0.000
21	1.063	3.182	0.000	0.000	8.900	4.200	0.000
22	1.039	1.987	0.000	0.000	0.000	0.000	0.000
23	0.999	-0.623	2.200	1.000	0.000	0.000	0.000
Total			128.100	61.300	129.826	65.437	0.000

Figure 5.8b: The results from the power flow solution by Newton-Raphson as they are printed in Matlab software in the case that 11.7MW are added in IWECO’s substation.

According to the results from the power flow solution by the Newton-Raphson method the existing wind farms can be extended at maximum for 11.7MW in the case of the Iweco’s wind farm near Mires substation. The results are shown in details in table 5.3.

Table 5.3: The results from the Newton-Raphson simulation are presented in this table. In the third and fourth column the nominal capacity of the wind farms and the capacity that can be added in the existing wind farms is shown respectively. In the fifth column the bus in which the voltage magnitude exceeds the 6% can be seen.

Wind Farm Name	Bus No	Present Nominal Capacity (MW)	Maximum capacity (MW)	Additional Capacity (MW)	Error Bus
Ahladia	14	10	13.9	3.9	18
Anemoessa	15	5	8.9	3.9	18
Kria	16	10	13.9	3.9	18
Iweco	11	5	16.7	11.7	18
Toplu	21	6.6	8.9	2.3	18
Rokka	20	10.2	12.3	2.1	18
Aeolos	18	9.9	12.2	2.3	18
Ksirolimni	19	10.2	12.3	2.1	18

After several iterations and test simulations, according to Newton-Raphson method in each bus, it was concluded that in all buses except those in table 5.4, the power generation that can be added can cover all the electricity demand in the island. Actually if this power is produced by wind turbines it will

result in many problems to the electrical grid because as it is known wind power is a variable, non constant and unpredicted energy source. Its fluctuations can be normalized by conventional power plants or power plants with constant operation such as biomass plants or solar thermal plants. This limits the percentage of wind penetration in the Cretan electric grid.

Table 5.4: The results from the Newton-Raphson simulation showing maximum wind penetration in buses without present electricity production from wind farms.

Bus Name	Bus No	Maximum capacity (MW)	Error Bus
Aghios Nikolaos	12	5.0	18
Mires	6	11.7	18
Stalida	7	8.6	18
Maronia	22	4.0	18
Sitia	17	2.3	18
Ierapetra	13	4.0	18

5.3.3 Gauss-Seidel Method

Same procedure as the one in Newton-Raphson method was used in Gauss-Seidel power flow solution. The busdata and linedata files that were used were exactly the same to those in Newton-Raphson method but concluded to different results. A main difference between the two methods was the numbers of iterations that were needed by Matlab in order to print the results. More specific, in Newton-Raphson method usually three (3) iterations were enough for Matlab to print the results, while in the contrary in Gauss-Seidel method up to a hundred (100) iterations were needed. In addition in the Gauss-Seidel method the maximum mismatch was 5 to 100 times more than the one in Newton-Raphson method. An example with results from a power flow solution provided by Gauss-Seidel Method is as follow.

Power Flow Solution by Gauss-Seidel Method							
Maximum Power Mismatch = 0.000993071							
No. of Iterations = 96							
Bus No.	Voltage Mag.	Angle Degree	-----Load-----		---Generation---		Injected Mvar
			MW	Mvar	MW	Mvar	
1	1.000	0.000	2.100	1.000	20.449	6.237	0.000
2	1.000	-0.533	23.000	11.000	28.500	20.610	0.000
3	0.994	-0.646	17.100	8.200	0.000	0.000	0.000
4	0.998	-0.088	7.900	3.800	0.000	0.000	0.000
5	0.996	-0.246	23.400	11.200	0.000	0.000	0.000
6	1.017	0.864	6.900	3.300	0.000	0.000	0.000
7	1.012	0.677	8.400	4.100	0.000	0.000	0.000
8	1.000	-0.021	0.000	0.000	0.000	0.000	0.000
9	0.999	-0.066	13.500	6.500	0.000	0.000	0.000
10	0.998	-0.699	4.800	2.300	0.000	0.000	0.000
11	1.020	1.121	0.000	0.000	16.700	8.200	0.000
12	1.026	1.362	7.300	3.500	0.000	0.000	0.000
13	1.038	1.973	6.800	3.200	0.000	0.000	0.000
14	1.039	2.010	0.000	0.000	10.000	4.800	0.000
15	1.039	2.028	0.000	0.000	5.000	2.400	0.000
16	1.038	2.003	0.000	0.000	10.000	4.800	0.000
17	1.062	3.121	4.700	2.200	0.000	0.000	0.000
18	1.063	3.204	0.000	0.000	9.900	4.700	0.000
19	1.063	3.165	0.000	0.000	10.200	4.900	0.000
20	1.063	3.181	0.000	0.000	10.200	4.900	0.000
21	1.063	3.189	0.000	0.000	8.900	4.200	0.000
22	1.038	1.993	0.000	0.000	0.000	0.000	0.000
23	0.999	-0.623	2.200	1.000	0.000	0.000	0.000
Total			128.100	61.300	129.849	65.747	0.000

Figure 5.9a: The results from the power flow solution by Gauss-Seidel as they are printed in Matlab software a scenario with the existing power system.

Power Flow Solution by Gauss-Seidel Method							
Maximum Power Mismatch = 0.000987586							
No. of Iterations = 96							
Bus No.	Voltage Mag.	Angle Degree	-----Load-----		---Generation---		Injected Mvar
			MW	Mvar	MW	Mvar	
1	1.000	0.000	2.100	1.000	19.670	5.767	0.000
2	1.000	-0.538	23.000	11.000	28.400	20.635	0.000
3	0.994	-0.648	17.100	8.200	0.000	0.000	0.000
4	0.998	-0.088	7.900	3.800	0.000	0.000	0.000
5	0.996	-0.246	23.400	11.200	0.000	0.000	0.000
6	1.017	0.887	6.900	3.300	0.000	0.000	0.000
7	1.012	0.682	8.400	4.100	0.000	0.000	0.000
8	1.000	-0.021	0.000	0.000	0.000	0.000	0.000
9	0.999	-0.066	13.500	6.500	0.000	0.000	0.000
10	0.998	-0.705	4.800	2.300	0.000	0.000	0.000
11	1.021	1.157	0.000	0.000	17.600	8.700	0.000
12	1.026	1.371	7.300	3.500	0.000	0.000	0.000
13	1.038	1.984	6.800	3.200	0.000	0.000	0.000
14	1.039	2.021	0.000	0.000	10.000	4.800	0.000
15	1.039	2.039	0.000	0.000	5.000	2.400	0.000
16	1.039	2.015	0.000	0.000	10.000	4.800	0.000
17	1.062	3.132	4.700	2.200	0.000	0.000	0.000
18	1.064	3.215	0.000	0.000	9.900	4.700	0.000
19	1.063	3.176	0.000	0.000	10.200	4.900	0.000
20	1.063	3.192	0.000	0.000	10.200	4.900	0.000
21	1.063	3.200	0.000	0.000	8.900	4.200	0.000
22	1.039	2.004	0.000	0.000	0.000	0.000	0.000
23	0.999	-0.628	2.200	1.000	0.000	0.000	0.000
Total			128.100	61.300	129.870	65.802	0.000

Figure 5.10b: The results from the power flow solution by Gauss-Seidel as they are printed in Matlab software in the case that 12.6MW are added in IWECO's substation.

According to the results from the power flow solution by the Gauss-Seidel method the existing wind farms can be extended at maximum to 12.6MW in the case of the Iweco's wind farm near Mires substation. In details the results are shown in table 5.5.

Table 5.5: The results from the Gauss-Seidel power flow solution in buses where wind farms exist.

Wind Farm Name	Bus No	Present Nominal Capacity (MW)	Maximum capacity (MW)	Additional Capacity (MW)	Error Bus
Ahladia	14	10	14	4	18
Anemoessa	15	5	8.9	3.9	18
Kria	16	10	14	4	18
Iweco	11	5	17.6	12.6	18
Toplu	21	6.6	9.2	2.6	18,20,21
Rokka	20	10.2	12.6	2.4	18
Aeolos	18	9.9	12.1	2.2	18
Ksirolimni	19	10.2	12.0	1.8	18,20

Simulations were also made for all the other buses concluding that in all buses, except those in table 5.6, power enough to cover all Crete’s electricity demand can be added.

Table 5.6: The results from the Gauss-Seidel power flow solution in buses where wind farms do not exist.

Bus Name	Bus No	Maximum capacity (MW)	Error Bus
Aghios Nikolaos	12	5.3	18
Mires	6	12.6	18
Stalida	7	8.2	18
Maronia	22	4.3	18
Sitia	17	2.7	18
Ierapetra	13	4.3	18

5.3.4 Line Flow Analysis and Losses

An important parameter for the analysis of a power system is the computation of line flows and losses. This was achieved using the *lineflow* program described in paragraph 4.8. An example of the output of this program is being shown below. In the first two columns the two buses connected by the transmission line can be seen. In the third, fourth and fifth column the active and reactive power flow entering the line terminals and line losses as well as the net power at each bus are being displayed respectively. In the last two columns the total real and reactive losses in the system can be seen.

Line Flow and Losses						
--Line--	Power at bus & line flow			--Line loss--	Transformer	
from to	MW	Mvar	MVA	MW	Mvar	tap
1	18.326	4.927	18.976			
2	4.789	-1.148	4.924	0.011	0.044	
3	13.879	3.316	14.270	0.043	0.175	
4	15.765	6.487	17.048	0.015	0.035	
5	15.590	8.679	17.843	0.027	0.103	
6	-25.853	-11.151	28.155	0.258	0.580	
7	-19.347	-7.761	20.846	0.145	0.326	
8	3.947	1.907	4.384	0.001	0.002	
9	9.564	4.617	10.620	0.008	0.017	
2	5.500	9.610	11.073			
1	-4.778	1.192	4.924	0.011	0.044	
3	3.272	5.094	6.054	0.009	0.035	
23	7.006	3.324	7.755	0.004	0.015	
3	-17.100	-8.200	18.964			
2	-3.263	-5.058	6.020	0.009	0.035	
1	-13.837	-3.142	14.189	0.043	0.175	
4	-7.900	-3.800	8.766			
1	-15.750	-6.452	17.020	0.015	0.035	
5	7.850	2.652	8.286	0.013	0.028	
5	-23.400	-11.200	25.942			
4	-7.837	-2.624	8.265	0.013	0.028	
1	-15.563	-8.576	17.769	0.027	0.103	
6	-6.900	-3.300	7.649			
11	-16.674	-8.095	18.535	0.026	0.105	
1	26.110	11.731	28.625	0.258	0.580	
13	-16.336	-6.936	17.748	0.208	0.468	
7	-8.400	-4.100	9.347			
12	-27.892	-12.187	30.438	0.221	0.498	
1	19.492	8.087	21.102	0.145	0.326	
8	0.000	0.000	0.000			
1	-3.946	-1.905	4.382	0.001	0.002	
9	3.946	1.905	4.382	0.002	0.005	
9	-13.500	-6.500	14.983			
8	-3.944	-1.900	4.378	0.002	0.005	
1	-9.556	-4.600	10.606	0.008	0.017	
10	-4.800	-2.300	5.323			
23	-4.800	-2.300	5.323	0.002	0.009	
11	16.700	8.200	18.605			
6	16.700	8.200	18.605	0.026	0.105	
12	-7.300	-3.500	8.096			
13	-35.412	-16.184	38.936	0.257	0.578	
7	28.112	12.684	30.842	0.221	0.498	
13	-6.800	-3.200	7.515			
6	16.544	7.404	18.125	0.208	0.468	
12	35.669	16.762	39.412	0.257	0.578	
17	-34.019	-15.389	37.338	0.466	1.050	
22	-24.994	-11.977	27.716	0.003	0.012	
14	10.000	4.800	11.092			
22	10.000	4.800	11.092	0.001	0.004	
15	5.000	2.400	5.546			
22	5.000	2.400	5.546	0.001	0.004	
16	10.000	4.800	11.092			
22	10.000	4.800	11.092	0.001	0.003	
17	-4.700	-2.200	5.189			
13	34.485	16.440	38.203	0.466	1.050	
19	-10.197	-4.889	11.309	0.003	0.011	
20	-10.196	-4.885	11.306	0.004	0.015	
21	-8.896	-4.185	9.832	0.004	0.015	
18	-9.895	-4.680	10.946	0.005	0.020	
18	9.900	4.700	10.959			
17	9.900	4.700	10.959	0.005	0.020	
19	10.200	4.900	11.316			
17	10.200	4.900	11.316	0.003	0.011	
20	10.200	4.900	11.316			
17	10.200	4.900	11.316	0.004	0.015	
21	8.900	4.200	9.841			
17	8.900	4.200	9.841	0.004	0.015	

22		0.000	0.000	0.000		
	14	-9.999	-4.796	11.090	0.001	0.004
	15	-4.999	-2.396	5.543	0.001	0.004
	16	-9.999	-4.797	11.091	0.001	0.003
	13	24.997	11.989	27.724	0.003	0.012
23		-2.200	-1.000	2.417		
	2	-7.002	-3.309	7.745	0.004	0.015
	10	4.802	2.309	5.328	0.002	0.009
Total loss					1.735	4.157

Figure 5.11: The line flow analysis and losses results as they are printed in Matlab software.

As it can be observed from the results, after several iterations trying to specify the levels of power penetration in each bus in the Cretan electric system, power losses were in a low level because of the short distances between the wind farms and the main buses used to distribute the energy. Only in the case of Iweco's wind farm power losses were in a higher level, since the distance between the wind farm and the nearest bus in Mires were quite further than in all other cases.

In addition the total power losses for November 2003, as they are calculated from the lineflow program in Matlab, reach the 1.53MW thus the energy losses would be:

$$\text{Energy Losses (November)} = \text{Power Losses} \times \text{Days} \times \text{Hours} = 1.55\text{MW} \cdot 30\text{days} \cdot 24\text{hours} \approx 1,120\text{MWh}$$

According to the PPS's annual report for 2003, total energy losses, including transmission lines and substation losses, for November 2003 were up to 2.200MWh, while the losses from the transmission lines reached 1,300MWh. This value is not far from the value calculated above. Also it should be considered that the above model simulates the electric system in ideal conditions thus differences are reasonable to be observed.

The results from the line flow analysis and losses were used together with the results from the power flow solutions by Newton-Raphson and Gauss-Seidel method in order to see how energy losses affect wind penetration in Crete. As it was mentioned before the maximum wind penetration in the existing wind farms can be achieved in Iweco's wind farm. After the analysis of line flow and losses it was observed that between Iweco's wind farm and Mires substation, power losses had the maximum value because of the distance between them. However the total energy production that can be added in the existing wind farm is more than the power that can be added in Stalida substation. In specific in Mires 11.7MW (with Newton-Raphson method) can be added near the Iweco's wind farm causing losses that reach 0.2MW. In the contrary in the case of Stalida 8.6MW can be added causing losses that reach 0.14MW.

The line flow analysis was also used for the specification of the thermal limitations of the transmission lines.

5.4 Thermal Limitations

Another parameter that was investigated was the thermal limits. Considering the power losses estimated in the previous paragraph, the thermal flow as well as the thermal capacity of the

transmissions lines was calculated and tested respectively. This analysis was made in order to see how the increase of power losses could affect to the increase of power production as it was described in our scenario.

According to the Public Power Company that is responsible for the Cretan electric grid, the thermal capacity of the transmission lines is at 90MVA. From table 5.7 it can be observed that in none connection this capacity is over the one given by PPC.

In the first two columns of table 5.7, the code number of the buses connected together is shown. In the third column the power flow (in MVA) can be seen as it was estimated after running the lineflow program as it was described in the previous paragraph. The power flow value that was used in these calculations was the maximum one that was added in buses where energy is produced, as it was presented in the results from Newton-Raphson method.

Table 5.7: The results from the lineflow program concerning the power flow. Comparing these values to the one given by PPC (90MVA as the maximum thermal capacity) in none connection the thermal capacity is above the limit.

From (Bus code)	To (Bus code)	Power Flow (MVA)	From (Bus code)	To (Bus code)	Power Flow (MVA)
1	2	4.588	12	7	28.442
1	3	7.189	13	6	21.466
1	4	17.048	13	12	38.148
1	5	17.843	13	17	34.939
1	8	4.384	14	22	15.345
1	9	10.620	15	22	9.884
2	3	12.862	16	22	15.345
2	23	7.755	17	13	38.251
4	5	8.286	18	17	13.375
6	1	18.825	19	17	13.642
7	1	19.901	20	17	13.642
8	9	4.382	21	17	9.841
10	23	5.323	22	13	27.716
11	6	5.546			

5.5 Environmental Benefits

The uncontested reason for which a wind energy project should be developed is the environmental benefits. Electricity produced from renewable energy sources such as wind causes no emissions at all. On the other hand using Fossil Fuels serious damage can be caused to the environment, resulting in undesirable phenomena that may affect the planet's climate. The emissions caused by conventional energy sources during electricity production are presented on the following table

Table 5.8: The emissions caused by several energy plants during electricity production.

Energy Source	CO ₂	SO ₂	NO _x	Particulates
Coal	247,000	320	725	45
Gas-CCGT	136,000	0	3	0
Oil Plants	204,000	3,750	1003	108
Diesel Plant	191,000	301	3,276	30
Wind Turbine	0	0	0	0

Units in kg/TJ

Source: Sustainable Energy Ireland http://www.sei.ie/uploads/documents/upload/publications/emissions_data.pdf

In 2003 only wind turbines of 84MW nominal power operated without problems in Crete. These wind turbines produced 227GWh. The power coefficient in that case is:

$$C_p = \frac{\text{ActualPower}}{\text{TheoreticalPower}} = \frac{227\text{GWh}}{736\text{GWh}} = 0.31 \quad (5.9)$$

In this scenario it is assumed that the power coefficient for the additional 11.7MW of nominal wind energy is also 0.31. Taking this for granted, the energy that will be produced is:

$$E = C_p \cdot P \cdot h_{\text{year}} = 0.31 \cdot 11.7\text{MW} \cdot 8760\text{h} = 31,772\text{MWh} \quad (5.10)$$

Using the data provided on Table 5.8, the emission savings due to the partial replacement of diesel plants by wind turbines are the following:

Table 5.9: The emissions savings after adding the 11.7MW. in tns.

Energy Source	CO ₂	SO ₂	NO _x	Particulates
Diesel Plant	21,852	34.43	374.8	3.43

6 CONCLUSIONS

The aim of this thesis was to investigate, from a technical point of view, how much more wind energy can be developed in the remote island of Crete, considering suspending parameters concerning the distribution network. Restrictive parameters for the increasing of wind penetration appear in the eastern part of the island where 8 wind farms are located producing 10% of the total electricity in the island.

For the determination of the capacity of wind energy projects that can penetrate in the electric grid of Crete, the power flow solutions by Newton-Raphson and Gauss-Seidel were used. After several iterations it was concluded that the maximum wind energy capacity which can be developed in the already installed wind farms in Crete is 11.7MW according to the Newton-Raphson method and 12.6MW according to the Gauss-Seidel method. The Eastern part of Crete is adequate for the installation and operation of wind farms, due to the high available wind potential of the region and the topography. In the central and western part of Crete according to the aforementioned power flow solutions there would be no serious problem in installing new power plants. However, the methods used in this analysis are conducting a static and not a dynamic study of the system. In this case, the fact that wind power is a dynamic and variable source of energy is not taken into account. What is being studied is the effect of the induction of any mode of power plant in the electric system.

In this project the possible power losses, as well as the thermal capacity of the transmission lines, were also determined, resulting in that these parameters will not affect negatively the installation of more power plants in the island. However, they have to be considered before developing any kind of power plants.

To conclude, the analysis made in this thesis showed that the electric grid of the island of Crete is capable of being connected to new power plants especially in the western part. Unfortunately the western part of the island is not available for the development of wind farms. The main reasons are the low wind potential, in comparison to the one at the eastern part, the topology and the high prices of buying or lending land. The only parts in western Crete that wind farms can be installed effectively are the south west areas and some sites near Kastelli substation, where wind potential exceeds 10m/sec. However in the first case it is difficult and expensive to connect this wind farms to the electric grid because of the inaccessibility of the area between the southern and northern part, where Chania, Kastelli and Agia substations are located. In addition, the areas in the central part of Chania prefecture belong to Natura 2000 Network and therefore have to be protected by human activities and industrial development is restricted there. Furthermore the areas near Kastelli substation that are suitable for the development of wind farms are few and this means that no large wind farms can be developed.

In the contrary, in the eastern part of Crete the main annual wind speed in many areas is more than 10-12m/sec. Due to the existence of barren areas the cost of buying or lending land is much cheaper. However, in this case as it was concluded by the power flow analyses, the development of more wind farms in sites where wind farms already exist will cause several problems to the island's electricity

system. Solution will be given if new transformers are added in these areas in order to control fluctuations from the wind turbines more effectively.

According to CRES's wind energy potential report for Crete it can be seen that in the central part of the island and near the Heraklio III and Rethimno substations, the wind potential is enough for the installation of energy effective wind farms. Also in these areas, sites are offered for an economically viable development of wind farms. Connecting new power plants in these two substations will not cause any problems to the electric grid as it was shown from the power flow solutions by Newton-Raphson and Gauss-Seidel in chapter 5.

The main advantage of the utilisation of a system as the one described above (where 11.7MW are produced by wind energy) is the environmental benefits. As it was analysed and estimated, 31,772MWh will be annually produced by wind turbines, saving 21,852tn of CO₂, 34.43tn of SO₂, 374.8tn of NO_x and 3.43tn of particulates.

REFERENCES

- [1] Law 2773/99 (Official Journal of the Hellenic Republic 286/22-12-99): «Απελευθέρωση της Αγοράς Ηλεκτρικής Ενέργειας, ρυθμίσεις ενεργειακής πολιτικής και λοιπές ρυθμίσεις». (“Liberalisation of the electricity market, regulation on subjects of energy policy and other regulations”).
- [2] Regulatory Authority for Energy - General Information on the Greek Electricity Sector for the period 2000-2003: Installed capacity, production & consumption levels, Renewable Energy Sources and Long Term Energy Planning.
- [3] Regulatory Authority for Energy - Report for the development of Renewable Energy Sources in Greece, Feb. 2003.
- [4] Ελληνική Δημοκρατία, Υπουργείο Ανάπτυξης – «2^η Εθνική Έκθεση για το επίπεδο διείσδυσης της ανανεώσιμης Ενέργειας το έτος 2010» (Hellenic Republic, Ministry of Development 2nd National Report for Renewable Energy Sources Penetration in Greece)
- [5] Directive 2001/77/EC of the European Parliament and of the Council of 27 September 2001 on the «Promotion of electricity from renewable energy sources in the internal electricity market».
- [6] The Annual Report of the IEA R&D Wind Implementing Agreement 2003
- [7] Deutches Windenergie-Institute, Tech Wise A/S, DM Energy, (2002) – “Wind Turbine Grid Connection and Interaction”, europa.eu.int/comm/energy/res/sectors/doc/wind_energy/maxibrochure_final_version.pdf
- [8] Energy Center of Wisconsin, “Wind Power Basics”- <http://www.wind.ecw.org/cat1.html>
- [9] British Wind Energy Association, “Best Practice Guidelines for Wind Energy Development”:
<http://www.bwea.com/ref/bpg.html>
- [10] Danish Wind Industry Association “Research and Education”, -: <http://www.windpower.org/>
- [11] J.T.G. Pierik, - “Electrical Systems in Wind Turbines and Integration of Wind Energy into the Grid”,(2002), [www.ecn.nl/_files/wind/ documents/Tilaran02_GridImpCR.pdf](http://www.ecn.nl/_files/wind/documents/Tilaran02_GridImpCR.pdf)
- [12] Henk Polinder, Sjoerd W.H. de Haan, Maxime R. Dubois Johannes G. Slootweg, - “Basic Operation Principles and Electrical Conversion Systems of WTs” (2004). www.elkraft.ntnu.no/norpie/10956873/Final%20Papers/069%20-%20electrical%20conversion%20systems.pdf
- [13] Han Slootweg, Eize De Vries, “Inside Wind Turbines – Fixed versus variable speed”, Renewable Energy World”, (Issue January-February 2003)

-
-
- [14] Markus A. Polle, “Doubly-Fed Induction Machine Models for Stability Assessment of Wind Farms”, (2002), http://www.digsilent.de/Consulting/Publications/DFIG_Modeling.pdf
- [15] Anca D. Hansen, Florin Iov, Poul Sørensen, Frede Blaabjerg, “Overall control strategy of variable speed doubly-fed induction generator Wind Turbine” (2004) www.elkraft.chalmers.se/Publikationer/EMKE.publ/NWPC04/papers/HANSEN.PDF
- [16] Econnect Ltd. & ILEX Associates, “A Technical Guide for Connection of Embedded Generators to the Distribution Network”, , November 1998
- [17] A.E. Kiprakis, G. P. Harrison and A. R. Wallace, -“Network integration of mini Hydro” (May 2003) www.see.ed.ac.uk/~gph/publications/REGEN-proof.pdf
- [18] Keith Jarrett, Jonathan Hedgecock, Richard Gregory and Tim Warham, - “A Technical Guide to the Connexion of Generation to the Distribution Network”, (February 2004) www.energynetworks.org/pdfs/FES_00318_v040211.pdf
- [19] Scott B. - “Decoupled Newton Load Flow, IEEE Trans. Power Apparatus and Systems”, PAS-93, May – June 1974
- [20] Scott B. and Alsac O - “Fast Decoupled Load Flow, IEEE Trans. Power Apparatus and Systems”, PAS-93, May – June 1974
- [21] EOT - GNTO - Greek National Tourism Organisation –“Statistics 2003”, <http://www.eot.gr>
- [22] PAE - RAE – Regulatory Authority for Energy – “The Energy System in Greece” - <http://www.rae.gr/energysys/main.htm>
- [23] ΔEH – PPC- Public Power Company – “Announcements”, “Press Releases”, “Annual Reports”, <http://www.dei.gr/%28CD8CD3E05032F1296E0A4A7622DF836865C1F84F73B46447%29/ecportal.asp?id=21&nt=19&lang=2>
- [24] Arthouros Zervos, Jolanda Crettaz and Christine Lins, - Renewable Energy Development and its impact on islands, European Renewable Energy Council, Proceedings of International Conference “RES for Island Tourism and Water, 26-28 May 2003 Crete Greece, pages 3-5.
- [25] National Statistical Services of Greece – “Real Population in each Region in Greece” (2001) http://www.statistics.gr/gr_tables/S1100_SAP_1_pinakas1b_i.HTM
- [26] Annual Report for the Electric Grid of Crete in 2003 – Public Power Corporation S.A., Islands Department of Transmission Sector of Crete and Rhodes
- [27] Hadi Sadaat - “Power System Analysis”, McGraw-Hill International Editions, Electrical Engineering Series, 1999.



- [28] School of Information Technology and Electrical Engineering, The University of Queensland, "Power Systems and Reliability", <http://www.itee.uq.edu.au/~elec4300/lflowadditional-04.pdf>